Université du Québec
à Rimouski

MODÉLISATION ET SIMULATION D'UNE PLAQUE EN ACIER 4340 CHAUFFÉE PAR INDUCTION UTILISANT UN MODÈLE DE SIMULATION PAR ÉLÉMENTS FINIS

PRÉDICTION ET OPTIMISATION NUMÉRIQUE

Mémoire présenté

dans le cadre du programme de maîtrise en ingénierie

en vue de l'obtention du grade « maître ès sciences appliquées »

(M. Sc. A.)

PAR

© RABII HOUTANE

Janvier 2022

Composition du jury :

Cherif Raef, président du jury, Université du Québec à Rimouski

Barka Noureddine, directeur de recherche, Université du Québec à Rimouski

Benabbou Loubna, codirecteur de recherche, Université du Québec à Rimouski

Sasan Sattarpanah Karganroudi, codirecteur de recherche, Institut technologique de maintenance industrielle

Vahid Sabri, examinateur externe, Mouvement Desjardins

Dépôt initial le 12 octobre 2021 Dépôt final le 12 janvier 2022

À mes parents.

REMERCIEMENTS

Je tiens à exprimer ma profonde gratitude envers Monsieur Noureddine BARKA pour son encadrement, ses conseils méthodologiques et pour son regard d'expert avisé. Il a été très présent pendant toutes les étapes de la réalisation de cette recherche. Ses conseils judicieux ont orienté mon choix du sujet et de la méthodologie, ils m'ont aidé à surmonter les difficultés et ils m'ont ouvert des pistes d'analyse pertinentes.

Je remercie également Monsieur Sasan Sattarpanah Karganroudi pour son attention de tout instant sur mes travaux, pour ses conseils avisés et son écoute qui ont été prépondérants pour la bonne réussite de ce travail.

J'adresse, également, de chaleureux remerciements à ma co-directrice Loubna Benabbou qui a fait partie des acteurs bienveillants de ma formation, elle a toujours été présente et à l'écoute, ses orientations éclairantes et ses conseils avisés ont été prépondérants pour la bonne réussite de ce travail.

Bien sûr, un grand merci à tous les membres du personnel du département de mathématique, d'informatique et de génie de l'université du Québec à Rimouski d'avoir mis à ma disposition tous les moyens techniques et logistiques pour réussir mes études.

Mes dernières pensées vont à mes deux parents. Leur amour, leur intérêt, leur soutien et leur encouragement m'ont beaucoup motivé à la réalisation de ce travail. Leur présence au cours de mon parcours était très précieuse et grâce à eux mon rêve est en train de se réaliser. Et sans eux je n'en serais pas là aujourd'hui.

Enfin, un merci très particulier à toute l'équipe de recherche, amis et collègues qui ont rendu ces années d'études agréables. Un clin d'œil particulier à Ilyasse, Haitam, Anass et Oussama pour tous les moments partagés.

RÉSUMÉ

Le traitement thermique par induction est une technologie importante dans l'industrie manufacturière. Avec sa vaste gamme d'applications allant du chauffage à la fusion, du brasage au soudage et du scellement des bouchons au collage, c'est souvent la clé pour ajouter de la valeur à un processus particulier dans l'industrie. Ceci est réalisé par le fait que le chauffage par induction fournit un taux de chauffage plus élevé que tout autre procédé de chauffage commercial disponible. En raison du chauffage rapide et de la bonne reproductibilité, il est couramment utilisé pour chauffer des matériaux conducteurs à la température exacte. La capacité de génération de chaleur en profondeur en combinaison avec une intensité de chaleur élevée rapidement et dans des régions bien définies sur la pièce est une caractéristique très attrayante de cette technologie conduisant à un temps de cycle de processus réduit avec une qualité reproductible. Néanmoins, beaucoup reste à faire pour construire le meilleur profil de température possible, c'est pour cela qu'il est nécessaire de caractériser et de contrôler l'effet des paramètres de contrôle du procédé. L'objectif de cette étude consiste alors à l'étude des paramètres géométrique, électromagnétique et mécanique intervenant en chauffage par induction, destinée à une géométrie tridimensionnelle à l'acier 4340 avec inducteur asymétrique. Pour bien mener cette étude, le projet est structuré en trois grandes parties combinant la simulation, la planification d'expérience, l'analyse statistique et l'optimisation pour la création d'un modèle prédictif du profil de température. À partir des équations de Maxwell pour l'électromagnétisme et les équations de transfert de chaleur, les phénomènes physiques ont été modélisés en éclairant les lois du comportement mécanique des matériaux et en établissant la densité de courant externe. Le problème a été entamé par la méthode des éléments finis avec un modèle en 3D et réalisé dans le logiciel COMSOL. Plusieurs simulations, et des mesures de profil de température ont été effectués pour chaque partie du modèle et permettent de confirmer avec succès les hypothèses du modèle et de vérifier la qualité des résultats de la simulation. Les conclusions de ce travail ont pointé l'aspect rentable des techniques utilisées et ont donné accès à l'industrie pour des recettes simples et fiables consacrées à la conception des profils de température uniformes et plus optimisés et qui rendent possible la production des composantes mécaniques de haute performance.

Mots clés : Traitement thermique par induction, Acier 4340, Plaque, Simulation, Profil de température, Taguchi, ANOVA, Prédiction.

ABSTRACT

Induction heat treatment is an important technology in the manufacturing industry. With its wide range of applications ranging from heating to fusion, brazing to welding, and cap sealing to gluing, this is often the key to adding value to a particular process in industry. This is achieved by the fact that induction heating provides a higher heating rate than any other commercial heating method available. Due to the rapid heating and good reproducibility, it is commonly used to heat conductive materials to the exact temperature. The ability to generate heat at depth in combination with high heat intensity quickly and in well-defined regions on the part is a very attractive feature of this technology leading to reduced process cycle time with reproducible quality. However, much remains to be done to build the best possible temperature profile, which is why it is necessary to characterize and monitor the effect of the process control parameters. The objective of this study is then to study the geometric, electromagnetic and mechanical parameters involved in induction heating, intended for a three-dimensional geometry in 4340 steel with asymmetric inductor. To properly conduct this study, the project is structured in three main parts combining simulation, experiment planning, statistical analysis and optimization to create a predictive model of the temperature profile. From Maxwell's equations for electromagnetism and heat transfer equations, physical phenomena have been modeled by illuminating the laws of mechanical behavior of materials and by establishing the external current density. The problem was started by the finite element method with a model in 3D and carried out in the software COMSOL. Several simulations, and temperature profile measurements were performed for each part of the model and allow to successfully confirm the model assumptions and to check the quality of the simulation results. The conclusions of this work pointed out the cost-effective aspect of the techniques used and gave access to the industry for simple and reliable recipes devoted to the design of uniform and more optimized temperature profiles and which make possible the production of mechanical components of high performance.

Keywords: Induction heat treatment, 4340 steel, Plate, Simulation, Temperature profile, Taguchi, ANOVA, Prediction

TABLE DES MATIÈRES

REMERCIEMENTS v

RÉSUMÉ vi

ABSTRACT vii

TABLE DES MATIÈRES viii

LISTE DES TABLEAUX x

LISTE DES FIGURES xi

INTRODUCTION GÉNÉRALE 1

0.1 MISE EN CONTEXTE 1

0.2 PROBLEMATIQUE 3

0.3 OBJECTIFS 6

0.4 METHODOLOGIE 7

0.5 ORGANISATION DU MÉMOIRE 9

CHAPITRE 1 LE CHAUFFAGE PAR INDUCTION À L'ÈRE DE L'INDUSTRIE 4.0 : UNE REVUE DE LA LITTÉRATURE 11

1.1 RÉSUMÉ EN FRANÇAIS DU PREMIER ARTICLE 11

1.2 INDUCTION HEATING IN THE ERA OF INDUSTRY 4.0: A LITERATURE REVIEW 12

1.2.1 Abstract 12
1.2.2 Introduction 12
1.2.3 History of induction 13
1.2.4 Induction heat treatment 14
1.2.5 Process simulation 25
1.2.6 Complex geometry 44
1.2.7 Challenges and future direction 55
1.2.8 Conclusion 60

CHAPITRE 2 MODELISATION ET SIMULATION DU PROCESSUS DE CHAUFFAGE PAR INDUCTION APPLIQUE SUR UNE PLAQUE EN ACIER 4340 62

2.1 RÉSUMÉ EN FRANÇAIS DU DEUXIÈME ARTICLE 62

2.2 MODELING AND SIMULATION OF THE INDUCTION HEATING PROCESS APPLIED TO A 4340 STEEL PLATE 64

2.2.1 Abstract 64
2.2.2 Introduction 64
2.2.3 Method and material 69
2.2.4 Simulation 77
2.2.5 Results analysis 81
2.2.6 Discussion 84
2.2.7 Conclusion 85

CHAPITRE 3 ÉTUDE DU PROFIL DE TEMPERATURE D'UNE PLAQUE EN ACIER 4340 TRAITE PAR INDUCTION EN FONCTION DES PARAMÈTRES MACHINES ET FACTEURS GÉOMÉTRIQUES 87

3.1 RÉSUMÉ EN FRANÇAIS DU DEUXIÈME ARTICLE 87

3.1 *STUDY OF THE TEMPERATURE PROFILE OF A 4340 STEEL PLATE TREATED BY INDUCTION DEPENDING ON MACHINE PARAMETERS AND GEOMETRIC FACTORS* 88

3.1.1 Abstract 88
3.1.2 Introduction 89
3.1.3 *Experimental design* 91
3.1.4 Effects of the parameters on temperature 94
3.1.5 Conclusion 109

CONCLUSION GÉNÉRALE 110

Réference bibliographique 115

LISTE DES TABLEAUX

Table 2.2-1: Geometric parameters of the inductor (mm) 71
Table 2.2-2 : Chemical composition of standard 4340 steel (%) 72
Tableau 2.2-3 : Material properties 76
Table 2.2-4 : Input simulation parameters 80
Table 2.2-5 : Proportion of the treated area 83
Table 3.1-1 : Input parameters and their level 91
Table 3.1-2 : Taguchi design of experiment 92
Table 3.1-3 : Simulations results 93
Table 3.1-4 : Analyze of variance for the temperatures at 1.25s 95
Table 3.1-5 : Analyze of variance for the temperatures at 2.5s 96
Table 3.1-6 : Model summary at 1.25s of heating time 99
Table 3.1-7 : Model summary at 2.5s of heating time 99

LISTE DES FIGURES

Figure 1.1.1 : Principaux éléments d'un système de chauffage par induction 2

Figure 1.1.2 Une gamme d'une variété pratiquement infinie de géométries d'inducteurs de chauffage 3

Figure 1.2.1: Principle of induction heat treatment, from Yuan and coll 2003 15

Figure 1.2.2 : Skin depth 16

Figure 1.2.3 : Induction heating model with a flux concentrator 17

Figure 1.2.4 : Temperature as a function of the hardened depth with the depth of hardening remaining at the surface in high frequency 19

Figure 1.2.5 : Temperature as a function of hardened depth for low frequency treatment 20

Figure 1.2.6 : Induction hardening of a gear by rotation relative to the inductor 21

Figure 1.2.7 : Sweep heating mode 22

Figure 1.2.8 : Progressive heating mode 23

Figure 1.2.9 : Power and frequency ranges of generators 24

Figure 1.2.10 : Section Distortion 31

Figure 1.2.11 : The Optimal S/N Results for Each Factor Analyzed Separately by Minitab Software 34

Figure 1.2.12 : Distribution of residual stresses in three directions calculated on the basis of d0 measured by ND for the surface and the d0ecore obtained by XRD for the core material 35

Figure 1.2.13 : Temperature distribution T (x, t) in the room domain at different times with uniform contours 37

Figure 1.2.14 : Calculation model before optimization 38

Figure 1.2.15 : Inductors after optimization at position x 38

Figure 1.2.16 : Inductors after optimization at position y 39

Figure 1.2.17 : Average temperature in the heated part with and without concentrator 42

Figure 1.2.18 : Experimental Validation of Predicted and Measured Hardness for, Edge(a) and Middle(b) 42

Figure 1.2.19 : Schematic presentation of the model geometry 43

Figure 1.2.20 : Sequential heating cycle 45

Figure 1.2.21 : Simultaneous heating cycle 45

Figure 1.2.22 : Gear hardness profiles obtained by induction 46

Figure 1.2.23 : Superposition of the etched microstructure with isotherms at 927, 816 and 704 °C (white lines, top to bottom). The dotted lines correspond to the profiles shown in the figure on the right 49

Figure 1.2.24 : Check the input u (t) as well as the trajectories of Tmax (t), Tavg (t) and Tmin (t) in Ωw for the surface hardening process 51

Figure 1.2.25 : the first quarter of the 2D section of the finite element model of the proposed coil with concentrator 53

Figure 1.2.26 : Interpolated microhardness maps for gears (treatments B and C) and corresponding profiles along roots and tips 54

Figure 1.2.27 : Typical Induction Hardness Curve 56

Figure 2.2.1 : Schematic representation of the induction heating process 66

Figure 2.2.2 : Geometric parameters of the inductor 71

Figure 2.2.3 : The dimensions of the 4340 steel plate 72

Figure 2.2.4 : Electrical conductivity of the AISI 4340 Steel 73

Figure 2.2.5 : Magnetic permeability of the AISI 4340 Steel 74

Figure 2.2.6 : Specific heat of the AISI 4340 Steel as a function of temperature 75

Figure 2.2.7 : Thermal conductivity of the AISI 4340 Steel as a function of temperature 75

Figure 2.2.8 : Final temperature versus the mesh size 78

Figure 2.2.9 : Arrangement of the plate vis-à-vis the inductor with the used mesh 79

Figure 2.2.10 : Characterization of gaps and the heating zone.....80

Figure 2.2.11 : Temperature profil.....82

Figure 2.2.12 : Point graph of the temperature distribution.....84

Figure 3.1.1 : The 4340 steel plate.....92

Figure 3.1.2 : Experimental data vs Predicted value for the temperatures at 1.25s.....100

Figure 3.1.3 : Experimental data vs Predicted value for the temperatures at 2.5s.....101

Figure 3.1.4 : Effects plot for the four temperatures ($T1, T2, T3, T4$) at 1.25s 103

Figure 3.1.5 : Effects plot for the four temperatures ($T1 - 2.5s, T2 - 2.5s, T3 - 2.5s, T4 - 2.5s$) at 2.5s.....104

Figure 3.1.6 : Response surface method plot for T1.....105

Figure 3.1.7 : Response surface method plot for $T2$.....105

Figure 3.1.8 : Response surface method plot for $T3$.....106

Figure 3.1.9 : Response surface method plot for $T4$.....106

Figure 3.1.10 : Response surface method plot for $T1 - 2.5s$.....107

Figure 3.1.11 : Response surface method plot for $T2 - 2.5s$.....107

Figure 3.1.12 : Response surface method plot for $T3 - 2.5s$.....108

Figure 3.1.13 : Response surface method plot for $T4 - 2.5s$.....108

INTRODUCTION GÉNÉRALE

0.1 MISE EN CONTEXTE

Il existe de nombreuses façons de chauffer les matériaux métalliques, notamment l'utilisation des appareils de chauffage par induction, de fours à gaz, d'appareils de chauffage à infrarouge, de fours électriques et à combustible, etc. Chaque méthode a ses propres avantages et limites. Il n'y a évidemment pas de méthode universelle qui soit la meilleure dans tous les cas.

Au cours des quatre dernières décennies, le chauffage par induction électromagnétique est devenu plus populaire ([1, 2]). La capacité de génération de chaleur en profondeur en combinaison avec une intensité de chaleur élevée (si nécessaire) rapidement et dans des régions bien définies sur la pièce est une caractéristique très attrayante de cette technologie conduisant à un temps de cycle de processus réduit avec une qualité reproductible. Des intensités de chaleur hautement contrôlables qui vont de vitesses modérées à des intensités de chaleur élevées permettent la mise en œuvre de recettes/protocoles de processus optimaux.

Le chauffage par induction est utilisé dans l'industrie au cours des trois dernières décennies pour lier, durcir ou ramollir des métaux ou d'autres matériaux conducteurs. En raison du chauffage rapide et de la bonne reproductibilité, il est couramment utilisé pour chauffer des matériaux conducteurs à la température exacte. Pour de nombreux procédés de fabrication moderne, le chauffage par induction offre une combinaison attrayante de vitesse, de régularité et de contrôle. Les principes de base du chauffage par induction sont compris et appliqués à la fabrication depuis les années 1920. Ces dernières années, il y a eu un intérêt significatif pour l'expansion de l'utilisation du processus de chauffage par induction dans

différents processus de fabrication. L'une des opérations de fabrication qui nécessitent un procédé de chauffage de surface à très hautes performances est la trempe par induction.

Le durcissement par induction est largement utilisé dans l'industrie pour minimiser la distorsion du traitement thermique et obtenir des contraintes résiduelles de compression favorables pour une meilleure performance en fatigue. Le processus de chauffage lors de la trempe par induction a un effet significatif sur la qualité des pièces traitées thermiquement. La modélisation numérique du chauffage par induction permet d'optimiser les variables du procédé [3]. Dans une configuration de chauffage par induction de base illustrée à la Figure 1.1.1, une alimentation RF à semi-conducteurs envoie un courant alternatif à travers un inducteur (souvent une bobine de cuivre) et la pièce à chauffer (la pièce) est placée à l'intérieur de l'inducteur [4].

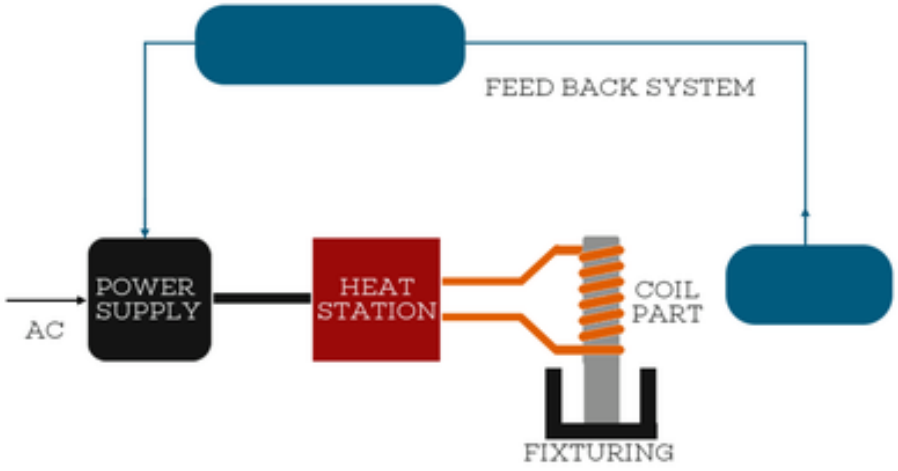

Figure 1.1.1 : Principaux éléments d'un système de chauffage par induction [4]

L'inducteur de chauffage et la bobine d'induction sont des termes utilisés de manière interchangeable pour l'appareil électrique qui fournit l'effet de chauffage dans la pièce positionnée à proximité. Un inducteur est souvent simplement appelé par les professionnels de l'induction comme une « bobine », mais sa géométrie ne ressemble pas toujours à la forme

de bobine circulaire classique. A titre d'exemple, la Figure 1.1.2 montre une gamme d'une variété pratiquement infinie de géométries d'inducteurs de chauffage nécessaires pour accueillir une variété infinie de pièces correspondantes. Un certain savoir-faire est associé à presque chaque application appliquant une géométrie de bobine/pièce différente.

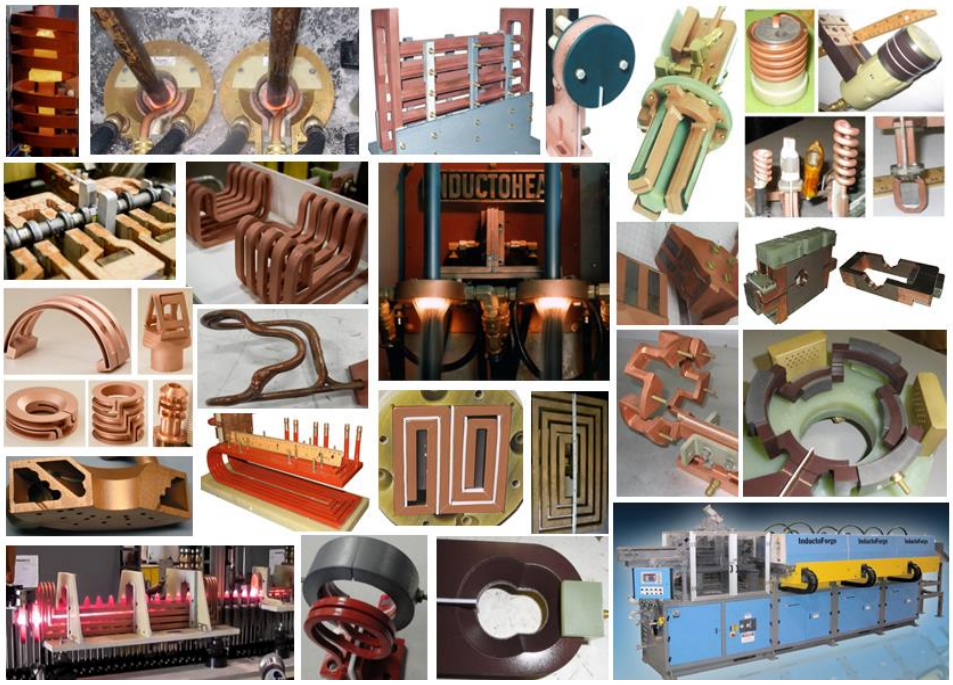

Figure 1.1.2 Une gamme d'une variété pratiquement infinie de géométries d'inducteurs de chauffage [5]

0.2 PROBLÉMATIQUE

La conception des traitements de durcissement superficiel exige la prise en compte de la nature et la forme des pièces, de l'effet du chauffage rapide sur les propriétés physiques du matériau utilisé, ainsi que les propriétés mécaniques recherchées à la suite du traitement. Le procédé de traitement thermique par induction est principalement appliqué à des nuances d'aciers faiblement alliés, et contrairement à d'autres procédés, ce type de traitement ne

modifie pas la composition du matériau. Par conséquent, un acier sélectionné pour le durcissement par induction doit avoir une teneur en carbone et un alliage suffisant pour obtenir le niveau de dureté superficielle souhaitée [6]. Les applications typiques de traitement thermique par induction incluent les aciers alliés et les aciers à moyenne et à haute teneur en carbone[7], utilisés dans des larges applications mécaniques comme les arbres de transmission, les engrenages, etc. Généralement, une teneur en carbone de 0,4% à 0,6% est nécessaire pour que le traitement par induction soit efficace [7]. En effet, le matériau étudié est l'acier AISI 4340 (AISI désigne American Iron and Steel Institute). Il possède une teneur en carbone d'environ 0.4%, il comporte des proportions assez importantes de chrome, de Nickel et de Molybdène. Il a une haute ténacité comparativement à la plupart des aciers outils. D'une autre part, les modèles de prédictions deviennent, pour les entreprises, des outils stratégiques pour le développement des meilleures recettes applicables dans leurs procédés à l'échelle industrielle. Par ailleurs, le développement des modèles de prédiction fiables et précis exige la connaissance du comportement thermo-électromagnétique des propriétés intrinsèques du matériau, ce qui nécessite de mener une large compagne d'essais de simulations et d'expérimentations pour comprendre le comportement du matériau face au procédé du traitement. L'obtention des microstructures entièrement martensitiques connues pour leur bonne résistance à l'usure et une bonne ténacité après le traitement de trempe a fait de cet acier un choix incontournable comparativement à d'autres aciers, qui contiennent plus de carbone et d'éléments d'alliage plus coûteux [8]. Il possède une excellente trempabilité à l'air. Cet acier présente une haute résistance et une bonne ductilité. De plus, il est immunisé contre la fragilisation et il peut être utilisé dans une variété d'applications, y compris les avions commerciaux et militaires, les systèmes automobiles et les systèmes hydrauliques forgés [9].

Dans le durcissement par induction, où les surfaces de pièces telles que les engrenages et les disques sont chauffées à haute température avec un refroidissement rapide, une contrainte résiduelle de compression pourrait être conçue par la génération de températures élevées et de gradients de propriétés microstructurales et mécaniques entre la couche de surface et le cœur du composant [10, 11]. Le passage de l'austénite en martensite après trempe

s'accompagne d'une augmentation de dureté et de volume proportionnelle au pourcentage de carbone contenu dans le matériau traité [12]. Cette dilatation thermique due au gradient de température et au changement de phase produit un état bénéfique de contrainte résiduelle de compression qui peut être prédit et/ou contrôlé en fonction de plusieurs facteurs impliqués dans le processus de chauffage par induction [13], tels que la vitesse de refroidissement [14] et la distribution finale de la température avant trempe [15, 16]. De plus, la résistance à la fatigue est proportionnelle à l'épaisseur de la couche superficielle durcie et change en fonction de la répartition de la dureté [17]. En effet, la région durcie est directement liée à la composition de la microstructure qui pourrait être interprétée à partir de la distribution de température finale du processus de chauffage [18]. La mesure de la distribution de la température pendant le processus de chauffage par induction est une tâche difficile à réaliser en raison de la vitesse de chauffage très rapide du processus d'induction [19] . Certains chercheurs ont développé des méthodes expérimentales et statistiques pour mesurer le profil de température de surface à la fin du chauffage par induction [20].

L'analyse numérique ou simplement la simulation sont des applications d'ingénierie de méthodes scientifiques extraites de la physique, des mathématiques, de la chimie et de la technologie informatique. Des processus comme le chauffage par induction peuvent sembler simples au premier abord, mais combinés à un champ électromagnétique, ils peuvent devenir très complexes. L'objectif lors de la simulation de certains éléments et de leur environnement est de simplifier les formes et les volumes autant que possible. Cela rend la tâche plus réalisable. Par exemple, s'il existe une symétrie axiale, l'analyse 2D peut être facilement utilisée. Il prend moins de temps en raison de sa configuration rapide et de son temps de calcul, qui est souvent de quelques secondes. D'autre part, l'analyse 3D nécessite plus de temps et de ressources qui lui sont dédiées. Les solutions sont complexes et les atteindre n'est pas une tâche facile.

Toutefois, la synthèse de la recherche bibliographique montre qu'il n'y a aucun des ouvrages qui a touché la géométrie tels que la plaque rectangulaire, et aucune étude n’a été réalisée concernant la modélisation 3D d’un inducteur asymétrique. Cependant, les travaux publiés

manquent de précision dans les modèles, et n'abordent pas clairement les effets de paramètres tels que la puissance, la vitesse et le facteur géométrique de la pièce et de l'inducteur sur le profil de dureté et sur les contraintes résiduelles. Les modèles FEM développés sont très utiles pour prédire avec précision le comportement réel de la distribution de température [21], et aident a éviter les longues compagnes d'essais couteuses et fructueuses. Par conséquent, il serait très intéressant de développer un modèle basé sur la simulation FEM pour étudier la sensibilité du profil de dureté d'une plaque mince en acier 4340 en fonction des paramètres du procédé et des facteurs géométriques.

0.3 OBJECTIFS

Le projet de recherche vise le développement de modèles de prédiction du profil de dureté de la plaque en acier 4340 en fonction des paramètres du procédé du durcissement par induction. En s'appuyant sur des modèles de simulation par éléments finis avec validation statistique. Le premier objectif spécifique de ce projet est de réaliser une revue de la littérature global, il s'agit d'une revue qui regroupe la majorité des travaux faits en chauffage par induction en détaillants l'origine et le principe incluant les différents éléments de base du traitement par induction. Ainsi de chercher et de traiter les points d'intersection entre les deux domaines, le chauffage par induction et l'industrie 4.0 pour exploiter les méthodes et les moyens de cette dernière dans le but d'améliorer le processus et d'ouvrir la discussion pour des travaux futurs. Le deuxième objectif consiste à réaliser un modèle numérique de chauffage par induction, qui commence par la conception du modèle complexe de l'inducteur 3D en forme de U suivi par la réalisation du volume de la plaque en utilisant le logiciel COMSOL Multiphysics. Ce modèle a pour but de simuler la chauffe par induction d'une plaque en acier 4340 et d'étudier les différentes affinités et l'influence des paramètres machines et géométriques sur l'évolution de la température à la fin de la chauffe. Une première caractérisation des paramètres les plus importants du procédé sera établie à partir des travaux de recherches précédents. Le modèle doit considérer la nature multi-physique du procédé, ainsi que le comportement non linéaire des propriétés du matériau en fonction de la température et du champ magnétique. Le troisième objectif vise à étudier les effets des

paramètres machines et géométriques, les paramètres seront les mêmes que ceux du deuxième travail, mais avec trois niveaux de valeurs. L'objectif sera de déterminer les interactions entre les paramètres, en se basant sur des analyses statistiques dans les zones d'intérêt afin de contrôler la distribution de la température sur la pièce au milieu et à la fin du temps de chauffe. Les résultats de l'analyse statistique seront nécessaires pour établir des modèles de prédiction robustes et fiables.

- Plus spécifiquement, le projet permet de : Mener une étude bibliographique du traitement thermique par induction pour les géométries simples et complexes ainsi qu'une revue des méthodes de l'industrie 4.0 appliquées dans le domaine de chauffage par induction.

- Modéliser et simuler le procédé de chauffage par induction appliqué à une plaque en acier 4340 traitée par un inducteur a géométrie complexe asymétrique en utilisant un modèle de simulation d'éléments finis en fonction des paramètres machines et facteurs géométriques.

- Analyser statistiquement les paramètres machines et géométriques pour déterminer les effets de chaque facteurs sur le profil de température, et développer des modèles prédictifs par la méthode d'analyse de la variance.

0.4 MÉTHODOLOGIE

L'installation du système de chauffage par induction n'est pas une simple tâche. La majeure partie du temps, les inducteurs sont dimensionnés de façon empirique. Sur la base d'expérience acquise par une succession d'essais-erreurs, il est de même pour le profil de puissance nécessaire pour le traitement souhaité. Ces essais sont cependant longs et coûteux, d'où la nécessité d'employer la simulation numérique pour comprendre des phénomènes physiques en se basant sur le couplage électromagnétique et thermique. Dans un premier lieu, il est nécessaire de faire une revue de la littérature pour bien documenter le projet et pour

bien situer la problématique. En deuxième lieu, les équations gouvernantes seront discrétisées par la méthode des éléments finis et la simulation se fera sur le logiciel multi-physique COMSOL sur un modèle en 3D. Dans ce sens, il est primordial d'établir un modèle multi-physique détaillé qui permet le couplage des effets magnétiques et thermiques. Les équations de Maxwell pour l'électromagnétisme mises en jeu devront être bien formuler autant que pour les équations de transfert de chaleur, de façons à bien repérer les paramètres de contrôle du procédé pour déterminer mathématiquement la physique du chauffage par induction, appliqué sur une pièce de géométrie simple. Toutes les simulations seront menées avec des études de convergence qui vont permettre d'avoir un bon ratio entre la précision des résultats et le temps de calcul de la simulation. Ces efforts vont permettre de cerner le comportement magnétothermique du matériau et aidera à dimensionner le générateur de puissance en spécifiant la puissance requise et la plage de fréquence désirée pour le matériau utilisés et la géométrie à traiter. Par la suite, le modèle sera validé en utilisant une batterie d'essais, un ratio entre la puissance de simulation et celle fournie par le générateur sera déterminé pour établir le lien entre la théorie et la pratique. Un ensemble de tests préliminaires sera effectué pour étudier l'effet des paramètres sur le profil de dureté de la plaque en aciers 4340, et déterminer les paramètres les plus influentes sur les résultats du traitement. La procédure utilisée ici s'inspirera des travaux classiques et plus récents des procédés de traitement thermique par induction sur les propriétés intrinsèques et les performances mécaniques de l'acier étudié.

En troisième lieu, Des plans d'expériences et une étude statistique des interactions entre les paramètres les plus influentes déterminées dans l'étape précédentes sera conduite dans le but de valider les résultats de la simulation numérique, L'ensemble des données d'apprentissage est tiré d'une suite de simulation effectuée sur le logiciel de simulation COMSOL Multiphysics avec les niveaux de paramètres et les nombres d'essais qui sont déterminés par la méthode de Taguchi, puisque l'objectif est d'atteindre le maximum de résultats avec un minimum d'essais vu la complexité du modèle. Cela va permettre d'optimiser le traitement et d'établir une recette complète des variables influentes sur le processus du chauffage par induction. Les variables ayant un potentiel d'effet important sur les résultats seront

considérées et contrôlées dans la dernière phase qui se finalise par la réalisation d'un modèle de prédiction efficace et flexible décrivant le comportement thermomécanique de notre plaque en fonction des variables d'entrées.

L'ensemble des travaux de simulation numérique sont réalisés avec le logiciel de simulation COMSOL Multiphysics. Comme son nom l'indique ce logiciel permet de simuler plusieurs phénomènes physiques et applications en ingénierie, et comme il supporte tous les phénomènes couplés de même que le cas des traitement thermiques par induction. Les analyses statistiques sont effectuées avec le logiciel MINITAB, et les figures utilisées sont dessinées avec des scripts dans l'environnement MATLAB.

Chaque étude finit par la rédaction d'un rapport sous forme d'article. Le mémoire suivant regroupe les trois articles élaborés pendant les études de maîtrise.

0.5 ORGANISATION DU MÉMOIRE

Le premier chapitre du mémoire consiste à mieux comprendre le processus du chauffage par induction. Ce chapitre présente une perspective générale sur le chauffage par induction, les méthodes existantes dans le procédé, les travaux et recherches antécédents réalisés dans ce domaine par les différents chercheurs et scientifiques et les résultats trouvés par ces derniers. L'étude apparaîtra sous forme d'une revue de littérature permettant une meilleure compréhension du sujet et des défaillances rencontrées dans des travaux antérieurs. Elle nous présente aussi une ouverture pour l'implémentation de l'industrie 4.0 dans le domaine de chauffage par induction.

Le second chapitre présente une modélisation et simulation numérique 3D asymétrique d'une plaque a géométrie simple en acier 4340 chauffée par un inducteur a géométrie complexe. À cet effet, le deuxième chapitre se focalise sur la présentation de toutes les équations qui régissent le procédé de traitement par induction ainsi que la validation du modèle et la

caractérisation des paramètres machine et facteurs géométriques qui influent la distribution de la température sur la pièce.

Le troisième chapitre est consacré à l'amélioration des résultats trouvés dans le travail précèdent. Dans ce sens ce chapitre présente une analyse des effets et des interactions des paramètres caractérisant le procédé de traitement thermique par induction sur la distribution de la température. Des modèles prédictifs sont développés par la méthode d'analyse de la variance.

Finalement, la conclusion générale, cette dernière partie du mémoire constitue une synthèse des résultats obtenus dans le cadre de ce projet en lien avec les objectifs énoncés. Ainsi qu'une ouverture sur d'autres pistes qui peuvent encore être explorées pour d'autres travaux de recherche.

CHAPITRE 1
LE CHAUFFAGE PAR INDUCTION À L'ÈRE DE L'INDUSTRIE 4.0 : UNE REVUE DE LA LITTÉRATURE

R.Houtane[1], N.Barka[1] , S.K.Kanganroudi[1] , L.Benabbou[1]

University of Quebec at Rimouski, Rimouski (Qc), Canada

1.1 RÉSUMÉ EN FRANÇAIS DU PREMIER ARTICLE

La revue de littérature est une étape essentielle afin de bien situer l'état de l'art de la recherche et de présenter le procédé de traitement thermique par induction dans son ensemble avant de détailler les avancées technologiques. De plus, dans cette revue, une attention particulière est portée aux aspects théoriques et aux différents modèles développés par simulation. Cet article propose un bref historique présentant les bases de l'induction électromagnétique depuis sa découverte par le chercheur britannique Michael Faraday. Ensuite, il met l'accent sur les efforts des simulations numérique et empirique du procédé de traitement thermique par induction appliqué à des géométries simples avant de présenter des travaux de recherche portant sur des géométries complexes dont les engrenages. La dernière partie fournit une synthèse détaillée à la suite de la revue de littérature pour mieux exposer l'état d'avancement de la recherche dans le domaine de l'induction et les enjeux du procédé, pour mieux situer les apports des stratégies de l'industrie 4.0 dans le domaine du chauffage par induction.

Mots clés - Chauffage par induction, Durcissement superficiel, Simulation, Industrie 4.0

Cet article, intitulé « *Induction heating in the era of industry 4.0 : A literature review* », fut essentiellement rédigé par moi-même ainsi que le professeur Noureddine Barka. En tant que premier auteur ma contribution à ce travail fut la recherche sur l'état de l'art, et la réalisation

des travaux nécessaires pour cette revue de littérature. Le professeur Noureddine Barka a fourni l'idée originale. Les professeurs Sasan Sattarpanah et Loubna benabbou ont contribué au développement de la méthode ainsi qu'à l'amélioration de la rédaction pour la version finale.

1.2 INDUCTION HEATING IN THE ERA OF INDUSTRY 4.0: A LITERATURE REVIEW

1.2.1 Abstract

The literature review is an essential step in order to properly situate the state of the art of research and to present the induction heat treatment process as a whole before detailing the technological advancements. In addition, in this review, special attention is paid to theoretical aspects and to the different models developed by simulation. This paper offers a brief history presenting the basics of electromagnetic induction since its discovery by the British scholar Michael Faraday. Then, it emphasizes numerical and empirical simulation efforts of the induction heat treatment process applied to simple geometries before presenting research works dealing with complex geometries including gears. The last part provides a detailed summary following the literature review to better expose the state of progress of research in the field of induction and the challenges facing the process, to better situate the contributions of the industry 4.0 strategies in the field of induction heating.

Keywords Induction heating, Surface hardening, Simulation, Industry 4.0

1.2.2 Introduction

Today's aerospace and automotive industries use surface hardening (heat treatment) processes to improve the mechanical strength, fatigue performance and wear resistance of their mechanical components such as gears, splines, drive shafts, cams, etc. It is more advantageous for these components to be surface heat treatmented versus deep (mass) heat treatment. The main objective of these treatments is to produce a surface layer with

characteristics that significantly improve friction and wear resistance while increasing mechanical fatigue and contact resistance [22]. The industrial surface heat treatment processes currently in use are the electromagnetic induction heat treatment process and thermochemical processes. Thanks to its many industrial advantages, induction heat treatment represents a very promising process due to its strong potential application in manufacturing production lines. To understand the industrial context, it is necessary to present this process with emphasis on its specificities and intrinsic characteristics.

A literature review is an essential step in order to situate the state of the art of research and to present the induction heat treatment process in its entirety before detailing the technological advances. Moreover, in this review, particular attention is paid to theoretical aspects and to the various models developed by simulation. Firstly, we will look at the history presenting basic notions on electromagnetic induction since its discovery by the British scientist Michael Faraday. Then, it will focus on the industrial aspects related to the induction heat treatment process and shed light on the technical difficulties encountered during the development phases of new components. He presents the numerical and empirical simulation efforts of the induction heat treatment process applied to simple geometries before presenting research work on complex geometries including gears.

1.2.3 History of induction

Historically, the first discovery of electromagnetic induction dates back to the British scientist Michael Faraday around the year 1831 [23]. This discovery constitutes the core and the basis of all scientific research in the field of electromagnetics. A few years later, in 1851, the French scientist Léon Foucault discovered the induced currents caused by the magnetic field in a metal part (Courants de Foucault) and demonstrated that these currents are responsible for heating by the Joule effect [24]. Then, the German physicist Heinrich Lenz formulated the law that states that the polarity of an electromotive force tends to produce a current that creates a magnetic flux opposing it to the imposed magnetic flux [1].

The first industrial applications of the magnetic induction phenomenon were devoted to the development of transformers and electrical machines. The efficiency of these machines has always been subject to losses in the form of heat that electrical engineering researchers have always tried to minimize. As for metallurgists and mechanical researchers, they have demonstrated over the years that these losses constituted a new avenue for thermally heating mechanical parts. In 1930, the advent of medium-frequency power generators made it possible to use the induction heat treatment process for the first time to heat treat shafts and bearing seats. In 1941, engineers from Caterpillar, a company specializing in heavy machinery, succeeded in setting up the first experimental set-up to treat gears using a 500 kW power generator operating at a medium frequency of about 10 kHz [1]. Since then, the technology has made significant advances in induction machines. Indeed, new power generators make it possible to generate very high frequencies and to modulate several frequencies in the same inductor to heat parts. The new induction machines being introduced are CNC programmable machines with high dimensional accuracy and good power setpoint repeatability that can be easily integrated into automated manufacturing cells [1, 25, 26].

1.2.4 Induction heat treatment

1.2.4.1 Principle of the process

Figure 1.2.1 illustrates the basic principle of the induction heat treatment process. The application of an alternating current (AC) across the inductor at a specific frequency creates a variable electromagnetic field, which generates and concentrates induced currents in the workpiece. Under the Joule effect, these currents heat a specific zone whose depth is controlled by the treatment frequency, the power applied and the heating time. A typical process cycle involves local heating of the component to be treated above a certain critical temperature of the workpiece material. The part is then rapidly cooled to achieve the desired hardness profile. Induction heat treatment can be used in a variety of industrial applications such as surface heat treatment, brazing, hot working of materials and molding processes.

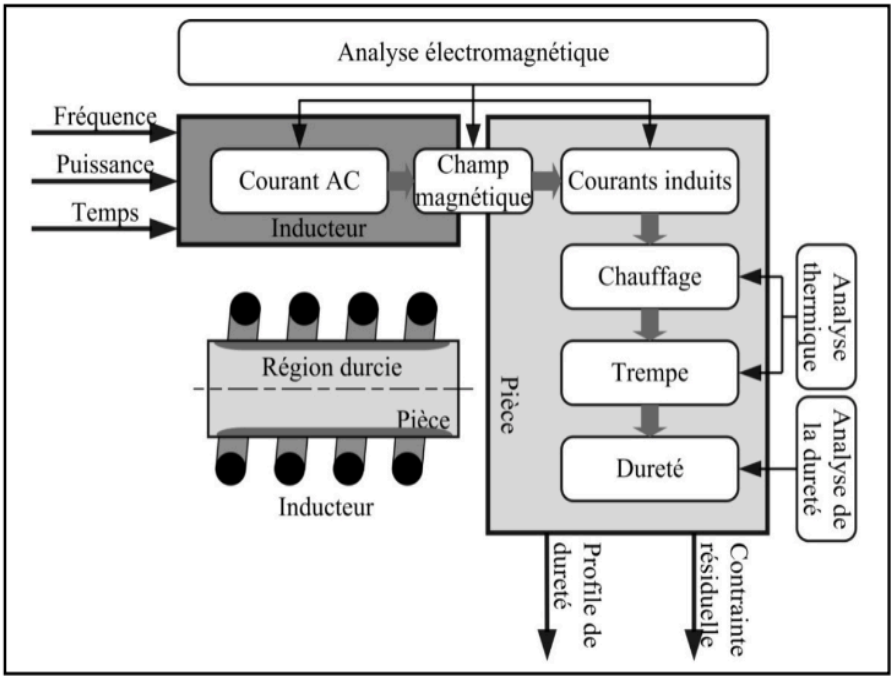

Figure 1.2.1: Principle of induction heat treatment, from Yuan and coll 2003 [27].

1.2.4.2 Electromagnetic effects

It is important to introduce some effects that greatly affect the behavior of the induction heat treatment process before listing the types and modes of treatment frequently used. Induction heat treatment is governed by the electromagnetic skin effect. In fact, a reminder of the basic notions of electricity shows that when a direct current (DC) passes through a conducting wire, its distribution is uniform throughout the section. However, when an alternating current (AC) flows in the same conductor, the distribution is not uniform. Indeed, the maximum value of the current is observed at the surface, while the value of the current in the core of the part is zero. This phenomenon is called the electromagnetic skin effect, which occurs in the case of medium and high frequency alternating current. This effect has a considerable impact on the final temperature distribution in an induction-treated room, since it is responsible for the concentration of eddy currents at the surface [28-30].

The electromagnetic skin effect is characterized by the depth of penetration, called skin depth. This depth is calculated using equation (3.1) and is expressed as a function of the processing frequency and the electromagnetic properties of the material (relative magnetic permeability and electrical conductivity). In practice, the layer having as its depth concentrates 63% of the density of the induced currents and 86% of the electromagnetic power transmitted to the part as shown in figure 1.2.2. This power is then converted into heat under the Joule effect. The properties of the material are considered constant as a function of the temperature in the room.

$$\delta = \frac{1}{\sqrt{\pi . \mu_r . \mu_0 . \sigma . f}}$$

where, μr is the relative magnetic permeability, μ0 is the magnetic permeability of vacuum, σ is the electrical conductivity and f is the processing frequency.

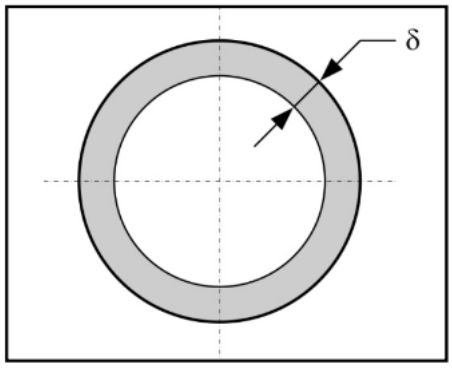

Figure 1.2.2 : Skin depth

The electromagnetic edge effect greatly affects the induction heat treatment process. Indeed, the magnetic fields at the edge of the inductor are greater and consequently the induced currents are more concentrated in these regions than in the middle of the parts treated in the

presence of the high frequency. The magnetic fields are thus responsible for the non-uniform heating of the mechanical parts. Thus, if the width of the inductor is greater than the width of the workpiece, the hardness profile is deeper at the edges of the parts compared to the mid-plane. The hardness profile obtained is greatly affected by these electromagnetic effects and mainly in the case of high-frequency heating [28]. The design of the inductor also plays a very important role on the distribution of induced currents in the inductor and in the treated part and on the temperature distribution in the part which has a direct impact on the hardness profile obtained.

To overcome this problem of electromagnetic edge effect, the authors use flux concentrators, a technique used nowadays to control the dispersion of electromagnetic fields. The use of these concentrators allows to concentrate the electromagnetic fields on specific regions of the workpiece, and to prevent the electromagnetic flux from diverging and developing in undesired areas. This technique allows to increase the efficacity of the process treatment and to obtain more uniform temperature profiles between the edge and the middle of the room. The shape of these concentrators is also dependent on the shape and geometry of the treated part as shown in Figure 1.2.3 [31].

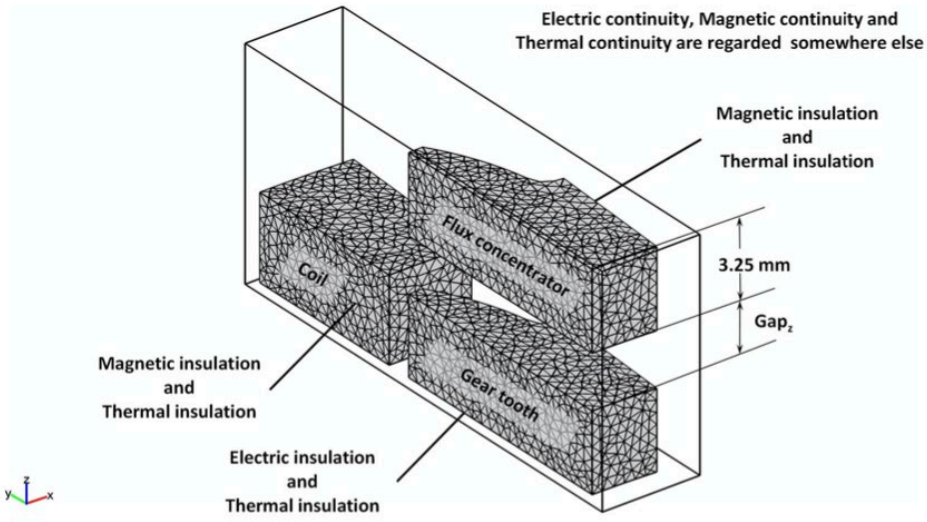

Figure 1.2.3 : Induction heating model with a flux concentrator [31].

1.2.4.3 Types of induction treatment

The induction heat treatment process can be advantageously used to perform treatments such as induction hardening, tempering and annealing. In addition, it allows for surface treatments that can be located in specific areas without having to heat the entire part. Indeed, because of its ability to concentrate heat locally in mechanical parts and the possibility of controlling the heating time and machine power, the process can be used for selective hardening, for annealing of parts and for tempering after quenching [32]. The process can heat treat materials such as steels, aluminum alloys, titanium alloys and nickel alloys. For steels, there are four categories that can be treated by the induction heat treatment process: low carbon steels, medium carbon steels, high carbon steels, and stainless steels. Medium and high carbon steels can be alloyed with alloying elements or heat treated to improve their behavior and strength. Low-alloy steels are used for machine elements since they offer high strength and better behavior under mechanical stress conditions.

a) *SURFACE HARDENING*

Surface hardening is made possible by induced currents concentrated in a thin layer, usually using high-frequency power generators. As a result, thin surface areas are austenitized and are transformed into hard martensite after cooling. This type of treatment has the advantage of generating a martensitic layer on the surface at a specific depth, thus locally improving the mechanical properties without affecting the characteristics of the core of the part.

Some researchers are interested in surface hardening since it is possible to obtain sufficient repeatability of the thickness of the hardened layer on the part as well as a desirable or even prescribed hardened layer profile, ensuring sufficient hardness and favorable distribution of residual stresses in the hardened layer all this taking into account the interdependence between the heating parameters, i.e. power density and generator frequency (high frequency),

as a function of the specified depth of the hardened layer and the heating time required for better surface hardening control [33].

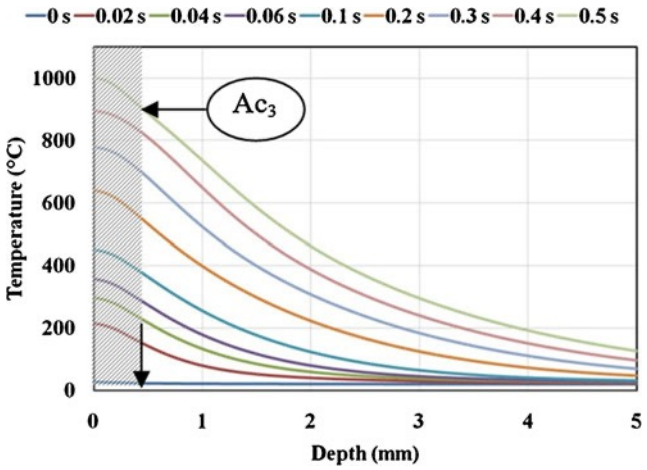

Figure 1.2.4 : Temperature as a function of the hardened depth with the depth of hardening remaining at the surface in high frequency [34]

b) *THROUGH-HARDENING*

Through-heart hardening produces a martensitic structure through the workpiece. Low- or medium-frequency generators are more suitable for this type of application and allow a depth distribution of the induced currents throughout the room. Thus, the part is completely austenitized before being rapidly cooled to produce the desired martensitic structure. The hardenability of the material plays an important role in the treatment process as well as the hardening conditions, grain size and geometry of the part. Surface hardening and through-hardening can be localized in a selective region that requires local hardening, as in the case of bearing seats, cams and gears. This type of treatment has the advantage of transforming a specific area without affecting the entire mechanical component.

It is also important to be aware that a frequency that is too low can cause the eddy currents induced by the induction coil in the part to be cancelled. This can lead to a dramatic reduction

in electrical efficiency during through-hardening of the parts, in addition to which it is necessary to heat as uniformly as possible the entire cross-section of the part to temperatures high enough to allow the formation of an austenitic structure with a sufficiently homogeneous distribution of carbon and other chemical elements (i.e. alloys and residual elements) [35].

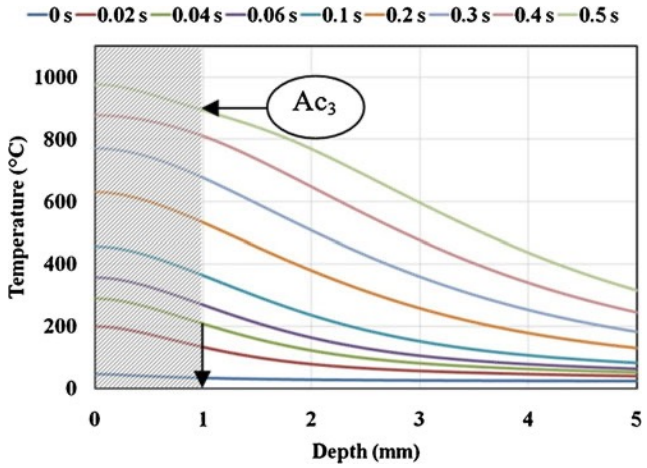

Figure 1.2.5 : Temperature as a function of hardened depth for low frequency treatment [31]

c) *INDUCTION ANNEALING*

Induction heat treatment can also be used for annealing. This type of treatment can restore the microstructure of parts already treated by induction. In addition to being carried out for a short period of time, it allows parts that have already been treated to be reused in the development process. It consists of heating the part to a temperature close to the austenitizing temperature (Ac1) for a few seconds and then allowing it to cool in the open air. Compared to conventional treatment, the holding time must be relatively very low.

d) *INDUCTION TEMPERING*

Induction tempering is a heat treatment that is carried out for a few seconds, but by heating and holding the treated part at temperatures significantly higher than conventional tempering temperatures. This treatment improves the resistance to brittle fracture by reducing the surface hardness and the level of residual stresses.

1.2.4.4 Induction Heat Treatment Modes

There are also four induction hardening modes: static mode, scanning mode, progressive mode and pulse heating.

a) *STATIC HEATING MODE*

This mode represents the simplest way to heat a workpiece by induction. In this case, the workpiece is usually rotated during the treatment without any movement in the axial direction. This heating mode is effective in the case of selective hardening or localized heating of a portion of a mechanical component such as gears, bearing seats or thin rings.

Figure 1.2.6 : Induction hardening of a gear by rotation relative to the inductor [36]

b) *SCANNING HEATING MODE*

This treatment mode becomes particularly effective in the case of long parts. Consequently, the workpiece to be treated is held on a suitable support and is moved with the continuous hardening method (the workpiece is moved in a continuous motion through a number of in-line inductors during heating in relation to the inductor. Heat is generated while the part is moving until the austenitization temperature is reached along the entire length of the part. This mode of heating is affected by the length of the part and by the variations in speed, power and the amount of heat required for heating. Figure 1.2.7 illustrates the basic principle of this mode of induction heat treatment.

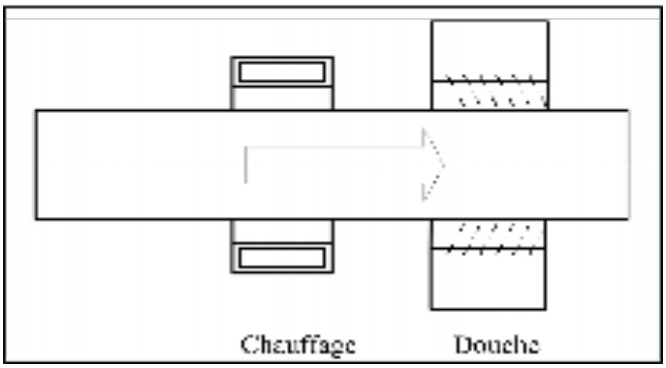

Figure 1.2.7 : Sweep heating mode [1]

c) *PROGRESSIVE HEATING MODE*

The progressive heating mode allows the processing of workpieces or bars with large lengths. In this heating mode, three phases are mandatory: preheating, intermediate heating and final heating. Since the heat is induced mainly by the skin effect, the various phases are required in this heating mode to allow the heat to penetrate into the heart of the workpiece. This means that during the initial heating the temperatures anywhere in the room are below the critical

temperature Ac2, so the maximum power density is located at the surface and decreases sharply towards the basement and the core. The generation of the heat source is localized by the thin surface layer of the room. This leads to a rapid increase in temperature at the surface with a minor change in the core. This step is characterized by a high electrical efficiency often reaching about 90%. During the intermediate phase the near-surface layer is heated above the critical temperature Ac2, at this stage the power density distribution along the radius has a unique non-exponential "non-corrugated" distribution. Finally during the final heating phase the classical exponential power density distribution will then take place, and the depth of the hardened layer has increased dramatically during the two previous stages, resulting in a deeper heating effect [37]. Figure 1.2.8 illustrates the basic principle of the progressive heating mode.

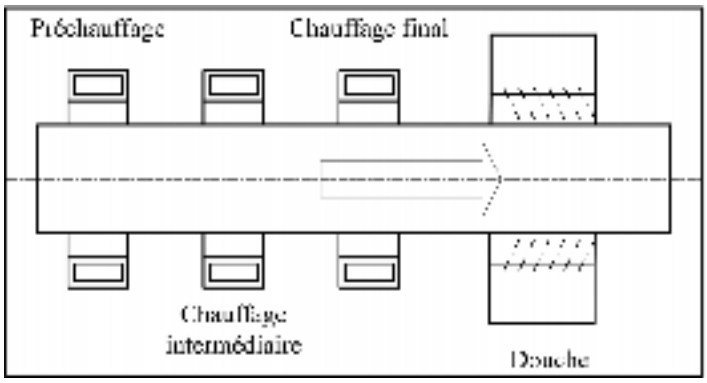

Figure 1.2.8 : Progressive heating mode [1]

d) *IMPULSE HEATING MODE*

Pulse heating mode consists of sending the machine power in the form of a series of pulses. A typical pulse hardening cycle should include on-off heating cycles until the desired results are achieved. This mode of heating is useful for hardening gears, critical components and high carbon steels, as well as cast irons with a high propensity to crack. In addition, it can be used with a combination of frequencies to perform dual-frequency heating. Indeed, for many

gear hardening applications, preheating is performed at medium frequency, while final heating is often performed at high frequency.

1.2.4.5 Power generators

Induction machines use MF and HF generators capable of delivering high power and concentrating it locally in the workpiece. As shown in Figure 1.2.9, there are three families of power generators: (1) frequency source systems (150 Hz - 540 Hz), (2) solid-state converter systems (500 Hz - 50 kHz) and (3) radio frequency (RF) systems (50 kHz - 10 MHz). Frequency source systems can provide power up to 100 MW, but they are very limited in frequency. These systems can, however, be used for mass processing of large parts. Solid-state converters offer an intermediate solution in power and frequency. These systems are generally used to process large gears and to preheat complex geometry parts such as gears or splines before heating them subsequently via a high-frequency generator. RF systems provide medium power at high frequencies and are used for contour processing of complex geometry part

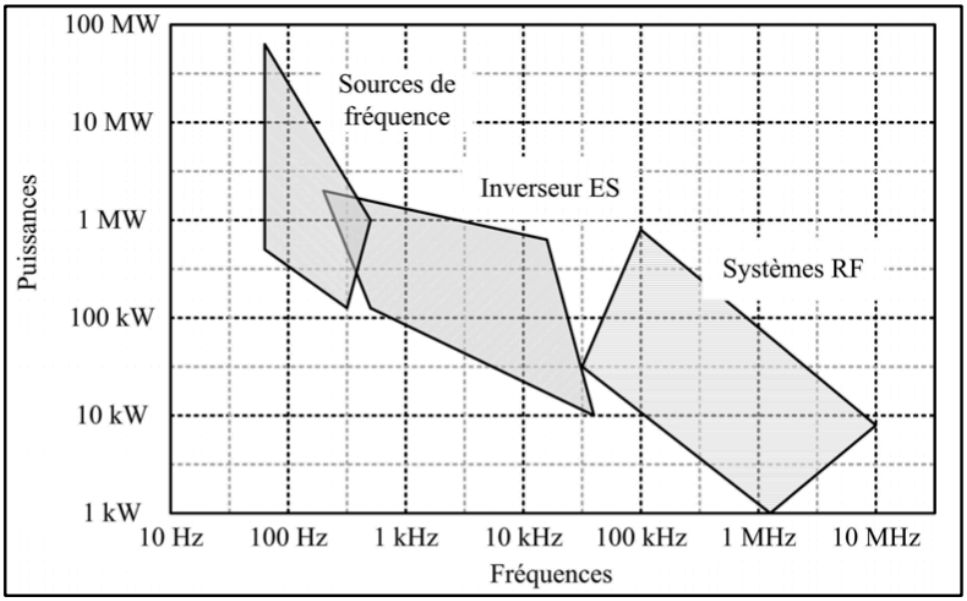

Figure 1.2.9 : Power and frequency ranges of generators [38].

1.2.5 Process simulation

The simulation of the induction heat treatment process represents a promising solution to explore the limits of the process and to help industrialists in the elaboration of practical recipes for the heat treatment of their mechanical components. Accompanied by validation tests, these models are an essential solution for mastering the induction heat treatment process. Thus, simulation allows to considerably reduce the development time and to decrease the rejection rate of parts during the development process. In this section, we present the state of progress of simulation efforts in the field of induction heat treatment over the last 50 years.

1.2.5.1 Evolution of simulation: simple geometry

The calculation of the temperature distribution for a one-dimensional problem considering induction heat treatment was first introduced by Baker [39]. Among the first relevant works in the field, Dodd and Deeds were the first to calculate analytically the electromagnetic potential vector in the case of an infinitely long cylinder subjected to a variable magnetic field and having a constant magnetic permeability [40]. The results obtained made it possible to determine the temperature distribution in a cylindrical piece of ordinary steel heated by induction by imposing a constant density of the current applied in the inductor. The work of Dodd and Deeds was taken up again in 1974 by Donea to calculate the magnetic potential vector using finite element methods in the case of simple geometry and using axisymmetric and 2D models [41].

Subsequently and as reported in their book, Davies and Simpson developed empirical models to calculate surface temperatures as a function of machine parameters for various mechanical components for specific industrial applications. The experimental tests were carried out on an experimental installation comprising a medium-frequency (20 kHz) power generator with a maximum power of about 200 kW. The models developed made it possible to calculate the surface temperature as a function of the machine power and the heating time with fairly good

accuracy [42]. Then, the effect of Curie temperature on relative magnetic permeability was partially analyzed by Masse et al. using the finite element method. These researchers considered that a steel heated above this temperature becomes diamagnetic and that its relative magnetic permeability drops drastically as a function of temperature to become unitary at high temperature [43].

The analysis of hardness profile and residual stress distribution for inductive heating followed by quenching was first introduced by Melander. The established finite element models were based on a weak coupling between the electromagnetic and thermal fields. The models developed were applied to an infinitely long cylinder and subjected to a uniform magnetic flux over its entire length. Experimental tests were also conducted on a high-frequency source (300 kHz) to validate the simulation results and the results obtained during this research showed a concordance between the simulation and the experimental results [44].

During the same year, Meunier set up 2D axisymmetric and 2D finite element models in order to calculate the magnetic potential vector at medium frequency and under different electrical conditions of voltages and currents. In its formulation, the part to be treated was considered to be decomposed into several complex electrical impedances and subjected to sinusoidal sources of voltages and currents. Overall, the models developed were validated using experimental tests carried out on a medium-frequency power source [45].

Until the late 1980s, modeling faced several technological limitations, including the computing capacity of computers. Nevertheless, the research carried out contributed to a global understanding of the process and the importance of machine parameters. Indeed, the first concrete simulation work was started in the 1990s and it allowed the Maxwell equations to be solved and coupled to the heat transfer equations using multiphysical finite element methods. In terms of experimentation, power electronics and generator technologies have also seen several advances. The new generations of induction machines are capable of delivering high frequencies and high powers and concentrating them in a room for a very short time.

In 1992, Wang et al. developed a new efficient approach using finite element methods to calculate the magnetic field, temperature distribution and stress field during induction heat treatment. The parts studied were made of a low carbon steel (AISI-1018) and the electromagnetic and thermal properties of the material were taken into account in the models developed. The 2D axisymmetric models developed used the finite element method based on weak coupling. The current density imposed in the inductor was 7x109 A.m-2 varying at a frequency of 60 Hz. The relative magnetic permeability of the material was fixed at 90 and heat losses by convection and radiation were neglected. Experimental tests validated the models developed to predict stress fields in the case of simple cylinders, square-section parts and cylindrical parts with notches (Wang, 1992). Wang et al. continued the same efforts to simulate induction heat treatment by applying it to nickel and aluminum alloy steels (AISI-2024) while comparing with the results obtained on 1080 steel. The results of the simulations allowed to establish preliminary recipes for the hardening treatment of nickel alloy steels and the precipitation treatment of aluminum 2024. The work of Wang et al. was of great importance; however, it was carried out at a very low frequency and for a very long heating time of several seconds which can be justified by the low power of the generator used for the experimental validation. In addition, the magnetic permeability was set at a constant value during heating [46].

Langeot et al. presented simulation models developed on mechanical components of simple geometries used for industrial applications. These researchers have implemented a new approach by taking into account the various interactions between electromagnetic, thermal and mechanical fields to determine phase changes and stress-strain. The coupling between the electromagnetic and thermal fields was of weak type. The results obtained were validated by experimental tests carried out on a simple geometry part made of a low alloy steel (equivalent to 4140) using a medium frequency source (15 kHz) and providing a maximum power of 40 kW. The 2D axisymmetric and 2D models developed have been useful to set up part development recipes and to optimize inductor design. In addition, they provided relevant data on induced currents and temperature distribution [47].

The models developed by Sadeghipour et al. have made it possible to predict the temperature distribution in transient conditions, to predict power density distributions and to calculate the total power consumed by the part during induction heat treatment. An axisymmetric 2D model was developed using finite element methods and based on weak coupling. This model consisted of a bushing with a carbon steel (AISI-1040) flange and an inductor in the form of a multi-wound coil. The numerical model was experimentally validated using a high frequency (150 kHz) power source. The results obtained showed that the errors between simulation and experiment were below 18% and that the surface temperature was measured using a type K thermocouple [48].

Chaboudez et al. set up a simulation based on an axisymmetric 2D model using weak coupling in order to study the temperature distributions obtained on a part of revolution with a simple stainless-steel geometry (X5CrNi 18/9). The model developed included a four-winding inductor and took into account the variation of material properties as a function of temperature. Validation tests validated the numerical simulation using a medium frequency (10 kHz) and low power (15 kW) power source. The heating time was very important (25 s). Two thermocouples placed on the surface of the part were used to measure the temperature to compare the measured temperature and the simulated one. They ruled that the discrepancies between the simulation and the experiment were mainly caused by manufacturing errors in the inductor [49].

In 1999, Enokizono et al. developed a numerical approach capable of determining surface temperatures for inductive heating applied to cylindrical parts. A 2D axisymmetric model was developed using weak coupling to solve electromagnetic and thermal fields and considering the non-linear behavior of the material. The model takes into account a non-uniform impressed current density in the inductor in the form of a solid square copper section. The material used in this study was a steel of an unspecified type. Three models were developed involving the same inductor and three cylindrical parts. In the first model, the part has the same width as the inductor while in the second model, the part is significantly wider than the inductor. In the third model, the inductor is placed close to a shoulder area. The

results obtained clearly demonstrate the electromagnetic edge effect in the case of the first model. Moreover, compared to experimental tests carried out on an 80 kHz power source, a concordance between simulation and experimentation was clearly identified for the first two models, while the third model demonstrated that it was difficult to predict surface temperatures in the shoulder region [50].

Then, in 2003, Favennec et al. were able to solve Maxwell's system of equations governing the electromagnetic field and to couple it with the heat transfer equations as well as the system of differential equations to calculate phase fractions for a 2D axisymmetric application where the workpiece was made of steel and was mobile during heating. They also attempted to optimize the induction process parameters, and the results obtained demonstrated the efficiency and robustness of the developed models based on weak coupling [51]. During the same year, Bay et al. presented an approach that allows the coupling of magnetic, thermal and mechanical fields to solve a problem of induction heat treatment applied to a part of revolution. The model developed used a weak coupling and took into account the non-linearity of the material behavior and solved the thermodynamic equilibrium equations in the treated part taking into account the thermo-elastic-plastic behavior of the material. The operating conditions were chosen according to the existing generators, i.e. frequency of the order of 500 Hz, the imposed current density was of the order of 8x108 A.m-2 and a very long heating time of 50 s [52].

Yuan et al. used the finite element method to build axisymmetric 2D models on Ansys commercial software using weak coupling to model the heating process applied to wheel supports made of carbon steel (AISI-1070) for the automotive industry. During the resolution steps, the researchers took into account the non-linear behavior of the material properties and used the temperature distribution during heating and the cooling curves to predict the hardness by estimating the phase fraction of the martensite. The frequency was of the order of 9.6 kHz, the initial current density was 1.26x107 A/m2 and a relatively long heating time of 7 s. A careful study allowed to identify the effects of the impressed current density, the frequency and the distance between the inductor and the workpiece on the hardened depth.

The results obtained made it possible to determine relationships between the hardness distribution and the final temperature distribution [27].

In 2003, Fireteanu and Tudorache advanced a numerical approach capable of evaluating the thermal field generated by constant flux induction heating on ordinary steel plates and long bars. The 2D models developed took into account the non-linearity of the magnetic field, the non-linear behavior of the material properties and the variation of the gap between the inductor and the part. The part was considered to move in the axial direction during processing. The operating conditions used in this case were frequency of the order of 807 Hz, inductor current of 7 kA and travel speed of 7.5 mm/s for the sheet metal [53].

In 2003, Nemkov and Goldstein proposed 2D axisymmetric, 2D and 3D models capable of studying electromagnetic edge and tip effects and using weak coupling. These studies were carried out at the Center for Induction Technology, Inc. The commercial software Flux 3D was used to develop the appropriate models and the processing frequency used in the simulation was 9.5 kHz and the parts were simulated at a frequency of 9.5 kHz and were moving linearly at a speed of 1.16 m/s. The simulation results were validated on a 9.5 kHz source using experimental tests with a medium frequency machine. Surface temperature measurement was performed using a type K thermocouple [54].

In 2005, Kawaguchi et al. proposed an analysis of the induction process and a technique for measuring the magnetic permeability of SUS430 material using a B-H analyzer for both 100 Hz and 100 kHz frequencies. The measurement was performed for field strengths ranging from 200 to 1600 A/m. These researchers then set up two 3D models using a weak coupling and two types of inductors, one with a circular section and one with a square section and a simple cylindrical part [55]; the results obtained showed that the simulated temperatures and those measured at the surface show a good agreement.

In 2006, Magnabosco et al. developed a numerical approach for induction heat treatment applied to carbon steel (AISI-1045 equivalent). The results of this work allowed the development of a 2D axisymmetric model capable of predicting the temperature and hardness

distribution in the part using weak coupling. The experimental validation was performed on a medium frequency generator (27 kHz) with a power of 31 kW and the part is moved at a speed of 20 mm.s-1 during heating. These researchers then compared the hardness profiles obtained by experimentation with those approximated by simulation [56].

In 2009, Kchaou et al. studied the effect of surface hardening on distortion and the state of stress applied to the bearing ring. Indeed, after surface inductive hardening, the section of the bearing ring undergoes a geometric deformation of perpendicularity. This distortion is the result of the forces induced in the hardening layer by the martensitic transformation and those appearing in the rest of the section. When heating, it is recognized that an angular distortion results in a lighter spacing of the flat (horizontal) face providing the cylindrical face. After cooling, these spacing decreases but persists with a small amplitude. The question is how to avoid this distortion. The answer can only be satisfactory once the heating parameters have been checked so that they remain within the required tolerance. If a hardening is carried out and the tolerance is exceeded, we propose to carry out a new hardening in another region of the part to create a counter distortion. The results of numerical simulations show a concentration of stress, especially in the center of the part. This concentration has a legitimate effect on the work and in particular on the service life of the part (ensures a good hardness of the surface layer) [57]

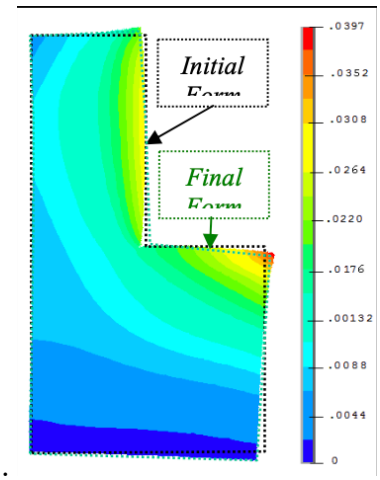

Figure 1.2.10 : Section Distortion [57]

In 2010, B.J. Yang et al. simulated the evolution of the microstructure of SAE1070 steel during induction heating, they demonstrated that the cellular automaton (CA) method is very effective in simulating the austenitizing of hypoeutectic steels during rapid heating. The kinetics of austenitization during rapid induction heating is simulated by simultaneously considering continuous nucleation, grain growth and roughness as a function of the heating rate. Numerical experiments show that the grain size distribution is strongly dependent on the local temperature history. Experimental validation of the size and distribution of the austenite grains in the radial direction confirms that the current model works well for a room or a domain with different heating rates. The simulated grain size profile and carbon concentration distribution are consistent with our experience and knowledge, respectively. The developed model has been applied to the induction hardening of steel and is able to provide information on austenitic grain size and homogeneity of composition prior to hardening, allowing the design and optimization of induction heating processes [58].

In 2011, AMIT KOHLI and HARI SINGH will address the optimization of treatment parameters in induction hardening using the response surface methodology. They have shown by experimental studies that the effect of process parameters such as speed, heating time, current and gap between material and induction coil on the hardness of AISI 1040 steel are under two different conditions, i.e., rolled and normalized during induction hardening. The optimum hardness values obtained were 56.4 HRC and 57.8 HRC respectively for the rolled and normalized condition at a speed of 3.21 mm/s, a heating time of 5 seconds, a current of 135 amperes and a gap between the material and the induction coil of 5.29 mm as the optimum value of the process parameters. The results showed that for the manufacture of shafts, axles or automotive components made of medium carbon steel, the raw material must first be normalized and then induction hardened in order to achieve uniform material hardness [59].

In 2011, K.D. Clarke et al. Induction Hardening of 5150 Steel: Effects of Initial Microstructure and Heating Rate, in fact the induction hardening heat treatments were studied using dilatometry on 5150 steel with initial microstructures of ferrite-pearlite and hardened

martensite to evaluate the effects of the anterior microstructure and heating rate. Transformation temperatures on heating are significantly higher for an initial ferrite-pearlite microstructure than for a previous hardened martensite microstructure. The difference between the transformation temperatures increases with the heating rate. The maximum hardness measured is equivalent, independently of the starting microstructure, for a given thermal cycle. Metallographic evidence indicates significant residual chromium enrichment in regions of anterior pearlitic cementite in the initial ferrite-pearlite microstructure. No evidence of alloy segregation was observed metallographically for the anterior hardened martensite microstructure. Further work is needed to understand the practical implications of local alloy segregation. Diffusion conversion simulations of induction heat treatment rates support ferrite-pearlite alloy segregation, indicate that residual alloy segregation is possible with previously quenched martensite, and can be used to tailor austenitizing heat cycles to process requirements. The results are applicable to general induction heating modeling [39].

In 2012 Mert Onan et al. Investigate the optimization of induction hardened 1040 steel using an experimental design method and material characterization analysis. Induction hardening optimization studies were conducted and the hardness and depth of the case were measured and analyzed. s and a distance between the coil and the workpiece of 4 mm were separated. According to the results of the F-test, the power ratio, scanning speed, and intersections were more effective than other factors. By applying higher power ratio or lower scan speed, induction hardening resulted in high surface hardness. A hard phase, called martensite, was not observed 100% of the time during optical microscopy. Microstructural characterization showed that four distinct regions from the surface to the inner surface were designated as martensite, pearlite, and ferrite, respectively [40].

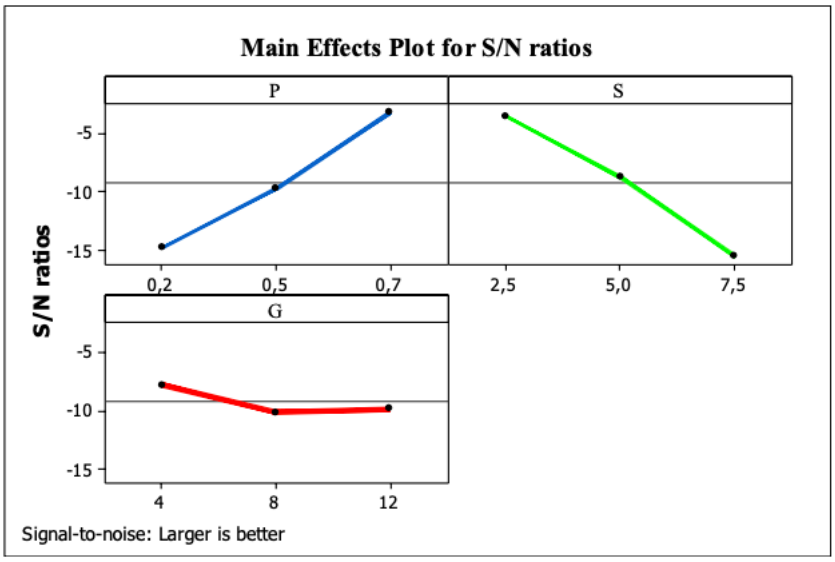

Figure 1.2.11 : The Optimal S/N Results for Each Factor Analyzed Separately by Minitab Software [40]

In 2013, J. Yi et al. conducted a study on the distortion and Residual Stress Measurements of Induction Hardened AISI 4340 disks. This study shows that the HI parameters (heating time and input power) and the initial hardness affect the distortion and hardening depth of the samples. For the same initial hardness, increasing the HI parameters (heating time or input power) increases both the depth of hardening and the distortion of the disk. However, for the same HI parameters, increasing the initial hardness of the disk increases the depth of cure because it decreases the deformation of the disk. Due to the large variation in hardness at the surface of a HI part, knowledge of the depth distribution d0 is necessary and can significantly affect residual stress results. A variation of 0.001A in d0 in the hardened layer can result in a residual stress difference of about 200 MPa in the same region. The measured d0 results ND (neutron diffraction) and XRD (X-ray diffraction) both show a visible difference in d0 values between the hardened layer and the core material. Therefore, it is more reasonable to use a d0 profile measured by ND to calculate the residual stress near the surface than to use a constant d0 surface value measured by XRD. However, for the core material, the d0core measured by XRD is more reliable [41].

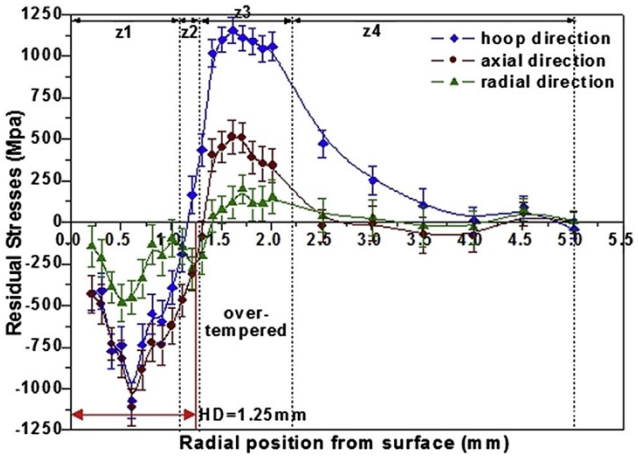

Figure 1.2.12 : Distribution of residual stresses in three directions calculated on the basis of d0 measured by ND for the surface and the d0ecore obtained by XRD for the core material [41]

In 2013, Tianxing Zhu et al. investigated the effects of the magnetic flux concentrator on the induction heating system using a coupled electromagnetic-thermal simulation model. In this work, they presented a 2D electromagnetic-thermal analytical model. The analytical model was constructed according to the configuration of the physical experiment with accurate material properties. The validity of the analytical model was verified by experiments. Fairly good agreement was obtained between the simulation and the experimental temperature profile at points on the surface of the part. The advantage of the analytical model is that it can be used to predict parameters such as the current density and the flow field inside the part, which are very difficult to measure directly. In addition to creating the model, the effect of the magnetic flux concentrator was also analysed. The magnetic flux concentrator uses the proximity effect and the gap effect to increase the productivity of the induction heating process by concentrating the current in critical areas. It can be used to improve part quality, production and process efficiency. The magnetic flux concentrator induction heating system is not only a fast and reliable process, but also can eliminate inconsistencies and quality problems that occur in other methods such as open flame and torch heating [42].

In 2013, Barka et al. investigated the sensitivity of the hardness profile of a 4340 sample. The results in the case of MF the temperature profiles at the edges and in the midplane are almost identical. Even though the temperature values are comparable at the surface, they are slightly higher in depth at the edges than in the mid-plane, while in the case of HF the depth of the hardened layer is greater at the edges than in the mid-plane [14].

In 2015, Sönke Rhein et al. investigated in their study the optimal control of induction heating processes using the software FEM. In this paper, a FOTD (first optimize and then discretize) approach of induction heating problems and its implementation with the software FEM is presented. The first order optimality conditions are derived using the formal Lagrangian technique. The gradient algorithm in combination with the COMSOL MULTIPHYSICS simulation software is used to numerically solve the canonical equations consisting of the partial multiphysics algebraic differential equation (PDAE). The main advantage of this approach is the seamless integration of the software FEM, to take advantage of the special solution methods for numerical integration in the optimization process. Due to the relatively small influence of the localized coil on the thermal behavior of the induction heating process, which is enhanced by the skin effect, the heat is mainly generated near the coil and propagates through conduction. To introduce most of the thermal energy into the workpiece, the maximum coil current is applied between the time interval [0 s, 92 s]. After that, the coil current decreases to achieve temperature homogenization inside the workpiece. The local temperature profiles of the space with uniform contour lines at selected time points can be seen in Figure 1.2.12. Despite the limited influence of the control input on the induction heating process, the digital solution of the optimum control problem (OCP) leads to the desired heating of the room at Td = 593K. The maximum temperature value is 638K at t = 94s [43].

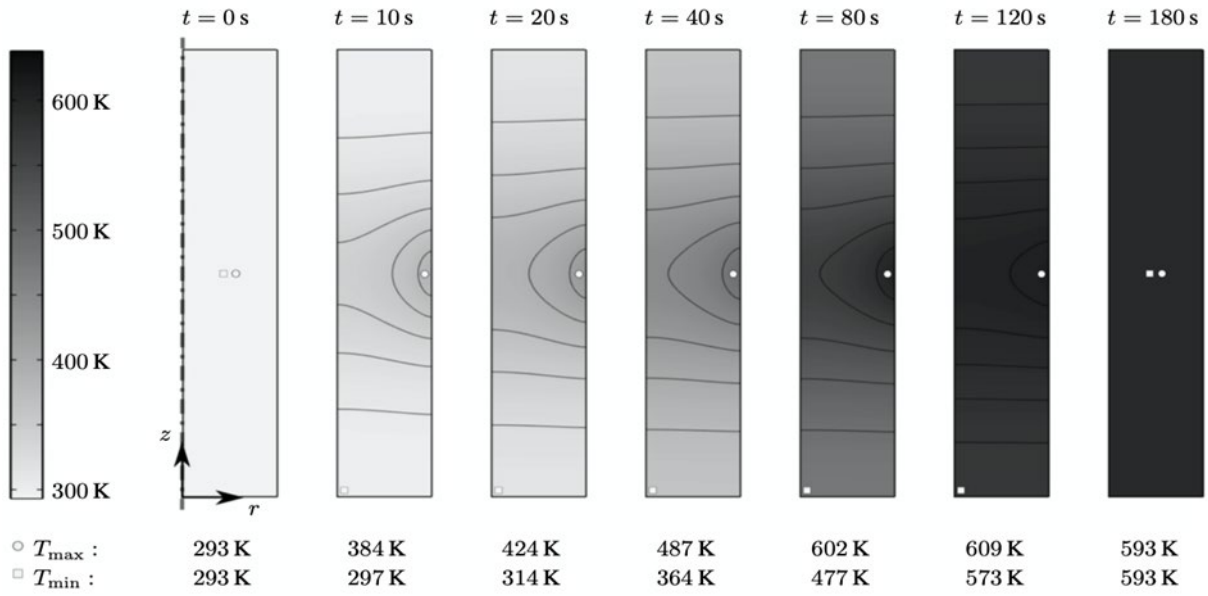

Figure 1.2.13 : Temperature distribution T (x, t) in the room domain at different times with uniform contours [43]

In 2015 W. Jomaa et al. a study of residual stresses and microstructure induced by machining of induction heated AISI 4340 steel In this study, orthogonal dry machining of induction heat treated AISI 4340 steel was carried out using a mixed ceramic tool. On the one hand, the results showed that a state of residual compressive stress can be achieved after dry hard machining, and the levels of these stresses were strongly affected by the machining conditions. On the other hand, a thin white layer formed on all machined surfaces. The authors suggest that proper selection of cutting speed and feed rate can lead to good surface integrity characteristics [60].

In 2016 Lenka Jakubovičová et al. optimized the induction heating process to achieve a uniform surface temperature. In their paper electromagnetic and thermal field equations were applied to solve the problem of induction heating. The numerical simulation of the induction heating process is presented as a coupling of electromagnetic and thermal problems leading to a transient thermal analysis system by the explicit Euler method used in time integration solutions. Through the numerical solution of the electromagnetic and thermal problem, it is

possible to observe the effect of individual variables related to electromagnetic induction as well as the resulting temperature or heat generated by the interaction of the surrounding environments for different time steps. By comparing Figures 1.2.13, 1.2.14 and 1.2.15, it is possible to see how the geometric position of the inductors influences the resulting temperature of the induction heating process. In Figures 1.2.14 and 1.2.15, it can be seen that the geometrically optimized parameters of the inductors lead to a uniform surface temperature required for many industrial processes. The combination of the numerical solution and the geometric optimization allows to optimize the uniform surface temperature on the heated sample [3].

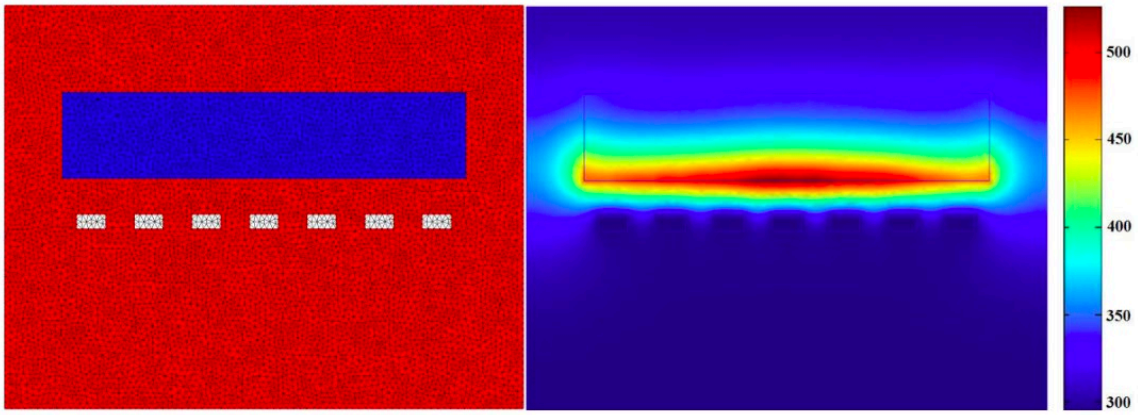

Figure 1.2.14 : Calculation model before optimization [3]

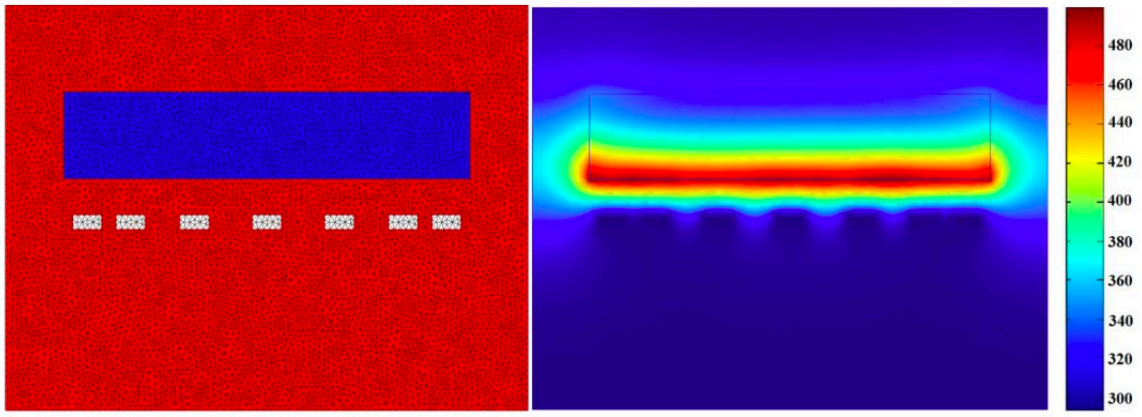

Figure 1.2.15 : Inductors after optimization at position x [3]

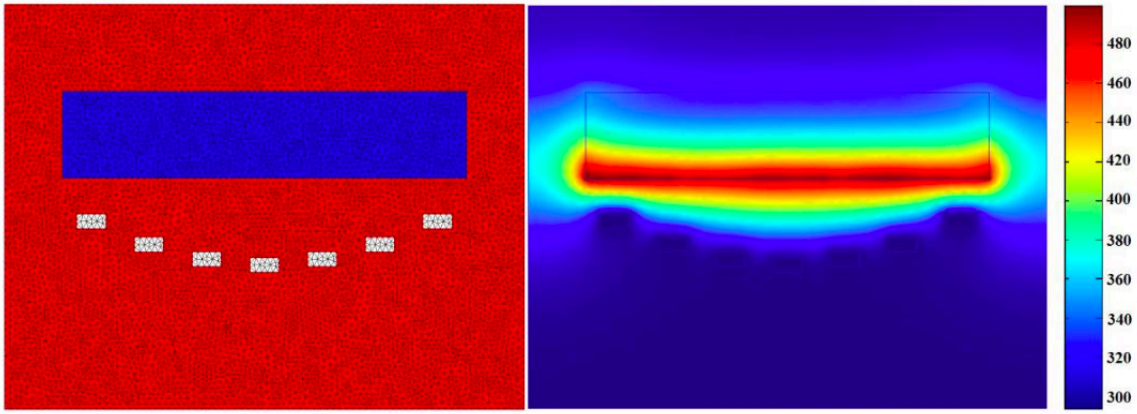

Figure 1.2.16 : Inductors after optimization at position y [3]

In 2016 Annika Vieweg et al. In their article Induction hardening and its differences from a conventional heat treatment process and optimization of its parameters. This study highlights the differences in microstructure and mechanical properties between a conventional and an induction heat treatment of a 50CrMo4 steel. An important difference between inductive and conventional heat treatment is that in inductive treatment, temperature gradients occur across the cross-section due to the skin effect. The gradient between the surface and the core is greater at higher heating rates because the power intensities must be increased. The calibration of the core temperature leads to overheating of the surface of the sample (up to 150 °C at a heating rate of 50 K/s). The induction heat treated samples were austenitized at higher temperatures (950 ◦C and 1000 ◦C) than the conventional sample (850◦C), resulting in an increase in the previous austenite grain sizes. Obviously, at higher temperatures during heat treatment, a larger volume fraction of carbides dissolves and the anterior austenite grain size increases. This is consistent with the fact that an increase in hardness and the amount of retained austenite was observed in the same samples, which can be attributed to a higher carbon content in the matrix. Subsequent quenching shows differences in carbide precipitation due to different amounts of dissolved carbon and different amounts of retained austenite. Further studies could be useful to analyse the kinetics of the tempering process as a function of the austenitization pretreatment, as well as a detailed analysis of the

precipitating carbides via e.g., TEM. A decrease in the toughness of the sample induced by austenitization, represented by the Charpy impact energy, can be attributed to a combination of three phenomena: Increase in hardness, increase in grain size and change in fracture behaviour - from ductile to partially intergranular. The reason for the latter requires further investigation, particularly of the state of the former austenite grain boundaries in terms of precipitates and impurities. Nevertheless, the samples inductively heated at T = 10K / s at both austenitizing temperatures show a good combination of hardness and Charpy notched impact energy. Despite the decrease of the impact energy compared to the chosen conventional method, it is still sufficiently high for the industrial specification of this steel (30 J). In addition, the samples have sufficient hardness and the treatment time is more than 10 times shorter than the conventional treatment. Heating rates of T = 50 K / s are difficult to control and lead to unsatisfactory toughness properties and are therefore not recommended according to this study [46].

In 2017, Senhaji et al. Modelled the temperature history and validated the rapid induction hardening process. The axisymmetric 2D model developed in this study was used to understand the effects of material properties on the induction heating behaviour. The sensitivity analysis of the material properties showed that the relative magnetic permeability is the property that most affects the surface temperatures. It is therefore necessary to carefully calibrate the evolution of this property as a function of temperature and magnetic field strength to obtain correct temperature predictions. The heat capacity also affects the temperature, while the effects of thermal and electrical conductivity are rather weak. Finally, by adjusting the thermal properties of the material, a good agreement was found between the simulation results and the temperature measurements at five different temperatures [47].

In 2017 Madina Yermekova and Sergei A. Galunin in their article on digital simulation and automatic optimization of induction heating system of disks. In this work, a double loop structure was applied to the optimization procedure in order to improve the shape of the objective function and in this way increase the efficiency of the optimization research. This

objective was achieved by dividing all design variables into two groups: Variables describing the shape of the induction coil and variables defining the position of the coil relative to the edge of the disk. Each of these two groups of variables is used in a separate, independent optimization search. The inner loop of the method finds only the optimal position of the fixed shape induction coils, which is given by the optimization algorithm of the outer loop. The outer loop algorithm is responsible for finding the optimal shape of the corresponding coil. Automatic optimal design is the only way to develop a new generation of highly efficient induction heating systems. A specially developed technology enables a very robust coupling of optimization algorithms with large digital packets. The two-loop optimization method, which separates the design of the inductor shape from the positioning of the coil, is much more stable and robust in operation than conventional research. Genetic algorithms combined with problem-oriented three-dimensional software can be recommended as efficient tools for optimal inductor shape design [48].

In the 2017 study by Iosko Balabozov et al. on the effect and modeling of magnetic concentrators in induction heating systems, a comparison of the mean temperature in the heated part for two cases (with and without concentrator) is given. It can be clearly seen that the temperature reached in the system with magnetic concentrator is about five times higher and the efficiency of the system is higher than in the system without concentrator (Figure 1.2.16). The results of the simulations of FEM clearly show that the use of magnetic concentrators around the coil significantly improves the efficiency of the two systems studied and leads to achieving several times higher temperatures in space. Further optimizations of the concentrator shape, size and material properties could also be performed to achieve better system performance [49].

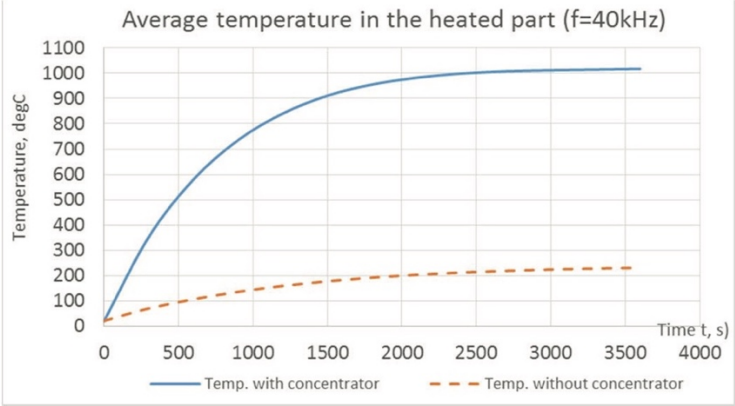

Figure 1.2.17 : Average temperature in the heated part with and without concentrator [49]

In 2018, Khalifa et al. Performed a sensitivity study of the hardness profile of a disk of induction hardened 4340 steel as a function of machine parameters and geometrical factors. Their work led to the development of a MATLAB algorithm that significantly reduced and optimized the simulation time. Statistical analysis using ANOVA showed the depth of the hardened layer and a great agreement between the mathematical model and the experimental results, with an average error of less than 15%. The obtained mathematical model implies a very good ability to predict the hardness and the overheating zone when the experimental values are close to the input of the simulation parameters [50].

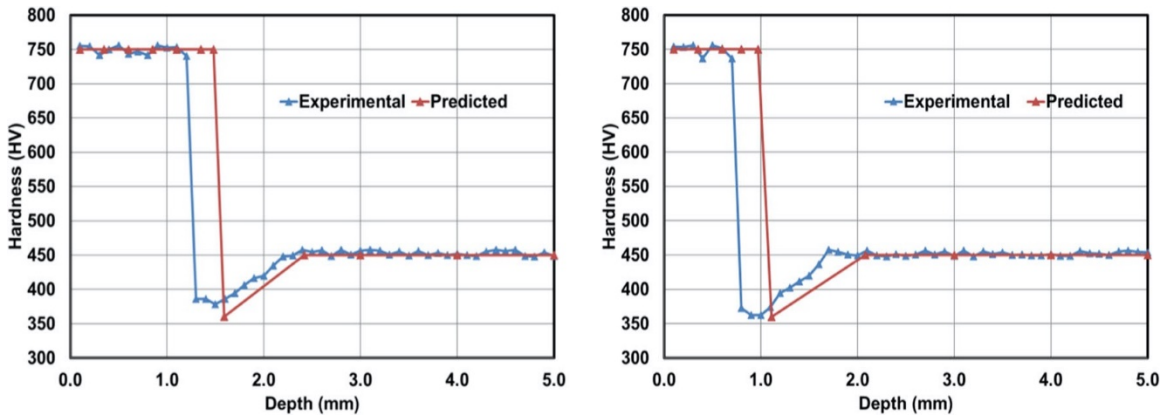

Figure 1.2.18 : Experimental Validation of Predicted and Measured Hardness for, Edge(a) and Middle(b) [50]

In 2019, Khalifa et al. Investigated the optimization of the edge effect of an inductively heated 4340 steel specimen with flux concentrators using axisymmetric finite element simulation and experimental validation. Of particular importance is the optimization of an approach to reduce the edge effect applied to a 4340 steel disk using a FEM model in conjunction with optimization algorithms that yield the best hardness profile. Moreover, the article proposes a particularly original method, namely the optimization of the geometrical parameters by placing the main disk between two identical disks with an axial gap acting as a flow concentrator on the central part. The simulation model was validated by a comparative analysis with the experimental results and it was found that it is possible to obtain the best hardness profile by using the flow concentrator and adjusting the geometrical parameters of the process: Gap, Frequency, Power and Time [51].

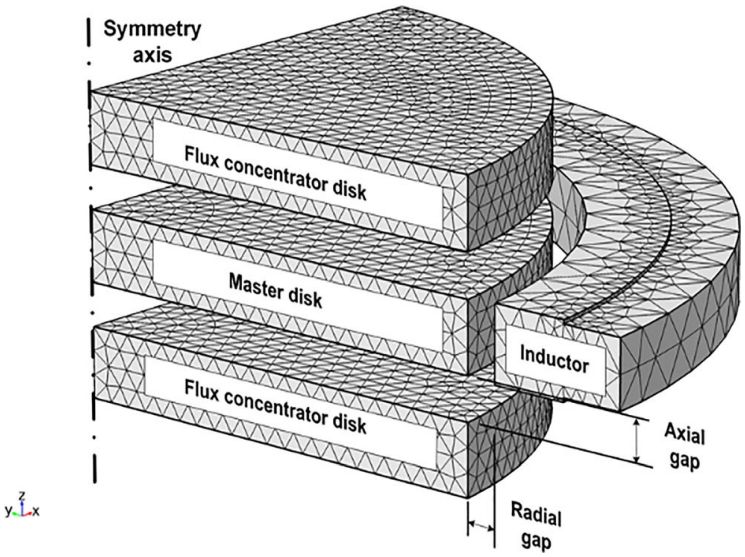

Figure 1.2.19 : Schematic presentation of the model geometry [51]

New developments in simulation tools and the resolution capacity of computers have made it possible to model increasingly complex geometries using a finer mesh with very good computational accuracy. The literature review on induction heat treatment simulation has shown that most of the processed applications are focused on parts with simple geometry. Moreover, the developed models do not guarantee good performance due to the assumptions

considered in the finite element resolution and the quality of the mesh used. The validation ranges of the developed models are very limited and therefore cannot be used to extrapolate the prediction of hardness profiles or residual stresses, especially since the validation tests were carried out in very specific cases and cannot be reproduced with new generation equipment. As far as the simulation of induction treated gears is concerned, the research results show that few researchers have addressed this issue. However, in parallel with the simulation, several industrial efforts have been made that have led to the understanding of some facets of the process, developing practical recipes and empirical models that help industrialists in the development process [[5][52][53]].

1.2.6 Complex geometry

Two heating concepts have been developed for the treatment of gears by induction in accordance with the development of power generators and gear geometries ([4][8][12]). The first concept is single frequency impulse heating (SIFH), which was developed in the 1940s and includes two different stages, namely preheating and final heating [12]. In this type of heating, the heat is not uniformly generated in the root and at the head of the gear teeth since the induced currents are concentrated deeper in the areas near the root. The advent of high frequency generators in the mid-1950s led to the development of dual frequency pulse heating (CDFI) [12] (US Army project, 1990). Originally, this heating method consisted of heating a room in two successive steps with appropriate power and the two available frequencies, the medium and high frequencies (Figure 1.2.19). Preheating is usually done at medium frequency, while the final heating is done at high frequency to distribute the heat appropriately along the contour of the teeth. Subsequently, the austenitized areas are transformed into hard martensite by quenching. Finally, tempering is performed to relax the residual stress field, give dimensional stability to the treated parts and slightly reduce the hardness, while significantly increasing the toughness of the material.

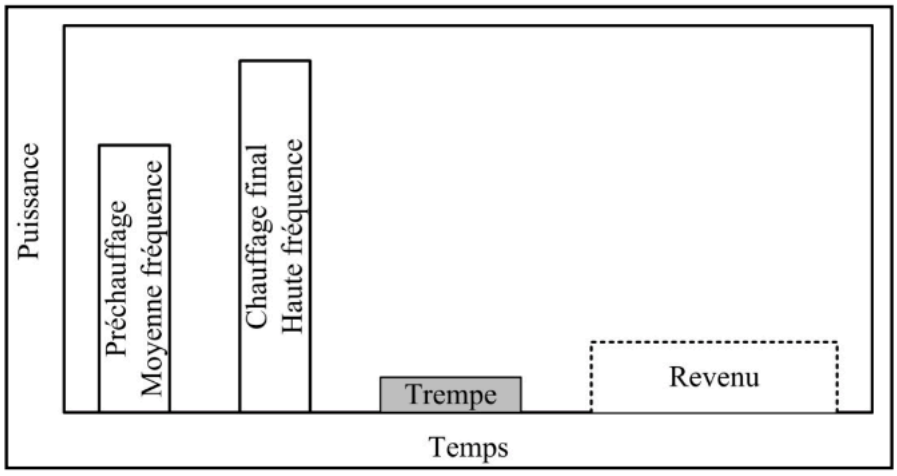

Figure 1.2.20 : Sequential heating cycle [1]

Recent technological advances in the field of power electronics have made it possible to combine both medium and high frequency powers in a single heating step (Figure 1.2.20). In fact, the simultaneous dual frequency heating makes it possible to modulate the medium and the high frequency by activating the two power generators at the same time. In addition, current generators can generate very high power and have the capacity to process mechanical parts of various sizes in less than a second.

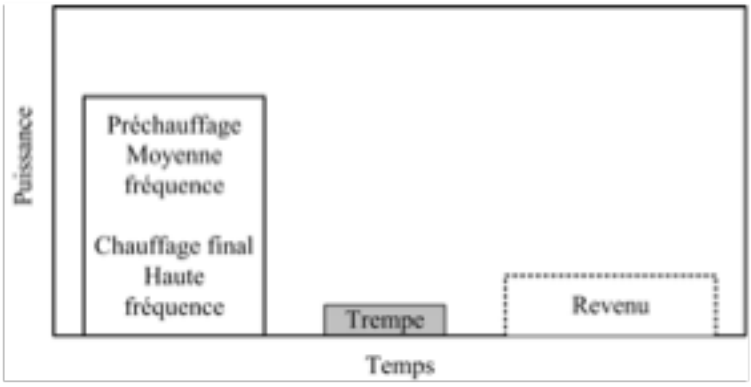

Figure 1.2.21 : Simultaneous heating cycle [1]

To understand the overall effect of MF and HF frequencies, Figure 1.2.21 illustrates an example of hardening using both frequencies. Thus, Figure 1.2.21.a illustrates an example of a hardness profile using only medium frequency power. Figure 1.2.21.b shows an example

of a gear hardening profile using only high frequency power. Figure 1.2.21.c illustrates the profile obtained by combining the medium and high frequency. The generated profile follows the contour of the toothing. It has a direct impact on the wear resistance and the life of the gears [52].

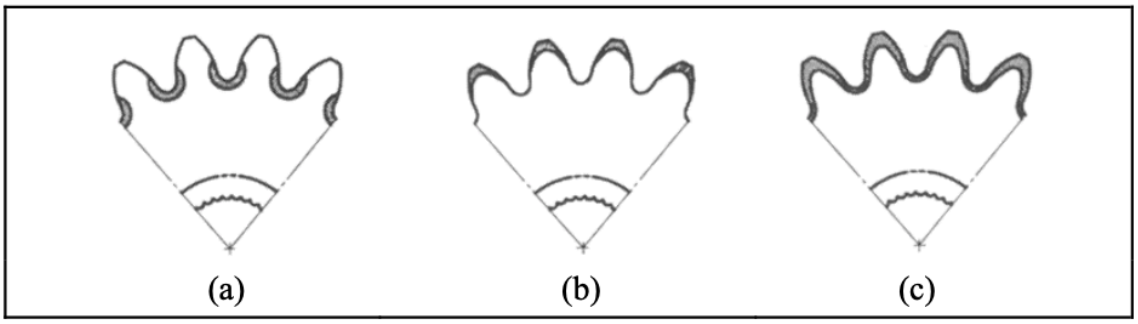

Figure 1.2.22 : Gear hardness profiles obtained by induction [1]

1.2.6.1 Gear simulation

In the last decade, a number of researchers have simulated the process of induction heat treatment of gears. One of the first works in this field was the numerical simulation of the process for spur gears, presented by Inoue et al. in 1999. These researchers developed 3D weak coupling models to solve electromagnetic and metallo-thermomechanical analyses by generating thermal energy equivalent to that theoretically generated by eddy currents. The treated gear was made of carbon steel (corresponding to AISI-1045) and had an outer diameter of 120 mm, a modulus of 3, a thickness of 20 mm, and 40 teeth. They then compared the simulation results with the experimental tests using the two heating concepts, single-frequency heating and sequential dual-frequency heating. The experimental tests were performed using a MF generator with a frequency of the order of 25 kHz and a power of the order of 165 kW for the single frequency heating. To validate dual-frequency heating, a MF generator with a frequency on the order of 3 kHz and a power on the order of 293 kW was combined with a HF generator with a frequency on the order of 150 kHz and a power on the

order of 339 kW. The total heating time was about 3 s in both cases. The obtained results allowed the comparison of the surface hardness profile and residual stresses with experimental results and showed agreement with the simulation results [54].

The 2003 work by Wrona and Nacke proposed a 3D model of the induction heat treatment process of spur gears. The 3D model, developed using Ansys software, allowed the coupling of electromagnetic and thermal fields using the concept of simultaneous dual-frequency heating and weak coupling to study the influence of machining frequency and power on the temperature distribution. The heating time was set to 1 s. First, they investigated the effect of the average frequency on the final temperature distribution by varying the frequency from 10 kHz to 40 kHz. They found that it is important to use a frequency of 20 kHz to obtain heat in the tooth flank, and that it is impossible to produce a hardness profile corresponding to the tooth contour with a single frequency. They also integrated the two frequencies, the medium frequency of about 5 kHz and the high frequency of 150 kHz, into the same 3D model and modulated them simultaneously while keeping the overall power constant. These researchers then tried to obtain the optimal profile of the heat generated by the Joule effect. The results obtained show that the optimal hardness profile is obtained at 20% of the HF power [55]. In this work, the properties of the material and their variation as a function of temperature were not really discussed.

The 2006 work by Wrona et al. Proposed a 3D model for machining an induction heat treated screw to calculate the final temperature distribution. The medium frequency range was between 5 kHz and 15 kHz and the high frequency range was between 150 kHz and 400 kHz. The researchers demonstrated the relevance of the Ansys simulation tool to solve the electromagnetic and thermal coupling using weak coupling. The researchers presented a comparison between the two heating concepts, the one frequency per pulse concept and the two simultaneous frequencies per pulse concept. The analysis of the single frequency heating concept showed that when the frequency is of the order of 20 kHz, only the root is strongly heated, while the root and part of the screw flank are heated when the frequency is increased to 40 kHz, while the head region is heated when the frequency is 100 kHz. Regarding the

concept of simultaneous dual-frequency heating, the results have shown that by combining the two frequencies and keeping the total power constant MF -HF and coupling the simulation with an optimization algorithm, that by applying about 50% of the power the hardness profile is near to the contour. In this work, the material properties as well as their evolution as a function of temperature have not been clearly discussed. The coupling used is a weak coupling with iteration, which provides that the resolution of the electromagnetic and thermal equations is done step by step [56].

In 2008, Kurek et al. Proposed 2D models to determine the temperature distribution on inductively heated gears. Induction heating was performed at an average frequency of the order of 10 kHz and at a high frequency of the order of 200 kHz. The material properties in thermodynamic equilibrium were taken into account in the resolution and the coupling used was of weak type. The simulation results were validated with experimental tests that proved the relevance of the developed numerical models. The material used was AMS 6414 (equivalent to AISI 4340). The efforts of Kurek et al. allowed the development of a 3D model for a spur gear tooth with a diameter of 100 mm, a thickness of 6 mm and 48 teeth using Ansys software. These researchers studied and compared the two cases MF and HF of heating. The heating was performed at a medium frequency of the order of 10 kHz and a high frequency of the order of 100 kHz, and the currents in the inductor were estimated to be 2500 kA and 1000 kA, respectively. The researchers did not provide clear information about the type and quality of the mesh used and the techniques used to measure the temperature [57].

In 2008, Niklewicz et al. used the same results as Kurek et al. to investigate the effect of geometrical parameters such as the air gap between the inductor and the component and the number of teeth on the temperature distribution during induction heat treatment. The 3D model was developed using Flux3D. Heating was performed at an average frequency between 5 kHz and 20 kHz for 1.5 s and at a high frequency of about 100 kHz for 0.3 s. The currents were of the order of 2.5 kA and 1.0 kA, respectively, and the number of teeth varied between 63 and 72 [58]. The quality of the mesh and the techniques used to measure the surface temperature were not clearly stated.

In 2013, Larregain et al. Method for accurate surface temperature measurements during rapid induction heating in a study accurately measured the thermal history on the side of a spur gear during HF heating using an image analysis technique. In particular, it is possible to document where and when a specific temperature is reached on the surface of a gear hardened by rapid induction heating. The final position of the isotherms was compared to the hardening transition line. The results suggest that the Ac1 transformation temperature varies depending on the position on the surface of the workpiece. The heating rates were estimated at two locations and showed that the temperature increased faster at the root than at the tip. Thus, this method confirmed the correlation between Ac1 temperature and heating rate [59].

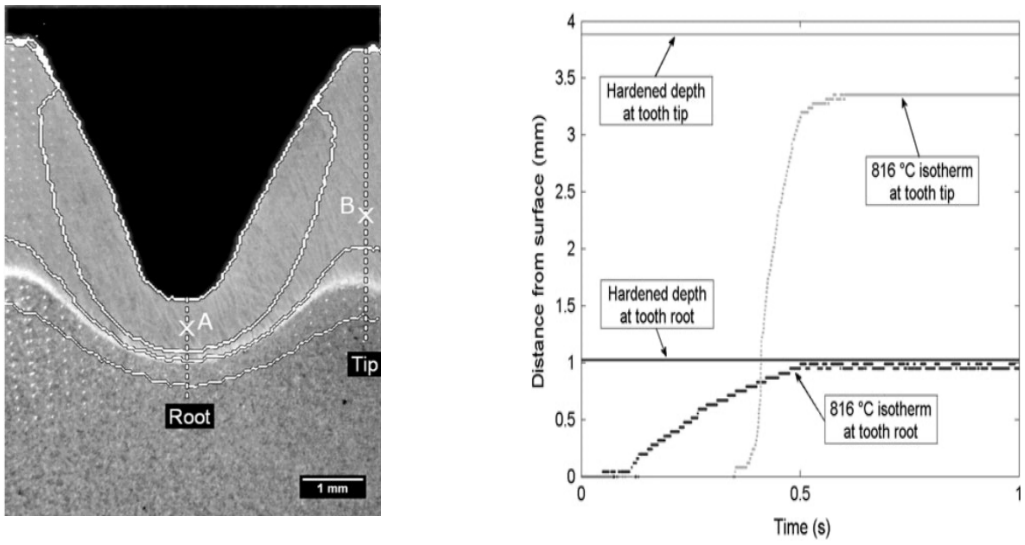

Figure 1.2.23 : Superposition of the etched microstructure with isotherms at 927, 816 and 704 °C (white lines, top to bottom). The dotted lines correspond to the profiles shown in the figure on the right [59]

In 2014, Zhichao Li et al. investigate the effect of quenching rate on distortion and residual stresses during induction hardening of a complete float axle shaft. Electromagnetic modeling using Flux2D and thermal stress modeling using DANTE were successfully coupled in this study. The power allocation process using Flux and DANTE is verified by directly comparing the temperature profiles predicted by the two packages. In this study, three spray quench rates

are modeled with heat transfer coefficients of 5, 12 and 25 kW / (m2 ° C). Higher cooling rate leads to higher surface compression and tension in the core and higher axial growth. The induction heating process parameters - frequency, power and sweep rate - affect the temperature profile, which significantly affects the distribution of residual stresses even without changing the case depth. The cooling rate was also found to be important for the final level of residual stresses and distortion [60].

In 2014, Barka et al. developed a new approach to optimize the induction heating process. First, a 3D model was built using Comsol by coupling electromagnetic and thermal fields,The simulation results show that only the area of the root circle and a small area around it can be converted into hard martensite when MF is applied at the edge and mid-plane. On HF, the induced currents generate much more heat in the tip and pitch diameter areas, making the edge effect very obvious (the root circle is strongly heated at the edge of the gear). Experimental tests show that there is good agreement between simulation results (temperature profile) and experiments (hardness profile) at both MF and HF. The temperature difference between the edge and the median plane, for the root and tip positions is closer when flux concentrators are used than in the case without flux concentrators [11].

In 2014 Jerzy Barglik et al. 3D modeling of induction hardening of gears, the paper presents a 3D numerical analysis of the nonlinear hardening process of a gear with respect to the temperature dependencies of all material parameters. The authors have not only modeled the process itself, but also tested the influence of the uncertainties of these parameters on the results. The results (both the temperature profiles and the final hardness) agree very well with practical experience, even if the uncertainties of the material parameters lead to their deviations. Many calculations show that the influence of the specific heat capacity is the most obvious. Here the temperature difference at the end of heating reaches about 50°C, i.e., about 6%. However, the resulting hardness of the teeth depends on the cooling time. And if this time is of the order of a few seconds, it exceeds 700 HV, which generally satisfies all operational requirements [61].

In 2015, Sönke Rhein, Knut Graichen in their paper Dynamic Optimization of Induction Heating and Surface Hardening Processes in Complex Spatial Domains presented an optimization framework to numerically solve the Optimal Control Problem (OCP) for induction heating and surface hardening processes. Considering the FEM software used, the numerical processing of OCPs can be performed using specialized algorithms. Moreover, complex spatial domains can be handled with relative ease. As shown in Figure 1.2.23, the control trajectory u (t) is optimized to minimize the difference between the desired temperature Td and the pinion temperature in the range Ωw, represented by the maximum Tmax (t), the average Tavg (t), and the minimum temperature Tmin (t), at tf = 8s. Three phases are observed in the optimized trajectory. During the first 0.6s, the control remains at the upper limit u + leading to the fastest possible temperature rise. After that, the coil current u (t) continuously decreases in the time interval [0.6 s, 4 s], so that the state constraint is satisfied. Finally, the coil current continues to decrease in the remaining time interval, leading to a homogenization of the temperature within Ωw. Current research concerns the study of temperature-dependent material parameters and the adaptation of the optimization framework to other multiphysics problems [62].

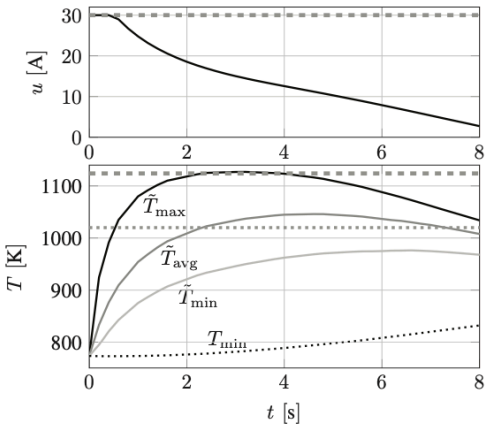

Figure 1.2.24 : Check the input u (t) as well as the trajectories of Tmax (t), Tavg (t) and Tmin (t) in Ωw for the surface hardening process [62]

In 2017, Barka et al. investigated the effects of parameters on heating depth. Before the results are available, a comparative study between cases MF and HF will be conducted to predict the depth of the hardened layer. MF hardens only the root and HF converts the tip of the gear into martensite. After experimental validation, simulation results show that only the root region and a small region around it are converted to hard martensite when MF is applied. However, when HF is used, only the head region and a small region near the pitch diameter are hardened. At this stage, the results confirm the validation of the tests. The sensitivity study shows the main parameters of the machine and their effect on the hardening profile. Depending on the control of the machine used, the very short heating time forces the machine to produce a high power quickly, which affects the quality of the response in terms of time and output. The results are also affected by geometric errors mainly due to the alignment between the part and the inductor (gap difference) [63].

In 2018, Hamdan F. Sabeeeh et al. investigated the effect of a flux concentrator on the surface hardening process of a steel gear. The results show that the use of both ferrite materials 3C90 and 4C65 leads to a reduction of the frequency to 50% compared to the conventional induction coil and the required power is reduced to about 30%. This results in a better temperature gradient and improves the temperature distribution in the gear during the heating process, as the magnetic flux is concentrated only on the required area. By using the same power required for the conventional coil, the processing time can also be reduced, which increases productivity. Finally, the proposed concentrator consists of two parts and contains a ventilation slot, which is neglected in the analysis for simplicity [64].

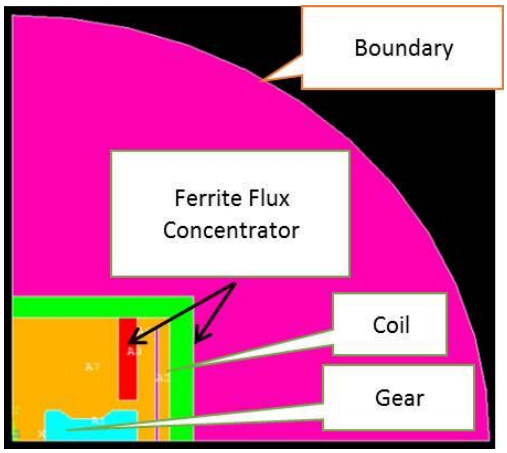

Figure 1.2.25 : the first quarter of the 2D section of the finite element model of the proposed coil with concentrator [64]

In 2018, N. Vanderesse et al. in their study Experimental Evaluation of High Heating Rates in Induction Heating with Thermosensitive Lacquers applied the method to induction hardening of parts made of AISI 4340 with variable geometry and parameters. Two gears heated simultaneously at single and double frequency were shown to have similar final microstructures and cured characteristics could be obtained with different thermal histories. This could only be demonstrated by recording the evolution of the isotherms during the process. Moreover, it was shown that the transformation temperature of the material varied according to the considered position on the surface of the part due to the different heating rates. In the case of simultaneous double frequency, it was observed that the phase transformation front can expand significantly at high speed after the end of the heating, especially at the end of the foot diameter. Therefore, for accurate control of the transformed layer in a complex shape such as a gear, great attention must be paid to the dwell time, i.e., the delay between the end of heating and quenching [65].

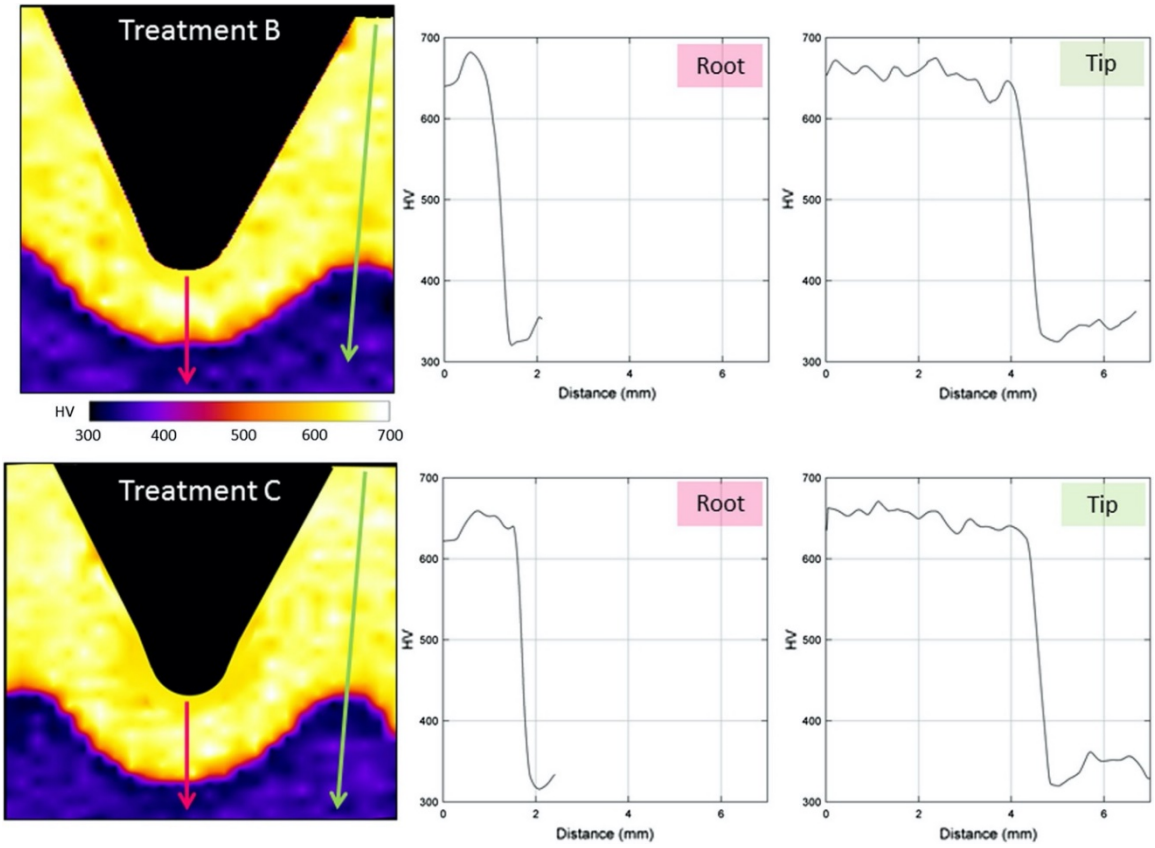

Figure 1.2.26 : Interpolated microhardness maps for gears (treatments B and C) and corresponding profiles along roots and tips [65]

In 2019, Khalifa et al. Address the reduction of the edge effect using response surface methodology and modeling the artificial neural network of a spur gear treated by induction with flux concentrators. As a result, a structured and comprehensive approach was developed to design models based on finite element analysis, ANOVA and ANN. These two techniques provided good prediction results, except that the neural network was much more efficient in terms of the depth difference between the root and the tooth tips of the gear and also in describing the behavior of the edge effect in terms of the input parameters. The experimental approach shows that the neural network model is an accurate and efficient technique for predicting and reducing the edge effect under different machines and geometric parameters and conditions [66].

In addition to simulation efforts, several empirical models and industrial methods have been developed over the years thanks to the concrete results and efforts of research centers and groups in this field. The Center of Induction Technology, the Inductoheat group, the company Contour Hardening, the Eldec group and the EFD group ([67][4]) have developed experimental tests and industrial expertise ([5][52][53][67][6]).

1.2.7 Challenges and future direction

1.2.7.1 Metallurgical and mechanical aspects

The process has limitations in terms of the materials and geometries to be treated, as the treatment of non-magnetic materials is not very efficient due to power losses. The induction heat treatment process can be used to treat large parts, but is not yet effective for complex geometries such as helical or bevel gears. Moreover, it is not yet fully mastered and the development of mechanical parts still requires a considerable investment of time and money. The investment cost of induction machines is still high for high power machines [68]. Although the current requirements demand a wide variety of tools made of high-quality steels, apart from the fact that it is a process that is still being tested and little work has been done on complex geometries in all their forms, we do not see induction hardening applied to helical wheels, splines or racks, as geometries that are found in many other industrial and domestic products and applications every day.

One of the major problems in recent applications of induction heating is the very high heating rate, reaching about 5000°C/s in less than a second. Therefore, the phase change and subsurface regions are locally tempered. This result leads to a region called "occurred" where the hardness can be significantly lower than the initial hardness before induction heating.

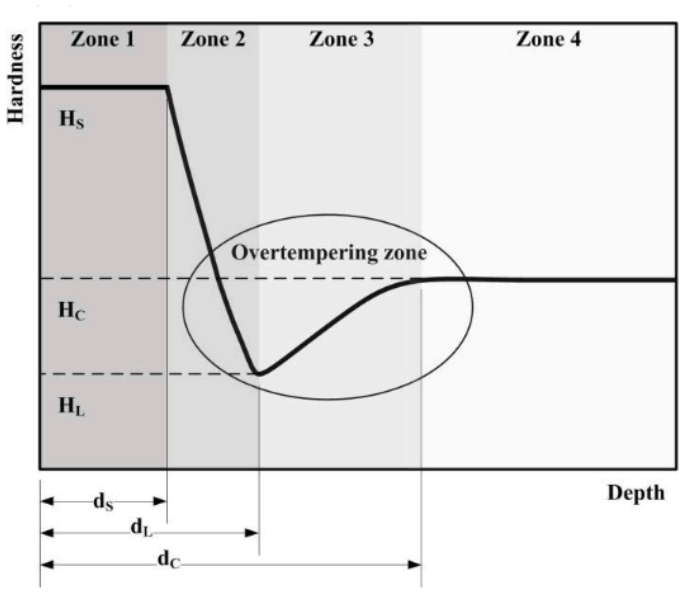

Figure 1.2.27 : Typical Induction Hardness Curve [34]

To address this issue and reduce this area of overheating, Barka et al. 2013 suggest using a high frequency and shortening the heating time, however this result has not yet been validated for a variety of initial hardness and with actual temperature measurements.

Annealing (also called process annealing, recrystallization annealing, or tempering) represents a large group of heat treatment processes that achieve microstructural changes and a change in mechanical properties without austenitization, except that this treatment does not know any development of knowledge about the induction heating process.

1.2.7.2 Simulation and validation of geometries other than gears

The articles on induction heating of complex geometries other than gears are rare. Although it would be interesting to study the effect of induction heating on all types of geometries and materials, Yi Han et all have studied the electromagnetic heating process of high-performance sprockets with civular coils and profile coils precisely matched to the geometry of the sprocket, an interesting comparison and analysis showing the importance of

the inductor. It was found that the inductor with the gear copy structure has a shorter heating time, a smaller temperature difference in the surface layer of the tooth profile and a better temperature uniformity. This improves the quality of heating of the gear rim and the heating efficiency [74]. A confirmation that justifies the following section of 3D printing of the inductors, which gives an exact geometry to the treated part.

An interesting application of induction heating is the treatment of crankshafts for heavy marine diesel engines, a complex geometry widely used and characterized by induction machining. A study of coupled electromagnetic and thermal analysis in conjunction with the equivalent circuit model confirms the validity of the analysis method through the experimental measurements of temperature for a variety of diameters, frequencies, input powers, and coil turns [75].

1.2.7.3 Additive manufacturing for inductors

In everyday practice, an inductor is also called an induction coil or simply a coil. There is an almost infinite variety of inductors/coils suitable for the almost infinite variety of induction heat treatment applications. However, their geometry often does not resemble the shape of a conventional coil. An inductor must be adapted to the part to be treated. Each geometry can have its own inductor with which to treat it, but the problem in this case is the manufacturing cost of these inductors, which are very expensive and require a lot of expertise, which leads us to think about the use of 3D printers, which reduce the cost and make the inductors accessible to any type of geometry without having to think too much about manufacturing costs, when this has the advantage of making the induction heating process a big step towards a leading heat treatment.

1.2.7.4 Induction heating and the industry 4.0

We can't move forward without addressing digital revolution and its impact on the heat treatment process. The fourth industrial revolution, often known as Industry 4.0, refers to the

transformation of industry and production systems as a result of the introduction of new technology.

If the previous industrial revolution was founded on the integration of robotics and process automation, we aim to take it a step further with Industry 4.0. Its purpose is to construct intelligent factories that can more easily adapt to changing production needs and processes. The Internet of Things (IoT), Cyber-Physical Systems (CPS), intelligent factories, big data and data analytics, and other concepts are all part of Industry 4.0.

Cloud computing is also one of the core elements of Industry 4.0, a powerful tool that allows users (companies) to simulate large projects in the cloud and only pay for resources when they are needed, rather than investing in large machines. This is part of the intelligent optimization of work processes.

In this section, we will provide our perspective on some of the issues that electromagnetic induction systems for heating and heat treatment in modern industry face in this part. Implementing Industry 4.0 strategies is one of them.

a) ***ADDITIVE MANUFACTURING / SMART MANUFACTURING***

The first challenge is 3D printing technology, which plays a crucial role in Industry 4.0 by lowering process complexity and enabling quick prototyping and highly distributed production processes [76] [77]. There is an almost limitless number of inductor geometries necessary to fit a matching infinite variety of workpieces [78]. The constraint here is in the fabrication of coils, a phrase typically used by induction professionals, but the geometry does not always resemble a traditional circular coil shape. Inductors are difficult to make and necessitate a great deal of experience. 3D printers will reduce the cost of inductors and make them available in a variety of geometries.

b) *CLOUD COMPUTING / SIMULATION / MODELING*

Cloud computing is a paradigm that allows users to access shared computer resources over the internet on demand. An internet-based model for managing, storing, and processing data. Cloud computing, as one of the core aspects of Industry 4.0, is a powerful tool for simulating massive projects so that the user (the organization) only pays for resources when they are used, rather than investing in large machines. This is part of the intelligent optimization of work processes. [79] [80], [81]. Before experimental validation, most induction heating operations are often simulated using numerical analysis methods such as the Finite Element Method, Finite Volume Method, and Discrete Element Method [82]. A simulation with a refined mesh might take a lot of space and computational time, which is where cloud computing comes in to help save time and improve the quality of results.

c) *POWER ELECTRONICS*

When it comes to generators, induction heating still necessitates advanced features, particularly the electrical parameters that influence the heating process [83]. It is difficult to alter the different combinations of frequency and power during the induction heating process. The majority of inverters on the market are unable to use a variable combination of frequency and power in different phases of the heating process at the same time. Rudnev has presented the new generation of Inductoheat's Statipower IFP inverter, which overcomes this constraint by allowing immediate control of frequency and power in a pre-programmed way during the heating cycle [5].

Despite the fact that induction heating systems have reached a certain level of maturity in terms of power electronics, there are still some challenges to address in order to improve performance. The advancement of semiconductor technology and the fast-growing of semi-conductor production need a greater focus on documentation and simple access to its data in order to plan for future research and development of new inventive products [84].

d) *MODEL/DESIGN/MONITOR*

Machine learning algorithms for data collecting and processing in a manufacturing environment have enabled real-time monitoring of equipment to reduce waste and increase efficiency at various stages to achieve new heights. Large corporations are employing a "internal AI development" strategy, in which they create and apply machine learning technologies for manufacturing. This enables the algorithm to be tailored to the various types of equipments used in companies [85]. Induction heating is becoming increasingly used in industrial settings. However, especially for sensitive applications, optimum process parameters have yet to be discovered. Cicconetal et al. 2017 examined two control systems, PID (Proportional Integral Derivative) and MRC (Model Predictive Control), for process control of induction heat treatment. The goal is to keep the temperature at 55 degrees for 210 seconds while keeping the disparity between the desired and output temperatures to a minimum. Because it predicts future process responses and optimizes future process behavior, the MRC has superior control over the output temperature [86]. Based on the mathematical models obtained, Tynchenko et al. developed algorithms for adaptive and intelligent control of the induction heating process in order to achieve uniform heating of the welded elements [87]. Although induction heating has achieved an acceptable degree of process monitoring, there is still work to be done to improve its control performance by implementing enhanced algorithms [88] for better measurement estimates and the formation of high-quality treated parts.

1.2.8 Conclusion

The literature review presented the main researches dealing with the simulation of the induction heat treatment process, mainly referring to research applied to simple geometries before dealing with more complex gears and geometries. This research made it possible to browse the main elements of the literature which brings together the majority of work done in induction heating from the development of the first mathematical model to the latest numerical developments by detailing the origin and the operating principle including the

different basic elements of induction heating treatment. The research carried out has clearly demonstrated the shortcomings and the challenges that facing the process during the past few years. As we move more towards industry 4.0, the implementation of its ideas should be part of the development of the process. Thus, to seek and treat the points of intersection between the two fields, induction heating and Industry 4.0 to exploit the methods and means in order to perfect the process and to open the discussion for future work. Finally, 3D printing has been proposed as an industrial application based on industry 4.0 answering the question that can it be possible at some point to print cooper coils to reduce the high cost of inductors production and make the inductors accessible to any kind of geometry at some point?

CHAPITRE 2
MODÉLISATION ET SIMULATION DU PROCESSUS DE CHAUFFAGE PAR INDUCTION APPLIQUÉ SUR UNE PLAQUE EN ACIER 4340

R.Houtane[1], N.Barka[1] and S.K.Kanganroudi[1]

University of Quebec at Rimouski, Rimouski (Qc), Canada

2.1 RÉSUMÉ EN FRANÇAIS DU DEUXIÈME ARTICLE

La présente étude vise à développer un modèle de simulation numérique traitant du processus de durcissement par induction. En utilisant les outils d'analyse numérique basés sur les éléments finis, nous avons réussi à développer et à réaliser une simulation 3D du processus en utilisant l'environnement COMSOL Multiphysics, qui comprend la présentation du champ magnétique, le transfert de chaleur et la dépendance temporelle. Les résultats présentés sont considérés pour deux des matériaux couramment utilisés ; cuivre et acier AISI 4340. La bobine de chauffage par induction est une forme de U complexe pour correspondre au chef-d'œuvre. Ce projet propose l'exploration des effets et influences des paramètres du procédé sur la répartition de la température lors du chauffage appliqué à la plaque. Cette exploration sera utilisée pour déterminer les plages optimales des paramètres du processus de notre modèle. Les résultats obtenus à partir du modèle sont assez intéressants, la température requise a été atteinte en 2,5 s, la propagation de la chaleur dans le cœur est grande et la répartition de la température est uniforme tout au long de la pièce.

Mots-clés - chauffage par induction, plaque en acier 4340, modèle 3D, bobines à géométrie complexe, simulation.

Ce deuxième article, intitulé *« Modeling and simulation of the induction heating process applied to a 4340 steel plate »* fut essentiellement rédigé par moi-même ainsi que par le professeur Noureddine Barka. En tant que premier auteur, ma contribution à ce travail fut la recherche sur l'état de l'art, le développement de la méthode, la création du modèle de simulation, la gestion des résultats et la rédaction d'article. Le professeur Noureddine Barka a fourni l'idée originale. Sasan Sattarpanah Karganroudi a contribué au développement de la méthode ainsi qu'à la révision d'article.

2.2 MODELING AND SIMULATION OF THE INDUCTION HEATING PROCESS APPLIED TO A 4340 STEEL PLATE

2.2.1 Abstract

The present study aims to develop numerical simulation model dealing with the induction hardening process. Using the tools of numerical analysis based on the finite element, we managed to develop and achieve 3D simulation of the process using the COMSOL Multiphysics environment, which includes presentation of the magnetic field, heat transfer and time dependence. The results presented are considered for two of commonly used materials; copper and AISI 4340 steel. The induction heating coil is a complex U-shape to match with the masterpiece. this project proposes the exploration of the effects and influences of process parameters on the temperature distribution during heating applied to the plate. This exploration will be used to determine the optimal ranges of the process parameters of our model. The results obtained from the model are quite interesting, the required temperature was reached in 2.5s, the heat propagation in the core is great and the temperature distribution is uniform all along the part.

Keywords Induction heating, 4340 steel plate, complex shape coils, 3D model, simulation

2.2.2 Introduction

Induction hardening [34] has been extensively used in the metallurgical industry due to its remarkable productivity, energy efficiency and ability to treat and process metal parts with complex geometric shapes. This process has been widely used in many industrial applications, such as brazing [61], casting [62, 63] and surface hardening, which is applied

to mechanical parts for the automotive and aerospace industries [21, 64]. The industrial advantages of induction heating include the ability to heat specific areas of the treated part, reduce manufacturing costs and achieve high mechanical properties [10]. However, the edge effect caused by the concentration of magnetic files on the edges of the workpiece is the main disadvantage in induction heat treatment. The distribution and penetration of the induced currents and the final temperature depend on several factors, such as the machine power, frequency, heating time, and the distance between the master part and the induction coil [21, 34, 65].

Therefore, in order to obtain the desired result, many preliminary tests and metallographic analyses are required, forcing practitioners to resort to trial-and-error methods in the development of their components. In this case, simulation plays a crucial role as it helps to approach the process first qualitatively and then quantitatively with the help of appropriate tests. A numerical model was developed using a genetic algorithm to optimize the temperature distribution of an inductively heated steel cylinder, where the input parameters were the position of a single coil loop, the amplitude and the frequency of the electric current in the coil [66].

In induction heating, heat generated by electromagnetic fields and induced currents is used with rapid cooling, in the hardening of steel application, to increase the surface hardness of steel [67, 68]. The process consists of generating a high intensity of heat in a concentrated area on the surface of the metal part. An alternating current characterized by its intensity and frequency is applied to a coil which is connected to the part to be treated. A magnetic field generated directly in the coil induces a current on the metal part. This current generates heat due to the Joule effect. Figure 1 illustrates the overall induction heating process. For a given heating time, the depth of hardening of the part depends on the frequency and current in the coil. The cooling rate directly affects the final hardness profile and the residual compressive stresses [69, 70]. As a result, the temperature on the heated part rises to the austenitization point. Induction heating can be applied to a wide range of shapes and sizes and does not require physical contact between the treated component and the induction coil [71, 72]. The

AC -induced current flow decreases in density from the surface towards the interior of the part. As a result, the generated heat distribution is concentrated from the surface to a certain internal distance, which is the depth of penetration. After quenching, a very hard martensitic structure is formed in the heated area extending from the surface to the penetration depth.

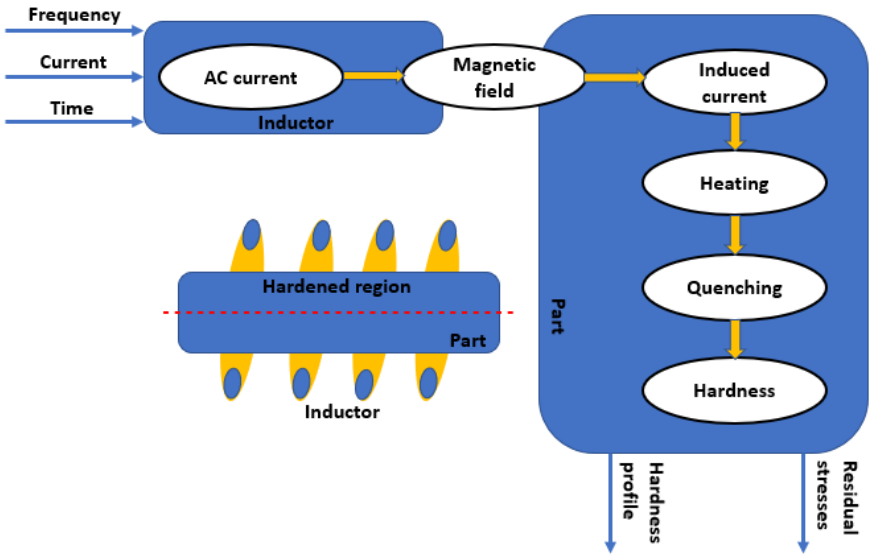

Figure 2.2.1 : Schematic representation of the induction heating process [27]

A classic industrial application of induction heating is to heat certain areas of a part above the austenitizing temperature (Ac3) so that martensite can be formed after quenching. The hardness profile must be controlled to improve wear resistance and increase contact fatigue life. Induction heating is also an environmentally friendly technology as it does not use a coating or produce carbon monoxide [1, 38].

Induction heat treatment study presents several difficulties at the level of simulation and experiment. It is difficult to master the complex electromagnetic and thermal physics involving multiple parameters and coupled physical phenomena, also the data on material properties are not accurate and vary with temperature. Adequate measurement of temperature and machine current during the heating process is a difficult experimental task because of the

rapid heating rate. Experimental and statistical methods were proposed to be suitable for solving like these problems. The right parameters must be selected to make a good statistical study, the experimental tests must be well conducted and the results obtained must be properly analyzed. There are researchers who have proposed this approach through simulation [21, 34, 73], simulation with validation [31, 74] and experiments with planning strategy [15, 75]. These studies are conducted to analyze various mechanical and thermal effects on a wide and different part shape using electromagnetic induction process to qualify or improve hardness, residual stress, deformation and final temperature distribution.

The induction process was attempted to be modeled to study the hardness profile and residual stress distribution of different geometries [56]. The accuracy and performance predictions of these models are limited by the approximations that are considered due to the non-linear behavior of the material properties. In addition, these models are specialized for some limited applications and cannot be used to understand the sensitivity of case depth to machine parameters or material properties. Consequently, it is a difficult task to reuse these results in other applications [64, 76].

Some studies have shown the important role of residual stress in the distortion of machined parts and has an important influence on the fatigue life and durability of engineering parts [77, 78]. Residual stress is the result of the part manufacturing and treatment process, especially in the process of volume expansion of the internal microstructure of the part due to heat treatment such as welding and rapid cooling of the surface hardening [78, 79]. Tensile residual stresses increase the likelihood of fatigue failure by promoting crack initiation and propagation, so they are not beneficial. In the other hand, the compressive residual stress in the surface layer is very helpful to offset the development of cracks and improve the resistance to stress corrosion cracking and fatigue behavior [79, 80]. Therefore, in the component manufacturing steps, the different processes and methods play an important role in the final distribution of residual stress [81]. In addition, many scientists are trying to develop finite element models (FEM) that can predict residual stresses caused by different manufacturing processes [82-85]. These models will then minimize distortion, while

reducing the number of steps, and modifying the processing method without affecting the properties of the part. In induction hardening, the surface of some parts is heated to a high temperature and quickly cooled. By generating a gradient of high temperature and microstructure and mechanical properties between the surface layer and the core of the part, the residual compressive stress can be imagined [10, 11].

The transformation of austenite to martensite after quenching is accompanied by an increase in hardness and volume, which is proportional to the percentage of carbon contained in the processed material [12]. This thermal expansion produces a favorable compressive residual stress state, caused by the temperature gradient and phase change, which can be predicted and controlled based on several factors involved in the induction heating process, such as the cooling rate [14] and the final temperature distribution before quenching [15, 16]. Furthermore, there is another method to measure some relevant surface temperatures and adjust the initial current in the coil by simulation to achieve the same surface temperatures. It depends on the quality of the temperature measurement equipment and on the assumptions considered in the simulation. The alternative solution is to consider the initial current density as the input variable and the maximum temperature as the simulation criterion and find the relationship between the initial current density and the power provided to the part, which is the simulation power. This power is obtained by mathematical integration of the heat source generated by the induced current, and it is useful because it is advantageously used to study the sensitivity of the hardening profile when the parameters are varied.

The synthesis of the bibliographical research shows that there is none of the works which touched the geometry such as the rectangular plate and the racks. However, the published work lacks precision in the models, and does not clearly discuss the effects of parameters such as power, speed and the geometrical factor of the part and of the inductor on the hardness profile and on the residual stresses. It would be very interesting to develop a model based on FEM simulation to study the sensitivity of the hardness profile of a thin plate in 4340 steel as a function of the parameters of the process and of the geometric factors.

The main objective of the present work is to study and test the developed model and to give another dimension to the induction heating treatment by introducing the speed as an important parameter for the treatment, thus analyze its effect on the plate and see how it affects the temperature profile at the end of treatment.

2.2.3 Method and material

2.2.3.1 Formulation

The formulation of the progressive induction heating process is described by an electromagnetic field extracted from Maxwell's equations in its time-varying form, while neglecting the displacement fields and introducing the magnetic vector potential related to the magnetic flux that could be written in the form of the equation (1).

$$\frac{1}{\mu}\nabla^2 A + j\omega\sigma A = -J_e \quad (1)$$

With A and Je, are the magnetic vector potential and the density of the current imposed in the inductor, respectively. ω = 2πf is the angular frequency of the current, and f is the frequency of the generator. μ and σ are temperature dependent properties and they respectively represent the magnetic permeability and the electrical conductivity of the material of the component to be treated. From equation (1), the density of the induced current Ji could be written as shown in equation (2).

$$J_i = -j\omega\sigma A \quad (2)$$

La résolution de l'équation (1) a permis de déterminer la densité du courant induit en fonction du potentiel vecteur magnétique, qui à son tour peut être déduit en résolvant l'équation (2). La quantité de chaleur générée à l'intérieur de la pièce métallique en raison du chauffage par effet Joule est évaluée en utilisant l'équation (3).

$$\dot{Q}_{ind} = \int_v \frac{|J_i|^2}{\sigma} dV \quad (3)$$

The heat produced by induction is fed into the heat transfer equation, in order to calculate the temperature distribution in the room. In this case, the heat transfer is described by the Fourier equation, and it is given by the equation (4).

$$\rho C \frac{\partial T}{\partial t} + \rho C V_{Trans} \nabla T = \nabla . (k \nabla T) + \dot{Q}_{ind} \quad (4)$$

Where T is the temperature. ρ, C and k are the temperature dependent properties and respectively represent the density, specific heat and thermal conductivity of the material. V_{trans} is the displacement speed field applied to the saw and which describes the translation of the latter with respect to the inductor. Part of the energy is lost by temperature differences due to convection and radiation between the room and the surrounding air. The losses of heat flow by convection $\dot{Q}_c$ and by radiation $\dot{Q}_r$ between the room and the open air are given respectively by equations (5) and (6).

$$\dot{Q}_c = h_c(T_s - T_a) \quad (5)$$

$$\dot{Q}_r = \varepsilon \sigma_s(T_s^4 - T_a^4) \quad (6)$$

Where $h_c$is the convection coefficient, ε is the emissivity and σ_s is the Stefan-Boltzmann constant.

2.2.3.2 Model

The induction heating mode applied to the part is by sweeping. The part is moved in translation along its axis of symmetry without any rotation to ensure uniformity of the temperature profile and thus the hardness profile. A simplified 3D finite element model for the part was constructed to assess the temperature distribution caused by induction heating. The inclusion of a limited part of the total length of the plate does not significantly influence the accuracy of the solution and is common practice for this type of geometry.

a) *GEOMETRY*

The plate used, the measurements of which are shown in figure 2.2.3, will be placed vertically against a U-shaped copper inductor of circular section and having a diameter of 0.25 in, in which flows a current I characterized by its external density I and its frequency. Fr. The different parts of the inductor are introduced under the COMSOL environment as shown in Figure 2.2.2.

For our model, the geometry of the inductor was set as indicated in Table 2.2-1, as well as the geometry of the plate that we will treat is indicated in Figure 2.2.3.

Table 2.2-1: Geometric parameters of the inductor (mm)

P_1	h_1	h_2	L_1	L_2	D_{ind}
15.24	20	20	22.23	38.1	6.35

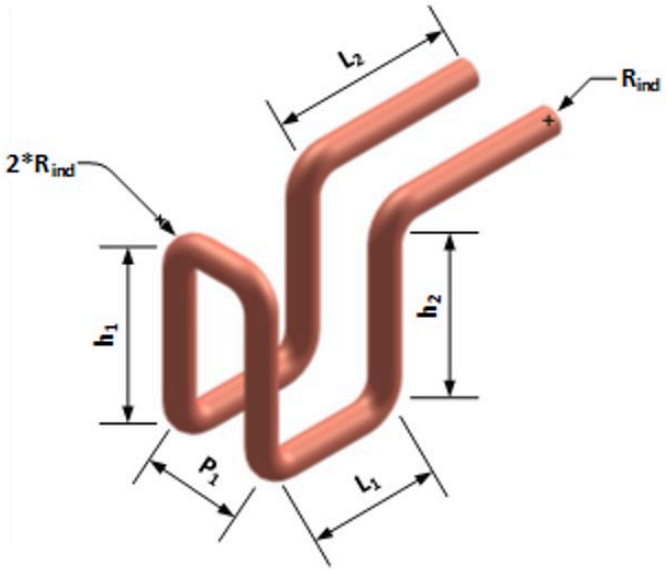

Figure 2.2.2 : Geometric parameters of the inductor

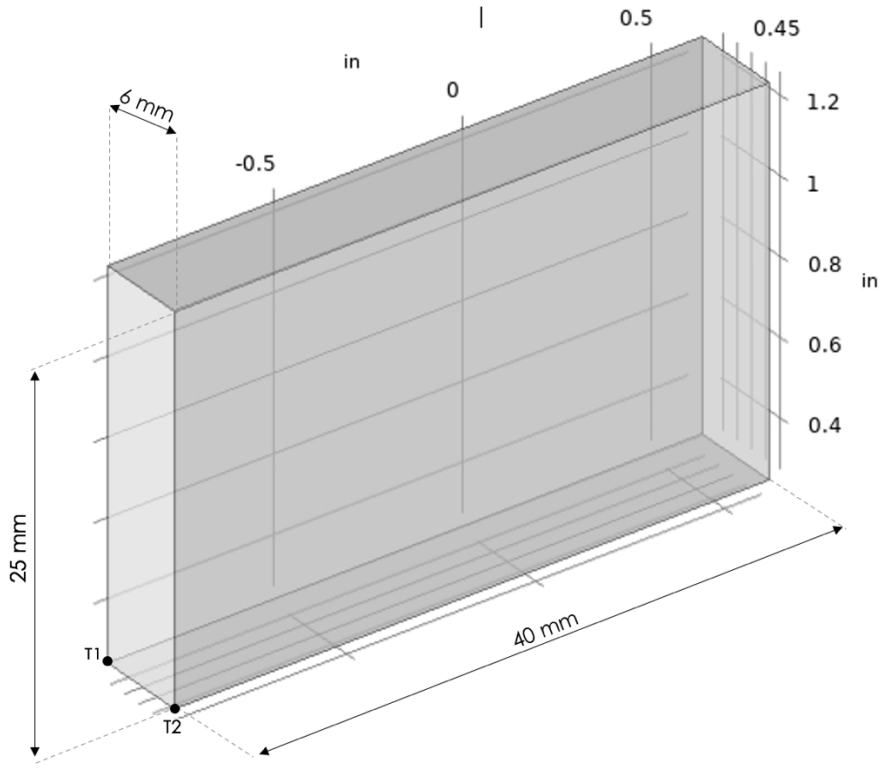

Figure 2.2.3 : The dimensions of the 4340 steel plate

b) *MATERIAL*

The material used for the plate is 4340 steel. The minimum temperature required to form austenite on the surface of the plate is approximately 850 ° C. The chemical composition of the material is shown in Table 2.2-2

Table 2.2-2 : Chemical composition of standard 4340 steel (%)

C (%)	Si (%)	Mn (%)	P (%)	S (%)	Cr (%)	Ni (%)	Mo (%)
0,38-0,43	*0,15-0,3*	*0,6-0,8*	*≤ 0,035*	*≤ 0,04*	*0,7-0.9*	*1,65-2*	*0,2-0,3*

The three material electromagnetic properties involved in the induction treatment process are: Electrical conductivity (σ), relative magnetic permeability (μ_r) and relative dielectric permittivity (ε_r). In this study, the relative dielectric permittivity is considered constant equal to 1. This assumption has no effect on the results since the displacement currents are negligible compared to the currents induced in the part.

Electrical conductivity

The electrical conductivity (σ) characterizes the ability of a material to let electric charges move freely and thus allow the passage of an electric current. It depends on temperature, chemical composition, microstructure and grain size. The electrical conductivity of the AISI 4340 steel is shown in figure 2.2.4, and from the curve we see that it decreases as a function of the temperature up to the temperature of the austenization Ac1, and beyond this temperature it can be considered constant.

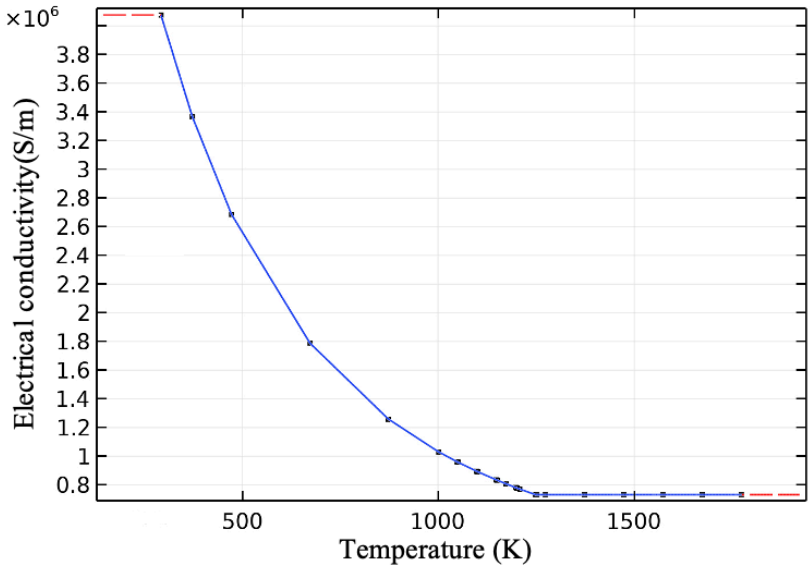

Figure 2.2.4 : Electrical conductivity of the AISI 4340 Steel

Magnetic permeability

The change of the relative magnetic permeability as a function of temperature is shown in Figure 2.2.5. First, the relative permeability remains constant (value at room temperature), then it drops rapidly until it reaches a value equal to 1 at the Curie temperature. From this temperature, the material becomes diamagnetic and its relative magnetic permeability remains constant (equal to 1) for temperatures above the Curie temperature.

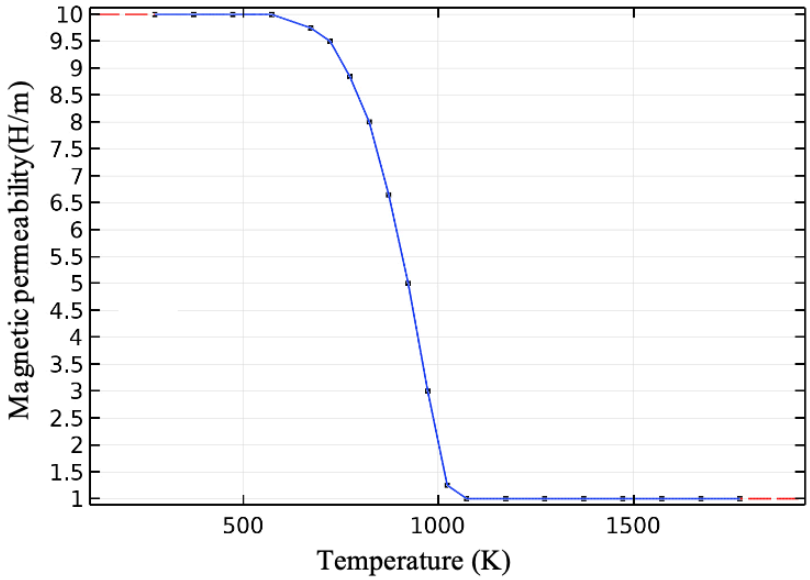

Figure 2.2.5 : Magnetic permeability of the AISI 4340 Steel

Specific heat

Specific heat (Cp) represents the amount of thermal energy that it is necessary to supply a body weighing 1kg to raise its temperature by 1°C. It depends on the structure of the material, the temperature and the heating rate. Figure 2.2.6 illustrates the evolution of this property as a function of temperature for 4340 steel. The specific heat increases slightly with temperature up to the temperature of the start of Ac1 austenitization. It then increases rapidly until reaching a maximum value of 1600 $J.Kg^{-1}.°C^{-1}$ which represents the latent heat of phase change between Ac1 and Ac3. Then, it decreases drastically before reaching Ac3 and it is assumed to be constant up to 1200 ° C. As Ac1and Ac3 temperatures depend on the heating rate, the peak latent heat is shifted to higher values.

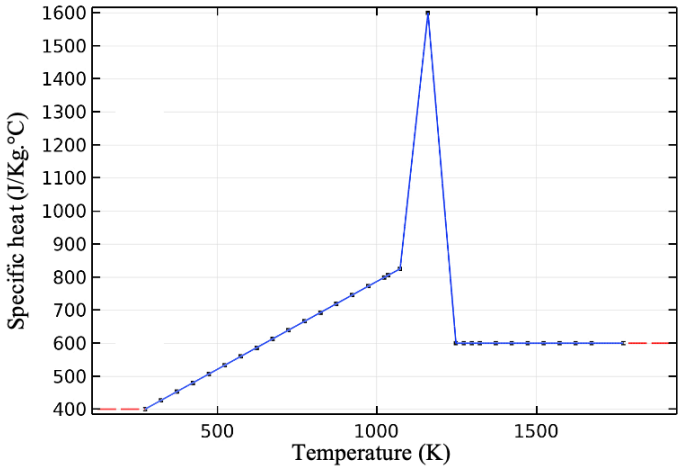

Figure 2.2.6 : Specific heat of the AISI 4340 Steel as a function of temperature

Thermal conductivity

Thermal conductivity k represents the ability of a material to conduct heat. This property is a complex function of the structure of the material (the initial treatment applied to the material), grain size, temperature and heating rate (Rudnev et al., 2003). Figure 2.2.7 shows the variation in thermal conductivity of AISI 4340 steel as a function of temperature, it decreases as a function of temperature up to the end of austenization temperature Ac3, and remains constant beyond this temperature.

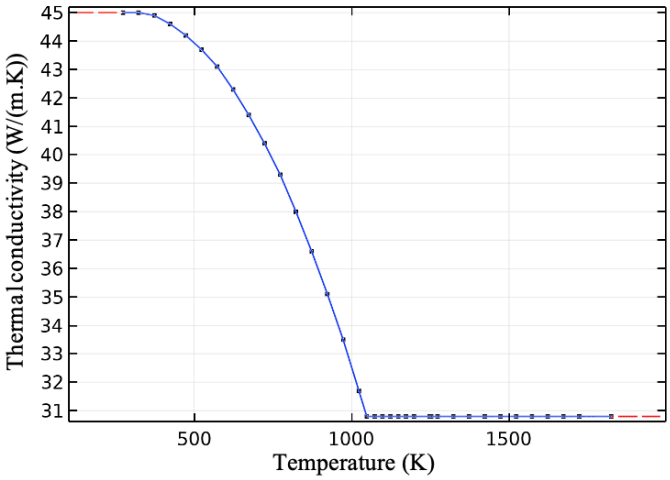

Figure 2.2.7 : Thermal conductivity of the AISI 4340 Steel as a function of temperature

The resolution domain is made up of three materials, namely AISI 4340 steel, the inductor copper and air, Table 2.2-3 summarizes the physical properties of these three materials

Tableau 2.2-3 : Material properties

Air	Material density	1.23	Kg/$\mathbf{m^3}$
	Thermal conductivity	0.5	W/(m.K)
	Relative permeability	1	1
	Specific heat	1000	J/(kg.K)
Copper	Material density	8700	Kg/m^3
	Thermal conductivity	400	W/(m.K)
	Relative permeability	1	1
	Specific heat	385	J/(kg.K)
	Electrical conductivity	5.998×10^7	S/m
AISI 4340 Steel	Material density	7850	Kg/m^3
	Thermal conductivity	k(T)	W/(m.K)
	Relative permeability	μ_r(T)	1
	Specific heat	C_p(T)	J/(kg.K)
	Electrical conductivity	σ(T)	S/m

2.2.4 Simulation

The simulation software COMSOL Multiphysics Version 5.6 was used to simulate the induction heating process. A 3D model was needed for this study, as the temperature and energy measurements had to be made at different positions across the width of the plate in order to take into account edge effects greatly affecting induction hardening.

2.2.4.1 Mesh convergence study

Once the numerical model is set up, a convergence study must be done in order to reduce the computation time without losing in terms of accuracy. This convergence study, which is focused on the mesh and the calculation time step, will allow the implementation of a robust and accurate numerical model.

Convergence was established by comparing the final values of the temperatures in order to determine the appropriate value of the mesh. The study is carried out by Comsol software, and the simulation parameters, heating time, the gap, the frequency, the current density and the speed were chosen so that the temperature at the points T1 and T2 situated the end of the plate are close to 950 °C to be sure that we will attend the austenization point.

Figure 2.2.8 illustrates the change in temperature as a function of the mesh size using the same parameter values for each of the mesh sizes studied.

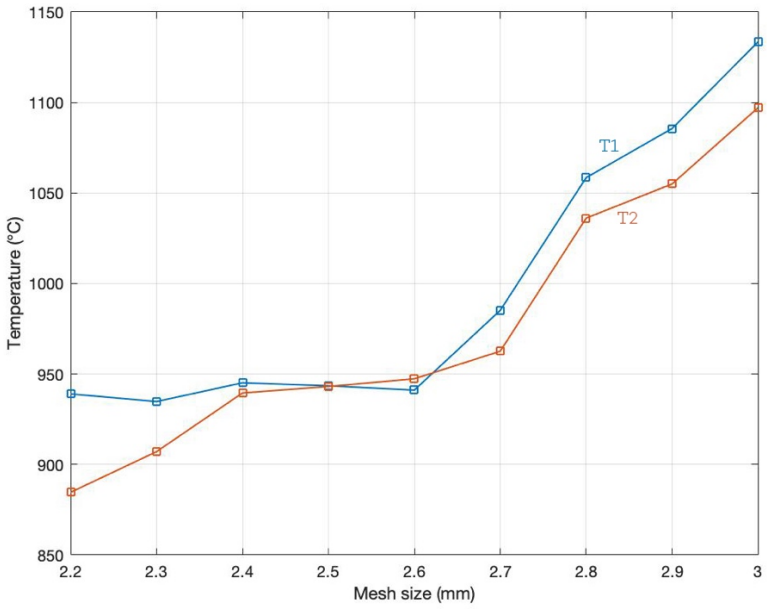

Figure 2.2.8 : Final temperature versus the mesh size

The results obtained show that there is more significant variation in temperature values from 2.6mm and below 2.4mm while the temperature at 2.5mm peaks at 945 °C for the two points T1 and T2.

The mesh size used in the study is 2.5mm. Lower values lead to very high computational efforts and time that the virtual machine cannot withstand. The elements used in the mesh are of the tetrahedral type, and the number of these elements is 12833 elements which leads to the number of degrees of freedom of 345195.

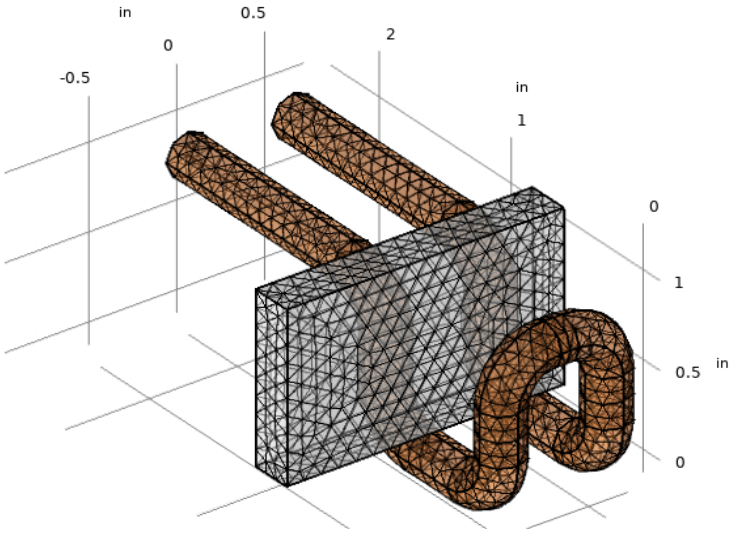

Figure 2.2.9 : Arrangement of the plate vis-à-vis the inductor with the used mesh

2.2.4.2 The process of choosing parameters

There are many parameters that are involved in the induction process, and each parameter has its degree of influence on the final temperature distribution. The approach used in this section is to adjust the current density and speed in such a way as to have an adequate temperature for the treatment. The speed of movement of the plate is along the x axis. The frequency has been adjusted to 40 kHz. The choice of this frequency is due to the small thickness and to allow the heat to penetrate deeper into the core of the plate. The imposed current density was varied until it reached a temperature of around 1000 ºC. In this case, we take a value of the order of 1.4×10^{10} A/m². The chosen simulation time is 2.5s to ensure that the plate has left the inductor and has been processed completely. The operating parameters are summarized in Table 2.2-4.

Table 2.2-4 : Input simulation parameters

Parameters	Frequency	External courant Density	Speed	Horizontal Gap	Vertical Gap	Heating time
Value	40	$1.4x10^{10}$	0.075	1/10	1/8	2.5
Unit	kHz	A/m^2	m/s	in	in	s

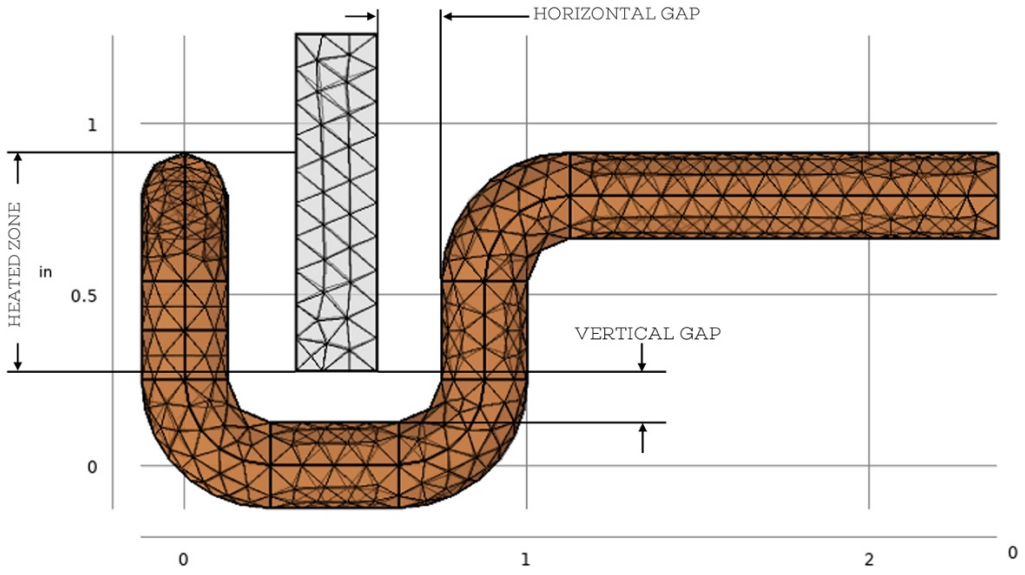

Figure 2.2.10 : Characterization of gaps and the heating zone

2.2.5 Results analysis

2.2.5.1 Temperature distribution

The history of the plate temperature as a function of time was analyzed. In order to verify the proposed heating model, the temperature on the part was measured as a function of time at the outer surface and in cross section along the length of the plate. The results of this analysis for the studied model are presented in the following paragraph.

The first configuration shown in Figure 2.2.11.a shows the volume distribution of the temperature at the end of the simulation. The second configuration shown in Figure 2.2.11.b shows equidistant cross sections of the temperature profile along the entire length of the plate. The third configuration shown in Figure 2.2.11.c shows a cross section at position x = 0 and measuring the rate of temperature propagation in the heart of the part.

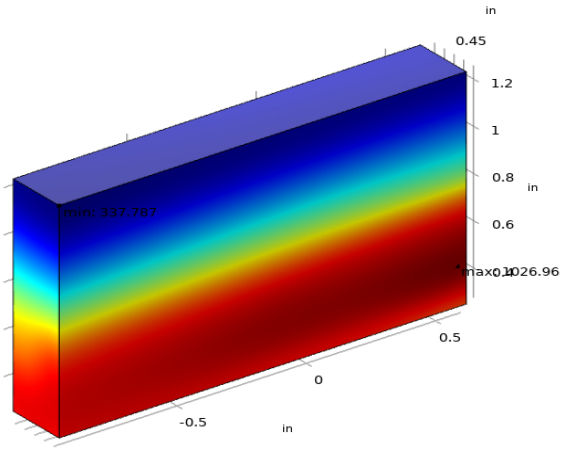

(a)

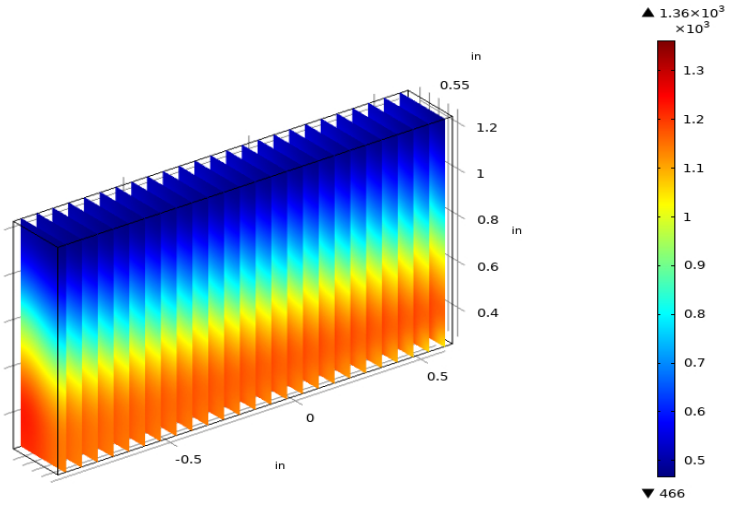

(b)

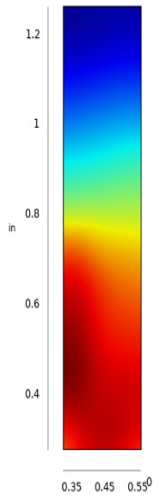

(c)

Figure 2.2.11 : Temperature profil

The history of the plate temperature as a function of time was analyzed. In order to verify the proposed heating model, the temperature on the part was measured as a function of time at the outer surface and in cross section along the length of the plate. The results of this analysis for the studied model are presented in the following section.

2.2.5.2 Évolution of the temperature

Heating started at a position on the x axis with coordinates x = 0mm and continued at the 100mm position in sequence with the heating time and rate. The maximum temperature increases successively depending on the position of the plate vis-à-vis the inductor. The maximum temperature reached is around 950 ° C. This temperature complies with the maximum limit required given the melting point of the material studied (around 1450 ° C). Similarly, the passage of the heat source does not necessarily immediately stop the temperature rise at all points because of the propagation of heat by conduction inside the heated body. On the other hand, all regions on the plate surface were heated to temperatures above the Ac3 in. Austenization temperature. The simulation can thus predict the hardened zones by assuming a complete transformation into martensite of the treated regions. These widths are directly related to the shape of the inductor and can be controlled by adjusting the geometric parameters of the latter. The height and proportion to the total height of the heat-treated areas for the model are summarized in Table 2.2-5.

Table 2.2-5 : Proportion of the treated area

Height treated (in)	1.1
Proportion treated (%)	60%

2.2.6 Discussion

In general, and after observing the results of Figure 2.2.11.c, heat penetrates deeper into the cross section of the plate, and where the inductor is closer to the part. This shows that the choice of speed and the appropriate gap according to the thickness guarantees us a greater heat propagation in the core and a more uniform distribution all along the part, as well as on both sides treated.

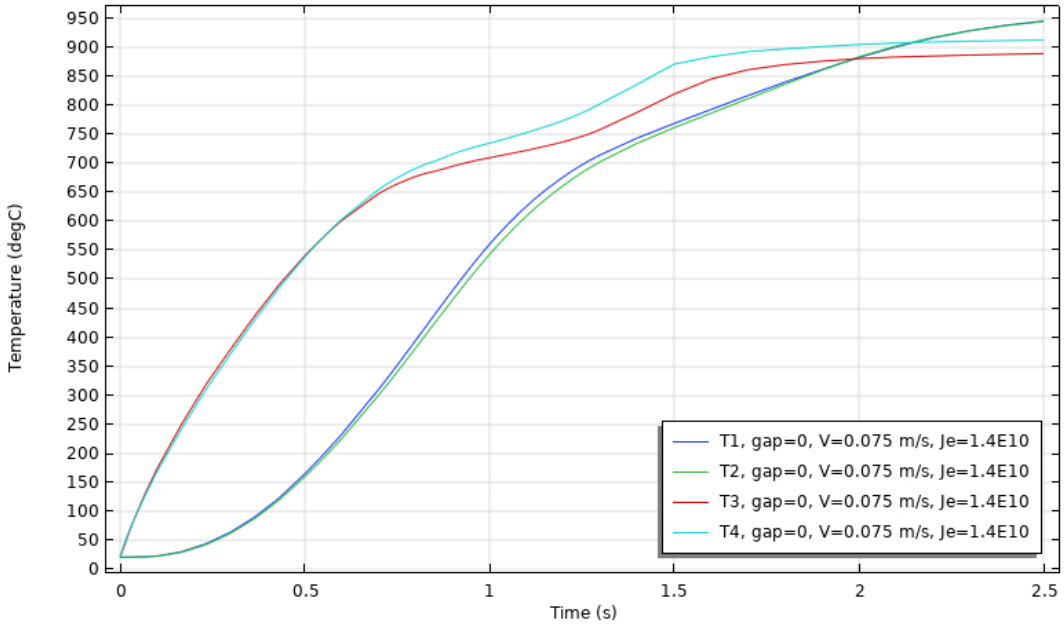

Figure 2.2.12 : Point graph of the temperature distribution

To better visualize the results, Figure 2.2.12 shows the plot of temperature evolutions for the lower quarter corners of the plate, at first sight we see that T1 and T2 (the two point of the beginning of the plate) have a similar profile, the same thing for the points T3 and T4 which are at the end of the room, the results show that the temperatures in the two corners either at the beginning or at the end of the room are almost similar especially for the two corners T1 and T2 , thus we were able to arrive at a temperature uniformity for at least two points which

are on the same plane (y, x), this proves the good parameters chosen for the simulation that we used.

At the end of the treatment (2.5s) we notice a small temperature difference between the three points knowing that for T1 and T2 they coincide in the same point 950 ° C but for T3 and T4 they have the respective values of 890 ° C and 915 ° C. We can say that we have arrived at a certain temperature uniformity since the values at the four corners are very close.

2.2.7 Conclusion

There are FEM induction models, but they are usually on axial-symmetric coils. We presented that this modeling method can also be used for windings with a more complex shape. We presented, for the first time, the induction heat treatment process applied to a 4340 steel plate using a medium frequency heat source. In this study we developed a numerical model of induction heating, which starts with the design of the complex U-shaped 3D inductor model followed by the realization of the plate volume using the COMSOL Multiphysics software used digital analysis in order to understand the different affinities and the influence of machine and geometrical parameters on the temperature evolution at the end of the heating time. The simulation therefore made it possible to define the main parameters for our model, which guarantees optimal and efficient processing.

During our study, we managed to achieve a successful 3D simulation of the induction heating process. The graphical representation and value of key parameters and their dependence on time gave a better view of the complex relationship between the electric field and the emerging asset temperature. Estimation of the specified electrical energy directly refers to the model consideration of the heating system.

In general, the results of this study made it possible to:

• Model and simulate the plate induction treatment process and thus provide enough information to understand the behavior of the cured profile based on key process parameters.

• Determine the temperature distribution at each point treated on the plate and at each instant of heating time.

• Select the optimal key process parameter ranges, note the current density, speed and horizontal gap, which ensure adequate and deep temperature distribution on the plate surface.

However, if this part constitutes a study and simulation of the thermal and metallurgical phenomena of the induction heating process, it is necessary to consolidate it by optimization studies targeting the various parameters of this process, as well as experimental validations.

CHAPITRE 3
ÉTUDE DU PROFIL DE TEMPERATURE D'UNE PLAQUE EN ACIER 4340 TRAITE PAR INDUCTION EN FONCTION DES PARAMÈTRES MACHINES ET FACTEURS GÉOMÉTRIQUES

R.Houtane[1], N.Barka[1], S.K.Kanganroudi[1] and L.Benabbou[1]

University of Quebec at Rimouski, Rimouski (Qc), Canada

3.1 RÉSUMÉ EN FRANÇAIS DU DEUXIÈME ARTICLE

La présente étude vise à déterminer l'effet de chaque paramètre impliqué dans le processus de chauffage par induction sur la distribution de température finale d'une plaque d'acier AISI 4340 et de développer des modèles de simulation numérique traitant du processus de durcissement par induction appliqué à une plaque d'acier 4340. Ce projet propose l'exploration des effets et influences des paramètres du procédé sur la répartition de la température lors du chauffage appliqué à la plaque. Une approche structurée et globale a été développée pour concevoir un modèle efficace basé sur l'analyse de la variance (ANOVA) pour l'estimation de la qualité et la prédiction des profils de température. Les résultats obtenus démontrent que le modèle statistique était capable de prédire avec précision le comportement de la température, et montre que l'effet de la densité de courant externe est important, aussi les graphiques RSM montre la meilleure combinaison des paramètres qui minimise l'effet de bord et améliore la qualité de la répartition de la température. Dans la phase finale, un test de simulation a été réalisé sur COMSOL pour valider les résultats et le modèle de prédiction.

Mots-clés - Chauffage par induction, tôle d'acier 4340, Simulation, Optimisation, ANOVA, RSM**.**

Ce troisième article, intitulé *« study of the temperature profile of a 4340 steel plate treated by induction depending on machine parameters and geometric factors »* fut essentiellement rédigé par moi-même ainsi que par le professeur Noureddine Barka. En tant que premier auteur, ma contribution à ce travail fut la recherche sur l'état de l'art, le développement de la méthode, la création du modèle de simulation et de prédiction, la gestion des données et résultats et la rédaction d'article. Le professeur Noureddine Barka a fourni l'idée originale. Sasan Sattarpanah Karganroudi et Loubna Benabbou, les troisième et quatrième auteurs ont contribué au traitement des données de simulation, au développement de la méthode ainsi qu'à la révision d'article.

3.1 *STUDY OF THE TEMPERATURE PROFILE OF A 4340 STEEL PLATE TREATED BY INDUCTION DEPENDING ON MACHINE PARAMETERS AND GEOMETRIC FACTORS*

3.1.1 Abstract

The present study aims to determine the effect of each parameter involved in the induction heating process on the final temperature distribution of an AISI 4340 steel plate develop numerical simulation models dealing with the induction hardening process applied to a 4340 steel plate. this project proposes the exploration of the effects and influences of process parameters on the temperature distribution during heating applied to the plate. A structured and comprehensive approaches was developed to design an efficient model based on analysis of variance (ANOVA) for the estimation of quality and the prediction of temperature profiles. The obtained results demonstrate that the statistical model was able to predict accurately the behavior of temperature, and shows that the effect of the external current density is important, also the RSM graphs shows the best combination of the parameters that minimizes the edge effect and improve the quality of the temperature distribution. In the final phase, a simulation test was conducted on COMSOL to validate the results and the prediction model.

Keywords **-** Induction heating, 4340 steel plate, Simulation, Optimization, ANOVA, RSM

3.1.2 Introduction

The induction hardening process is a revolutionary process that is currently used in the automotive and aerospace industry. Indeed, this process is distinguished by its multiple capacity and several advantages. Among these advantages, the process can be easily automated in production lines and it offers a very low cost compared to the thermochemical process [10]. Induction hardening of steels uses heat generated by magnetic fields and armature currents with rapid quenching to approve the hardness of the steel [31, 34]. The inductor, which can take different shapes depending on the heating model required and the shape of the room, is powered by the AC generator. The flow of alternating current through the inductor generates an alternating electromagnetic field which passes through the workpiece. This electromagnetic field induces currents that create heat which heats the room by the Joule effect [4]. The process thus exploits the heat generated by these induced currents and heats the part until it reaches the austenitization temperature followed by rapid cooling (quenching) in water or oil to increase the surface hardness of the part [57]. The process of induction heating depends on several parameters, and among the most important are the frequency of the current which is in direct relation to the depth of penetration of the heat, as well as the density of the current, the speed, the heating time [20] and the geometric parameters. the geometric parameters concern the shape, size, dimensions and position of the part relative to the inductor [21, 86]. The study of heat treatment by induction is done mainly by simulation [71, 87] or by an experimental study, it is difficult to manage the complexity of the geometries of the part and of the inductor [88], as well as the multitude of parameters and coupling of physical phenomena [3, 51]. Researchers are more likely to merge the two, simulation with experimental validation [31, 68, 86, 89]. Studies are often analyzed for the effects of parameters to determine the temperature distribution during the process and to improve hardness, residual stress and strain [3, 60, 90]. As well as the use of flux concentrators to better improve the quality of heat treatment [91]. They concentrate electromagnetic waves in specific regions of the 4340 steel plate, which gives us the ability to control the propagation of induced currents [89, 92, 93].

Foregoing studies have generally attempted to change the induction machine parameters such as the frequency, the amplitude of the induced current and the type of coil. In this case, magnetic flux concentrators are used to improve the quality of the heat treated parts [76, 94]. These magnetic concentrators concentrate the electromagnetic waves on very specific areas of the workpiece, which allows to control the penetration of the induced currents and the distortion of the temperature. A simulation model was developed to study the electromagnetic multiphysics transformation for a plane induction heating process using a metal powder-bonded magnetic flux concentrator (MPB -MFC). A response surface methodology (RSM) was applied to describe the comprehensive link between the induced current and frequency as input variables and the surface temperature as output [94]. Even if this technique improves the efficiency and quality of induction heat treatment, there is some disadvantages because of the metal powder-bonded magnetic flux concentrators which is affected in the operation, for example, by the degradation of magnetic particles and rust. They also need to be inspected and repaired at regular intervals, if necessary, which significantly increases the overall cost of the system [95].

Generally, to improve the efficiency of induction treatment, manufacturers try to modify machine parameters such as frequency, power of the machine or the shape of the inductor consequently they neglect the speed of movement of the part in relation to the inductor, a parameter often confused with the heating time. The effects of movement speed are not analyzed statistically, and no prediction model to estimate the temperature profile based on the parameters involved has yet been developed.

During this study, a modeling of the procedure was made taking into account the assumptions and realistic approximations by carrying out an adequate mesh study. As a large number of simulations have been performed, each simulation involves a unique combination of geometric and machine parameters that characterize induction heat treatment, such as current density, speed and horizontal gap. Finally, the results of the simulations are analyzed statistically, and prediction models have been developed using ANOVA to predict the temperature profile.

3.1.3 *Experimental design*

We have in our model three factors that we want to optimize and to control how they influent the heat transfer distribution, the design of experiment is presented in Table 3.1-2 and we mainly look as parameters the external current density "Je", the speed "V" and the horizontal gap "gap". The design of experiment presented below followed Taguchi method, as it is used in most simulation studies similar to this paper, this technique achieves a high level of quality while strictly limiting the number of tests needed to collect all statistically relevant data. The first machine parameter, the external current density varies from $1.4x10^{10}$ to $1.8x10^{10}$ A/m² with a step of $0.2x10^{10}$ A/m², while the second one is the transitional speed of the workpiece relative to the coil it's varies from 0.075 to 0.09 m/s with a step of 0.0075 m/s. The geometrical factor which is the original gap varies from 0 to 0.09 po with a step of 0.045 po.

Table 3.1-1 : Input parameters and their level

Parameters	**Unit**	**Code**	**Level 1**	**Level 2**	**Level 3**
External current density	($\times 10^{10}$ A/m²)	D	1.4	1.6	1.8
Speed	m/s	V	0.075	0.0825	0,09
Horizontal gap	in	G	0	0.045	0.09

Table 3.1-2 : Taguchi design of experiment

Tests	G	V	D
1	0	0.075	1.4
2	0	0.0825	1.6
3	0	0.09	1.8
4	0.045	0.075	1.6
5	0.045	0.0825	1.8
6	0.045	0.09	1.4
7	0.09	0.075	1.8
8	0.09	0.0825	1.4
9	0.09	0.09	1.6

After we've obtained the results of the nine simulations performed using COMSOL Multiphysics, the results extracted for each simulation are the four-temperature profile T_1, T_2, T_3, T_4 situated in the four lower corners of the workpiece as shown at the figure for the two periods of heating time 1.25s and 2.5s.

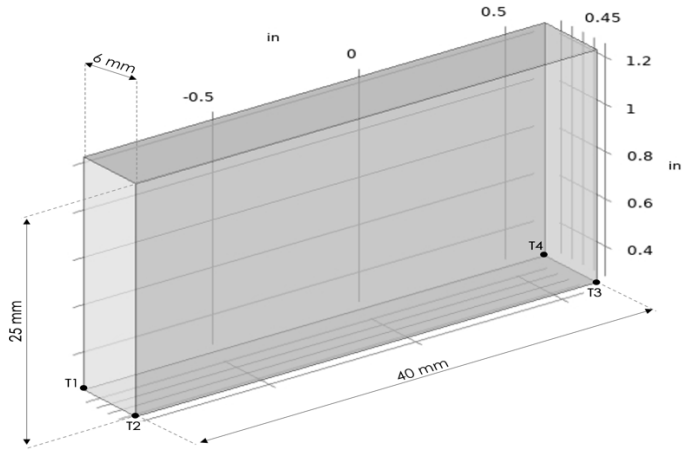

Figure 3.1.1 : The 4340 steel plate

The results obtained are shown on the Table 3.1-3 below.

Table 3.1-3 : Simulations results

Le temps	**1.25 s**				**2.5 s**			
Temperature at the four corners of the plate	T_1	T_2	T_3	T_4	T_1	T_2	T_3	T_4
1	697.95	684.58	747.27	787.84	946.64	945.65	890.36	913.69
2	860.77	860.66	905.19	926.92	1060.7	1058.2	994.23	1018.3
3	1021.8	1004.9	1019.6	1045	1299.1	1282.5	1226.23	1260.5
4	779.88	808.35	868.5	926.68	1017.6	1033.2	941.34	1006.9
5	934.51	969.9	951.26	1034.5	1205.7	1235.1	1135.5	1234.3
6	778.33	814.11	840.77	920.84	975.05	991.69	907.79	950.81
7	866.16	961.31	916.07	1062.9	1189.3	1258	1096.5	1272.1
8	737.87	809.82	762.88	921.71	964.18	1006.4	891.94	971.51
9	873.31	972.11	906.15	1030.9	1130.9	1205.9	1026.5	1196.9

As first impression we can already see that the temperature at the four corners doesn't go above the melting temperature of the AISI 4340 steel. Which means the configurations chosen are typical and considers the thermal constraints. And for the last heating time 2.5s we can also see that the temperature is higher that the austenization temperature of the 4340 steel at the four surface points of the part. Those results will be discussed using the ANOVA analysis and regression equations. The RSM models will also be presented in the next part of the paper.

In this study, to make a better presentation and discussion of our results we divided the work into two parts. The first part will discuss the analysis and the contribution of the parameters on the four temperatures at 1.25s. And the second part will be the same analysis bit this time for 2.5s and we will adopt this notation ($T_{1-2.5s}, T_{2-2.5s}, T_{3-2.5s}, T_{4-2.5s}$) for a better distinction between the two times.

3.1.4 Effects of the parameters on temperature

3.1.4.1 Anova results

Having the results of a simulation is only the beginning of the study itself. Since it is already apparent from the beginning of this study that the effects of the chosen parameters on the part are considerable. In fact, to further investigate the relationship between the variables within the simulation, we had to use an ANOVA method which is related to variance. And more precisely the stepwise method is the one used in this study with Minitab™.

As this is a statistical method based on the law of total variance, the variance is split into components attributable to different sources of variation[96]. In other words, we look for the effects of the different parameters on the temperature and with the ANOVA analysis we try to quantify these effects and calculate the contribution of each parameter on the temperature. The first step of this analysis is the ANOVA table that presents the sources for each temperature and those are the parameters affecting, the degrees of freedom (df) which is the number of independent variables in our regression model is also the amount of information in our data. The sequential sums (Seq SS) of squares are measures of variation for different components of the model, they are also used to calculate the p-value of a term. This also depends on the order of the terms that are entered into the model.

The contribution is as clear as the name and displays the percentage that each source in the ANOVA table contributes to the total sequential sum of squares[97]. The adjusted sum of squares is the same as the sequential one, but the order is not important. Adjusted mean squares measure the variation that a term or pattern explains, assuming that all other terms

are in the pattern, regardless of the order in which they were entered. Unlike adjusted sums of squares, adjusted mean squares take into account degrees of freedom. The F-value is the test statistic used to determine whether the term is associated with the response. And the p-value is a probability that measures the evidence against the null hypothesis [98]. Lower probabilities provide stronger evidence against the null hypothesis in this case, the null hypothesis would be that all temperatures are equal to the austenization temperature which would be equal to 850ºC. The results of the analysis of variance for the four temperatures at the two different times in this study are presented in Table 3.1-4 and 3.1-5.

Table 3.1-4 : Analyze of variance for the temperatures at 1.25s

Temperatures	**Source**	**DF**	**Seq SS**	**Contribution**	**Adj SS**	**Adj MS**	**F-value**	**P-value**
T_1	G	1	1774.4	2.16%	1774.4	1774.4	12.94	0.016
	V	1	18089.6	22,00%	18089.6	18089.6	131.90	0.000
	D	1	61675.5	75.01%	61675.5	61675.5	449.71	0.000
	Error	5	585.7	0.83%	685.7	137.1		
	Total	8	82225.2	100.00%				
T_2	G	1	6214.6	6.78%	6214.6	6214.6	37.24	0.002
	V	1	18914.7	20,65%	18914.7	18914.7	113.35	0.000
	D	1	65647.0	71.66%	65647.0	65647.0	393.39	0.000
	Error	5	834.4	0.91%	834.4	166.9		
	Total	8	91610.6	100.00%				
T_3	G	1	1260	2.09%	1260	1260.3	3.38	0.126
	V	1	9179	15,25%	9179	9179.1	24.59	0.004
	D	1	47884	79.55%	47884	47884.5	128.26	0.000
	Error	5	1867	3.10%	1864	373.3		
	Total	8	60191	100.00%				

T_4	G	1	10901.3	17.25%	10901.3	10901.3	92.41	0.000
	V	1	8016.9	12,68%	8016.9	8016.9	67.96	0.000
	D	1	43692.4	69.13%	43692.4	43692.4	370.36	0.000
	Error	5	589.9	0.93%	589.9	118.0		
	Total	8	63200.5	100.00%				

Table 3.1-5 : Analyze of variance for the temperatures at 2.5s

Temperatures	**Source**	**DF**	**Seq SS**	**Contribution**	**Adj SS**	**Adj MS**	**F-value**	**Pvalue**
$T_{1-2.5s}$	V	1	10543	8.48%	10543	10543	12.97	0.011
	D	1	108873	87.60%	108873	108873	133.99	0.000
	Error	6	4875	3.92%	4875	813		
	Total	8	124291	100.00%				
$T_{2-2.5s}$	G	1	5640	4.12%	5640	5640	4.76	0.081
	V	1	9861	7.21%	9861	9861	8.33	0.034
	D	1	115332	84.34%	115332	115332	97.43	0.000
	Error	5	5918	4.33%	5918	1184		
	Total	8	136751	100.00%				
$T_{3-2.5s}$	V	1	8995	7.90%	8995	8995	8.25	0.028
	D	1	98340	86.36%	98340	98340	90.22	0.000
	Error	6	6540	5.74%	6540	1090		
	Total	8	113876	100.00%				
$T_{4-2.5s}$	G	1	10252	6.00%	10252	10252	5.97	0.058
	V	1	7741	4.53%	7741	7741	4.51	0.087
	D	1	144426	84.46%	144426	144426	84.15	0.000
	Error	5	8581	5.02%	8581	1716		
	Total	8	171001	100.00%				

After looking to each column of the ANOVA table, the first thing we have to mention is the small value of the error for the eight temperatures. A small error means that the majority of the variation is due to the parameters as they are the ones who affects the most our results. It seems also that the external current density is the parameter that affect the most the temperature for all the times. This can be shown by the contribution percentage of the current density D in the eight ANOVA tables, this means that the external current density plays the big role in the variation if the temperature. We can also see the little effect of the speed V in the temperatures T_1, T_2 and T_3 above the horizontal gap G that have a negligible effect at these temperatures except for the T_4 in which it contributes 17,25% of the variation of this temperature. In the two tables of $T_{1-2.5s}$ and $T_{3-2.5s}$ we can remarque that the horizontal gap has no effect which justifies the fact that it does not appear in the analysis of variance table.
In general, this analysis of variance clearly shows that there is a relationship between the parameters and the result. Indeed, for all distances and for each parameter.
For the model analysis we will divide our study in two for the two heating times 1.25s and 2.5s to better analyze the results obtained.

3.1.4.2 Model analysis

ANOVA being such a strong statistical procedure to research data also can present us with the regression of y on x for every distance. this sort of equation is employed to get the connection between data sets if it exists [99] and therefore the existence of it's been proven within the analysis of variance in Table 6. the sector of modeling is extremely broad and there are several ways to make models of phenomena or maybe series of experiments. For the collected data, multiple linear regression was chosen because it's among the only in terms of calculation but has good reliability as shown by many researchers who have applied it in their work[100, 101] . Multiple linear regression equations contain an output calculated from the input parameters with coefficients calculated by the last mean square method. The model obtained for this study considers three parameters, external current density, speed and the horizontal gap and therefore the different interactions that appeared on the ANOVA table

presented. The models are going to be wont to predict approximations of the space variation for future experiments.

The generated models are represented below:

At 1.25s of heating time

$$T_1 = -558.9 - 382\ G + 7321\ V + 506.9\ D \quad (1.1)$$

$$T_2 = -610.4 + 715\ G + 7486\ V + 523.0\ D \quad (1.2)$$

$$T_3 = -251 - 322\ G + 5215\ V + 446.7\ D \quad (1.3)$$

$$T_4 = -165{,}5 + 947.2\ G + 4874\ V + 426.7\ D \quad (1.4)$$

At 2.5s of heating time

$$T_{1-2.5s} = -451 + 5589\ V + 673.5\ D \quad (2.1)$$

$$T_{2-2.5s} = -473 + 681\ G + 5405\ V + 693.2\ D \quad (2.2)$$

$$T_{3-2.5s} = -438 + 5163\ V + 640.1\ D \quad (2.3)$$

$$T_{4-2.5s} = -586 + 919\ G + 4789\ V + 775.7\ D \quad (2.4)$$

The effect of the external current density cannot be neglected, even if the value of the coefficient is small, as it emerged as a key factor in our study. Another important aspect of this model is its standard deviation and R-squared. These are the factors which will make sure that our models are reliable or not. In fact, the R-squared may be a statistical measure that represents the proportion of the variance of a variable explained by the variables within the regression model[102]. Adjusted R-squared may be a modified version of R-squared that has been adjusted for the number of predictors in our model. In this analysis the values of R-squared and the adjusted R-squared are quite high for all the temperatures. Table 3.1-6 and 3.1-7 presents the values of these factors simultaneously for the times 1.25 and 2.5s and it

appears that for all the temperatures (T_1, T_2, T_3, T_4) and $(T_{1-2.5s}, T_{2-2.5s}, T_{3-2.5s}, T_{4-2.5s})$ the R-squared is higher than 0.91 which shows a good reliability of the model and prevents it from overfitting.

Table 3.1-6 : Model summary at 1.25s of heating time

Source	**Standard deviation**	**R-squared**	**R-squared adjusted**
$\boldsymbol{T_1}$	11.7108	99.17%	98.67%
$\boldsymbol{T_2}$	12.9180	99.09%	98.54%
$\boldsymbol{T_3}$	19.3217	96.90%	95.04%
$\boldsymbol{T_4}$	10.8615	99.07%	98.51%

Table 3.1-7 : Model summary at 2.5s of heating time

Source	**Standard deviation**	**R-squared**	**R-squared adjusted**
$\boldsymbol{T_{1-2.5s}}$	28.5056	96.08%	94.77%
$\boldsymbol{T_{2-2.5s}}$	34.4048	95.67%	93.08%
$\boldsymbol{T_{3-2.5s}}$	33.0161	94.26%	92.34%
$\boldsymbol{T_{4-2.5s}}$	41.4279	94.98%	91.97%

One of the objectives of this study is to find a model that gives the most valid prediction of the temperature given current density, horizontal gap and speed. The statistical study ANOVA, gives equations that describe the predicted relationship between temperatures as a function of all parameters for the four lowest corners of the plate. The presented model also predicts the results for the same level of parameters that we defined in our experimental design in the previous section. The predicted results and the experimental result can be

presented in the same graph to compare the accuracy of our model. This comparison can be seen in Figures 3.1.1 and 3.1.2 for the two times 1.25 s and 2.5 s.

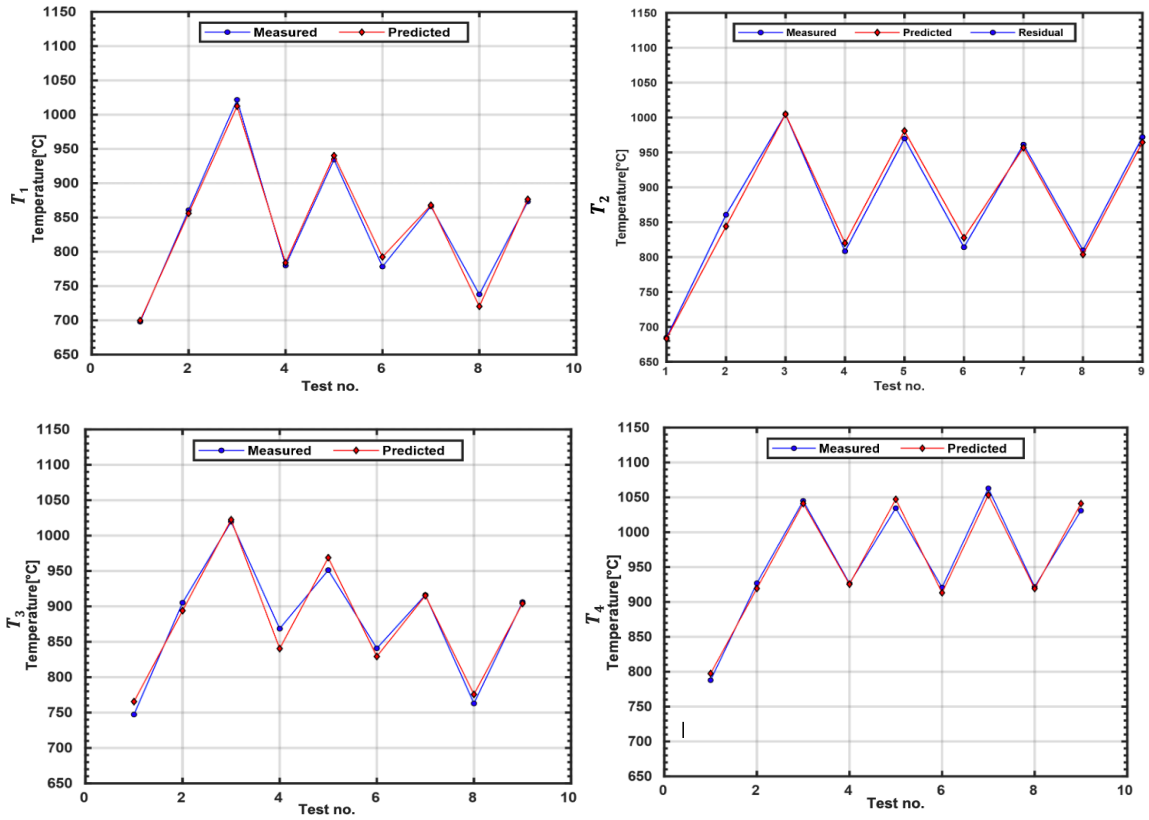

Figure 3.1.2 : Experimental data vs Predicted value for the temperatures at 1.25s

The experimental result and the prediction on one axis and the number of tests on the other, it is clear for each simulated response value, the predicted value is consistent with that measured, due to the low value of the residuals errors. Consequently, for each value of the temperatures, the predicted and simulated curves are nearly identical, which explains the good agreement between the predicted and the measured values. The results of the curves show that the prediction equation can provide a satisfactory level of accuracy with the simulation results.

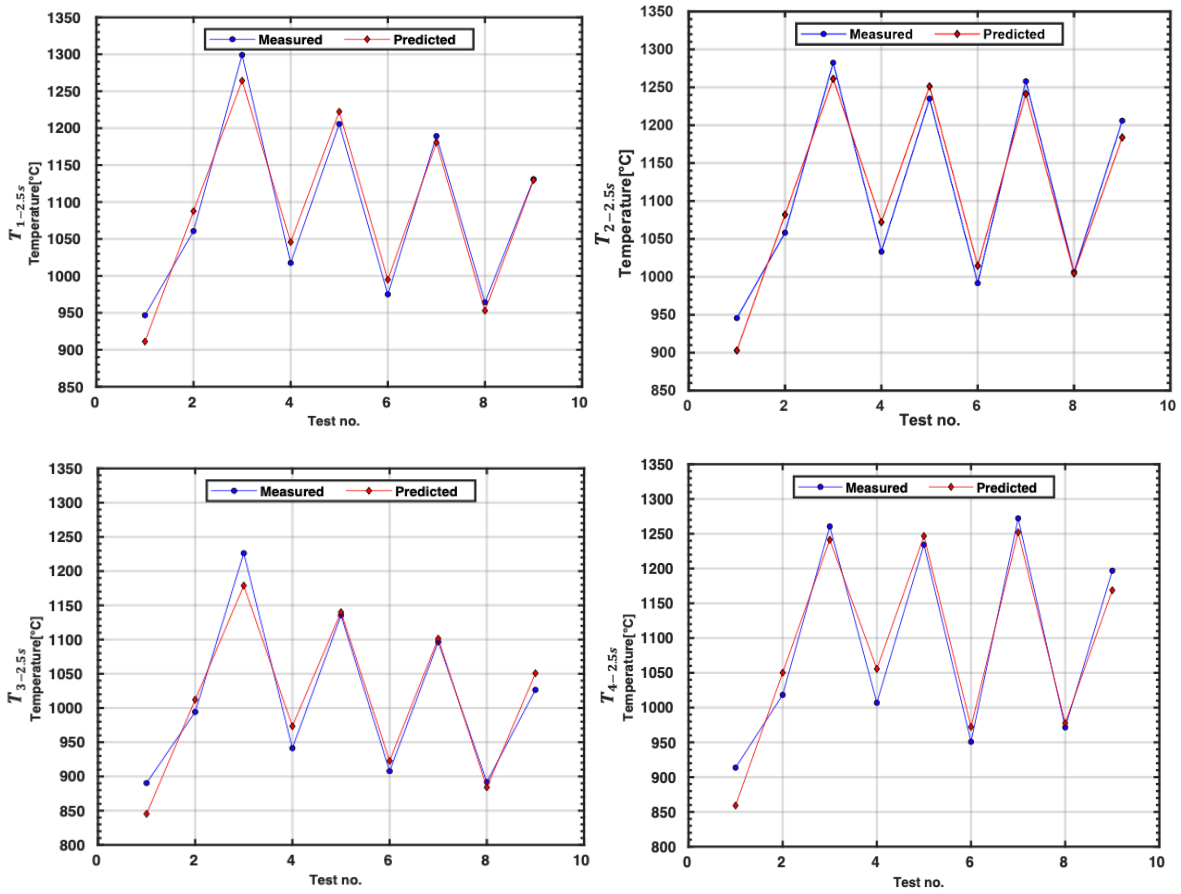

Figure 3.1.3 : Experimental data vs Predicted value for the temperatures at 2.5s

3.1.4.3 Effects plots

To have a far better visualization of the results presented in Tables 3.1-4 and 3.1-5 for the analysis of variance and to ascertain the consequences of every parameter on the result, we required the utilization of effect graphs on Minitab to offer a far better understanding of the result of our study. A main effects plot may be a plot of the typical response values at each level of a design parameter or process variable. This graph is often wont to compare the relative strength of the consequences of varied factors. The sign and magnitude of a main

effect would tell us about the direction of the effect, i.e., whether the mean response value is increasing or decreasing, and the magnitude tells us of the strength of the effect [103].
The next figures present us an overview of the effect of the different parameters on the outcome of our study for both times 1.25 and 2.5s.

At 1.25s of heating time

The figure 3.1.3 shows the effect of respectively, the horizontal gap, the speed and the external current density, on the temperatures at the four lower corners of the plate. From these plots, we can see for the temperatures $T_1$and T_3 at both corners 1 and 3 that a variation of 0.09[in] in the gap will provoke a small variation of 30 degºC on the temperature, in other words an increase of the gap decreases the temperature at these corners. The speed and the current density are different and their variation is more important on the outcome. The more both of those parameters increase, the more our temperature have an important value. In fact, an increase of 0.4×10^{10} A/m² of the current density, the temperature at the four corners increases for about 200 at T_1, 210 at T_2, 175 at T_3 and 180 degºC at T_4. The speed affects the temperature less than the current density does that is to say that when the speed increases for about 0.015m/s the temperature increases for approximately a mean of 96 degºC.

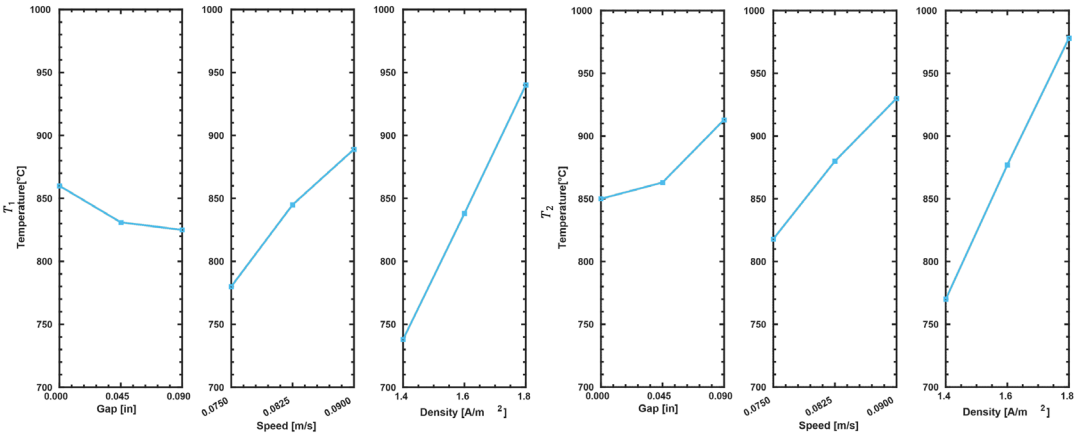

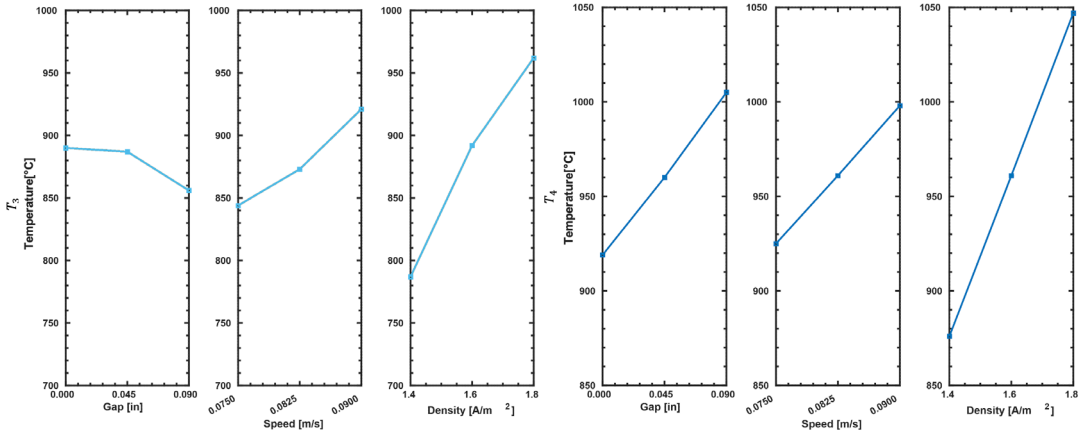

Figure 3.1.4 : Effects plot for the four temperatures (T_1, T_2, T_3, T_4) at 1.25s

At 2.5s of heating time

The of the effects for the other four temperatures at the last heating time 2.5s are presented in Figure 3.1.4 and the same observation can be made. The main parameters that affect the outcome are the external current density and with a degree less the speed. When the current density goes up from 1.4 to 1.8 ($\times 10^{10}$ A/m²), the temperature goes from 960 to 1230, from 980 to 1260, from 900 to 1150 and from 940 to 1250 degºC for respectively $T_{1-2.5s}, T_{2-2.5s}, T_{3-2.5s}$ and $T_{4-2.5s}$. The speed also plays a role in the variation of the outcome as it always affects the temperature by 80 degºC at each temperature. On another hand, the horizontal gap is the weakest parameter of the variation of the temperature is it affects depending on the value of the gap variation at 0.09[in] for the $T_{2-2.5s}, T_{4-2.5s}$ it goes respectively from 1050 to 1150 and from 1000 to 1160 degºC. And for the gap value when it goes from 0 to 0.045 the temperature decreases every time specially for the $T_{1-2.5s}$ *and* $T_{3-2.5s}$ it goes respectively from 1000 to 1065 and from 1035 to 995 degºC.

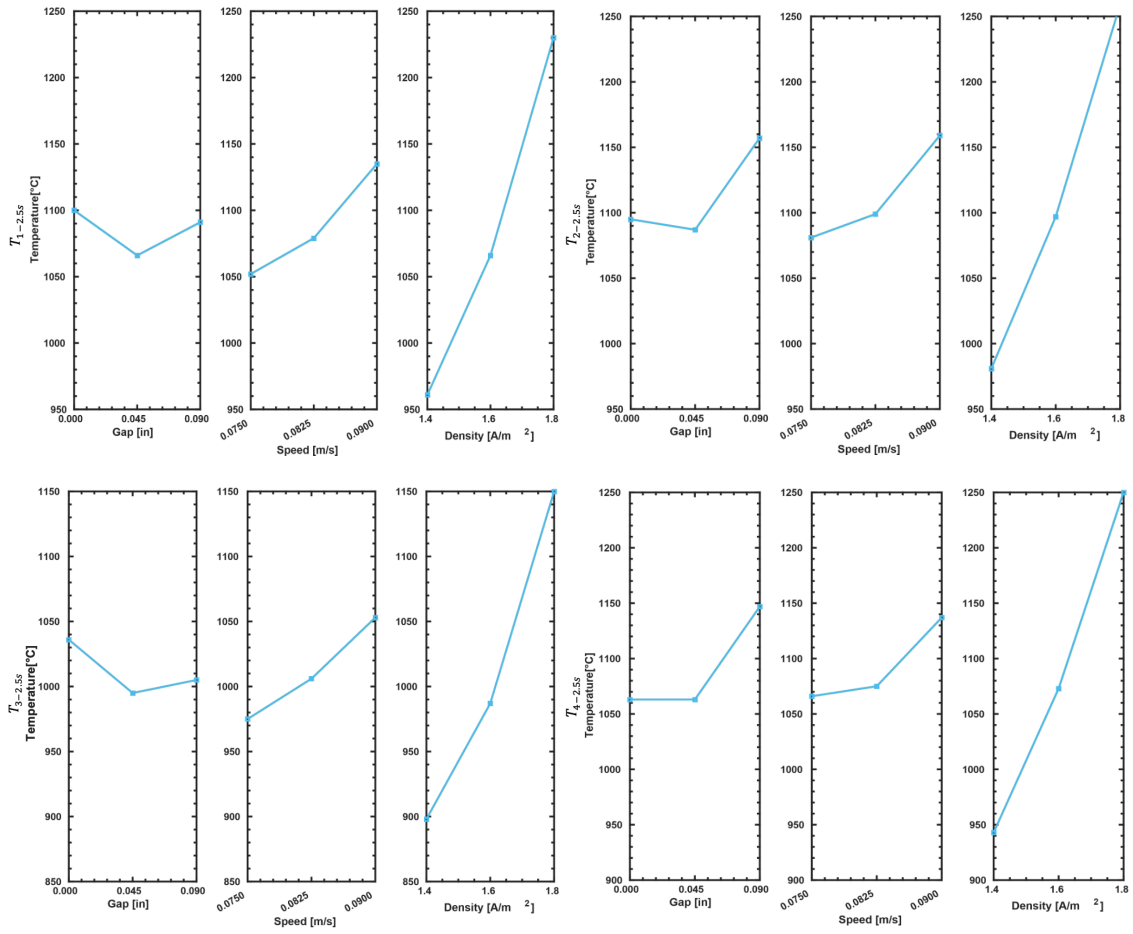

Figure 3.1.5 : Effects plot for the four temperatures ($T_{1-2.5s}, T_{2-2.5s}, T_{3-2.5s}, T_{4-2.5s}$) at 2.5s

3.1.4.4 Response surface method

Response surface method RSM is employed for modeling and analysis of problems during which a response of interest is influenced by several variables, with the aim of optimizing this response, CCDs are among the most RSMs utilized in experimental design. RSM is additionally presented during this study because it's a strong tool to output inferences and conclusions from the acquired results of various processes[94]. RSM creates contour lines that provides a clear idea of the consequences of the parameters on the result and may

help us optimize the results and avoid some critical points where the result could also be far outside the wants, we've defined for various studies. This method is one among the simplest for predicting values compared to other methods [104]. Response surfaces are plotted by holding the worth of 1 factor at one level and ranging the opposite factors to ascertain the response of the result. The main goal of this study is to try to have the same temperature value at the four corners at the same time.

At 1.25s of heating time

At this time, we don't worry about the value of the temperature since it's the middle of the heating time but the objective here is to have an equal value of the temperature for the four corners T_1, T_2, T_3, T_4.

Keeping in mind that the austenization temperature for the AISI 4340 steel is 850 ºC so it should be attended at the end of the treatment, this is why at 1.25s according to Figure 6 the temperature T_1 the best results would be acquired

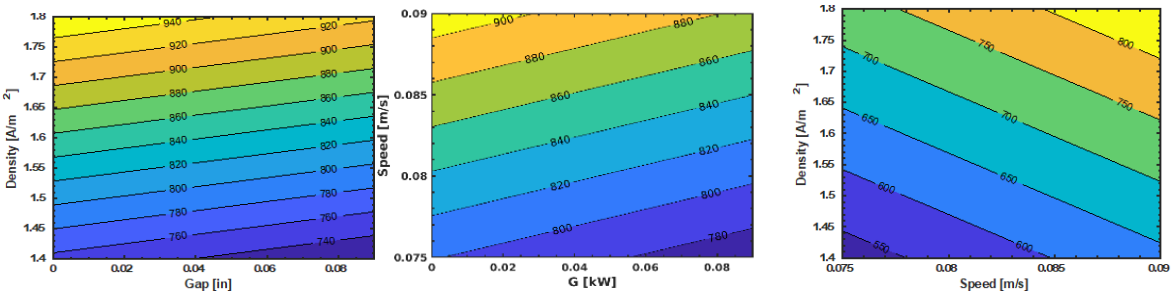

Figure 3.1.6 : Response surface method plot for T_1

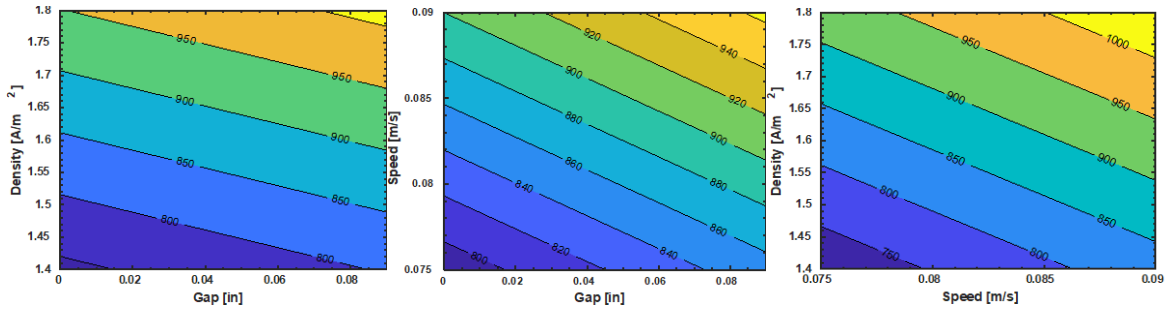

Figure 3.1.7 : Response surface method plot for T_2

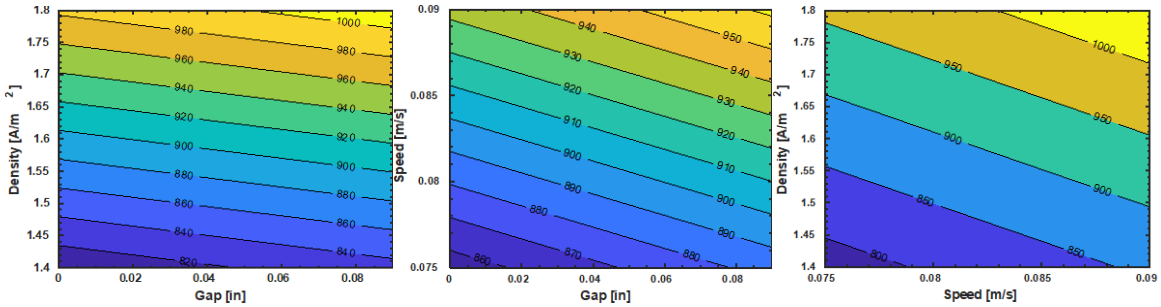

Figure 3.1.8 : Response surface method plot for T_3

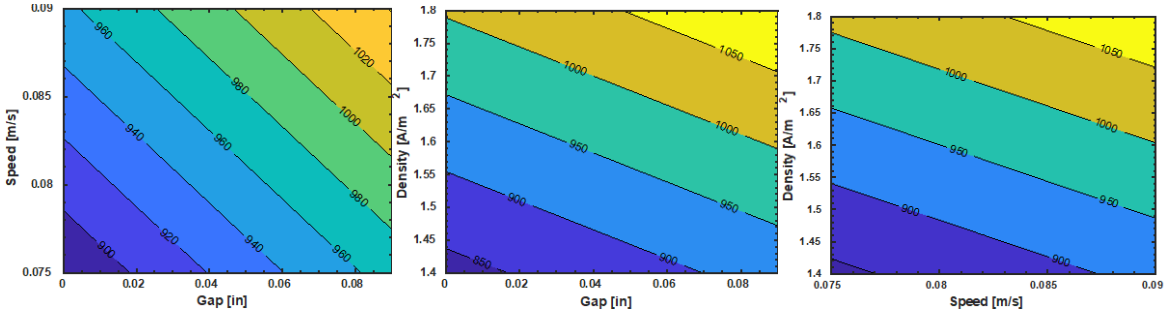

Figure 3.1.9 : Response surface method plot for T_4

At 2.5s of heating time

Here it comes the major role of the response surface analysis, since it's the last heating time, we should worry about the temperature range between 850 and 1100 degºC, remember the main objective of this study is to have an identical temperature at the four lower corners of the AISI 4340 Steel plate. As a first reflection we see from the figures that we have a linear variation between the temperature and the factors, temperature increases with the increasement of the both parameters that figures in every curve. From the Figure 3.1.9 of the temperature $T_{1-2.5s}$ the horizontal gap is not presented, since it has no effect at this temperature as we saw earlier at the main effects plot analysis. To be in the correct range of the temperature the figure shows that the current density should not pass the interval between 1.4 and 1.7($\times 10^{10}$ A/m²) without giving an importance to the speed value.

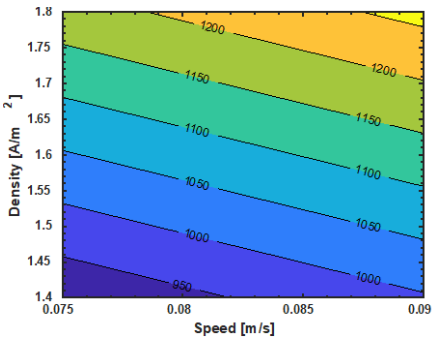

Figure 3.1.10 : Response surface method plot for $T_{1-2.5s}$

For $T_{2-2.5s}$ and $T_{4-2.5s}$ we can see that we have the effect between all the factors what can explain the three contour plots bellow for each corner. For the figure 3.1.10, when the external current density is held at 1.45($\times 10^{10}$ A/m²), the combination speed and gap don't play an important role as the value of the temperature always meets the requirements and is always near our requirement value of 1050 ºC for the end of the heating time. For a hold value of 0.079 m/s for the speed the requirements are met when the density is greater without exceeding the value of 1.6 for a gap lower than 0.02in. For a higher gap, the current density can go down to 1.4($\times 10^{10}$ A/m²) without exceeding the tolerance zone. A lot of combinations can be possible when holding the value of the gap to 0.06in, as long as the value of the speed is near of 0.075 m/s for a 1.5 ($\times 10^{10}$ A/m²) of the external current density.

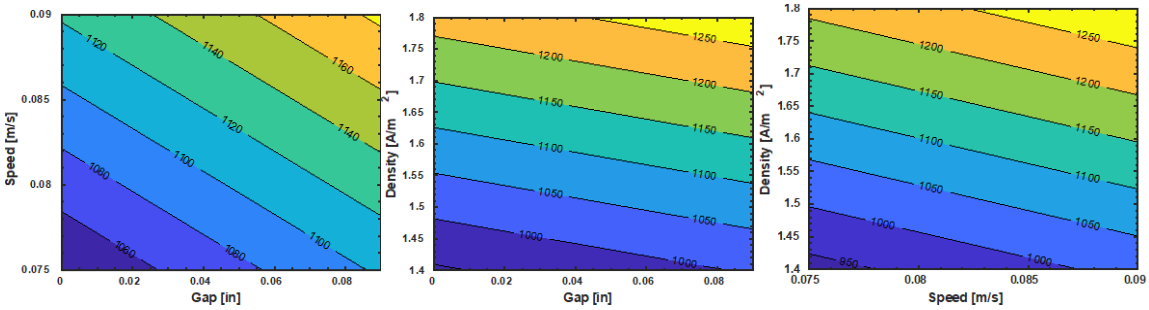

Figure 3.1.11 : Response surface method plot for $T_{2-2.5s}$

The exact same observation can be made for the surface response of the temperature $T_{3-2.5s}$ presented in Figure 3.1.11. In fact, for a hold value of 1.65 ($\times 10^{10}$ A/m²) of the external

current density, the value of the speed it is not important to have a temperature between 850 and 1100 ºC. The same goes for the gap since it's not represented.

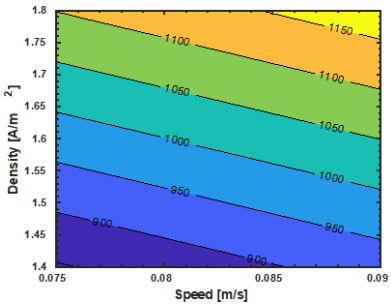

Figure 3.1.12 : Response surface method plot for $T_{3-2.5s}$

The last temperature $T_{4-2.5s}$ has the same exact analysis as the $T_{2-2.5s}$. It is clear that results confirm the linear behavior of different input parameters on the corners. As is seen in Figure 3.1.12 the effect of the horizontal gap and the speed are nearly the same, the temperature lines are parallel and equal so an increase of external current density and reduction of horizontal gap or speed leads to an enhancement in the final temperature on $T_{4-2.5s}$. Best temperature profile could be achieved for lower external current density and higher speed values. A better temperature profile can be obtained at the end of heating in the range of 0 to 0.02in of the horizontal gap.

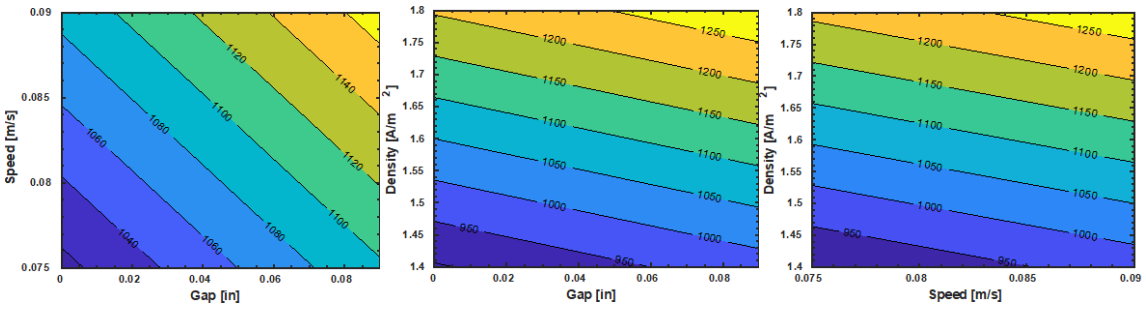

Figure 3.1.13 : Response surface method plot for $T_{4-2.5s}$

3.1.5 Conclusion

This paper presented a statistical study for our original model developed and designed of finite element analysis. This article aims to study the effects of machine and geometric parameters the parameters will be the same as those of the second work, but with three levels of values. The heating treatment simulations was performed following the Taguchi method for the design of experiment. The statistical analysis using ANOVA has demonstrated the effect of the parameters on the temperature profile for the four lower corners of our AISI 4340 steel. We also created a model for each outcome to be able to understand previous experiments and predict future ones. The models presented had an absolute mean error value of 0.46% at the middle time of the simulation (1.25s) and 4.6% as an absolute mean error value at the final time of the simulation (2.5s) which show us the reliability of the model. Thus, the statistical analyses demonstrated the good agreement between the prediction model and the simulation results, with an error not exceeding 50 ºC between the predicted temperature and the measured one. So that we have established a robust and reliable prediction model. This study aims to be a step toward the complex geometries design of the treated pieces and open new possibilities for the future like its implementation with industry 4.0.

CONCLUSION GÉNÉRALE

Pour améliorer le procédé de chauffage par induction, cette recherche propose de comprendre les différents phénomènes physiques d'origines électromagnétique, thermique et mécanique qui peuvent toucher à la structure de la surface extérieure lors du traitement et des nouvelles approches combinant des ordinateurs et des analyses statistiques. En ce sens, des études approfondies ont été faites concernant les différentes techniques du chauffage par induction comme méthode de durcissement des métaux. Dans le cadre des activités de recherche en maîtrise en ingénierie réalisées dans les laboratoires de l'UQAR, ce mémoire porte une attention particulière à la bonne compréhension du comportement thermomécanique des pièces en acier 4340 lors du traitement thermique par induction. Pour ce faire, une approche structurée en trois phases a été adoptée comme suit :

Réalisation d'une revue de littérature qui se focalise sur l'exploration des différentes méthodes du chauffage par induction et la mise en évidence des avancements et des travaux effectués dans ce domaine pour construire une idée claire sur les directions que nos études et nos recherches peuvent prendre.

Modélisation et simulation d'un modèle de plaque en AISI 4340 chauffée par induction. Un modèle 3D asymétrique chauffé par un inducteur à géométrie complexe en utilisant le logiciel multi-physique COMSOL afin de caractériser les paramètres qui influent le traitement et prédire la distribution de température dans la plaque traitée.

Réalisation d'un plan de simulation basé sur la méthode de Taguchi afin d'identifier et évaluer les effets des paramètres de contrôle sur la distribution de la température sur la plaque 4340 traité par induction. Et développement d'un modèle de prédiction avec ANOVA pour la prédiction de la distribution de la température au milieu et à la fin de chauffe afin d'avoir un profile uniforme sur toute la plaque.

La première phase du projet avait pour but de réaliser une revue de la littérature globale. Il s'agit d'une revue qui regroupe la majorité des travaux faits en chauffage par induction en détaillant l'origine et le principe incluant les différents éléments de base du traitement par induction**.** Ainsi la recherche des points d'intersection entre les deux domaines, chauffage par induction et l'industrie 4.0 pour exploiter les méthodes et les moyens de cette dernière dans le but d'améliorer le processus. Dans cette partie du mémoire, un bref historique présentant les bases de l'induction électromagnétique depuis sa découverte par le chercheur britannique Michael Faraday. Les principales recherches traitant de la simulation du procédé de traitement thermique par induction, se référant principalement aux recherches appliquées à des géométries simples avant d'aborder des engrenages et des géométries plus complexes. Ces recherches ont permis de parcourir les principaux éléments de la littérature depuis l'élaboration du premier modèle mathématique jusqu'aux derniers développements numériques. L'implémentation des méthodes de l'industrie 4.0 est aussi présente dans ce premier chapitre. En effet, on a ajouté une partie dédiée à l'industrie 4.0 qui montre comment ce domaine a évolué avec le temps pour répondre à des attentes élevées de la part des processus de fabrication et d'assemblage des pièces. Cette révolution, étant l'une des plus importantes dans l'industrie, s'avère essentielle à prendre part dans notre recherche littéraire. Cette phase du mémoire est importante dans le travail de recherche, elle nous permet de voir la bonne direction de nos travaux et nous donne une idée importante sur les résultats futurs qu'on peut avoir.

La seconde phase du projet fut dédiée aux travaux de modélisation en 3D par un logiciel de calcul par éléments finis avec couplage des phénomènes électromagnétiques et de transfert de chaleur. Cette phase du projet avait pour but de réaliser un modèle numérique de chauffage par induction, qui commence par la conception du model complexe de l'inducteur en 3D suivi par la réalisation du volume de la plaque en utilisant le logiciel COMSOL Multiphysics. Ce modèle avait pour but de simuler la chauffe par induction d'une plaque en acier 4340 et d'étudier les différentes affinités et l'influence des paramètres machines et géométriques sur l'évolution de la température à la fin de la chauffe. Nous avons présenté le procédé de traitement thermique par induction appliqué à une plaque d'acier 4340 en utilisant une source

de chaleur à moyenne fréquence. Dans cette étude, l'analyse numérique a été utilisée afin de comprendre le comportement thermique lors de la modification des paramètres de chauffage, notamment la vitesse et la puissance. La simulation a donc permis de définir les intervalles de puissance et de vitesse de balayage pour notre modèle, ce qui garantit un traitement optimal et efficace. Au cours de ce chapitre, nous avons réussi à réaliser une simulation 3D réussie du processus de chauffage par induction. La représentation graphique et numérique des paramètres clés et de leur dépendance temporelle a permis de mieux comprendre la relation complexe entre le champ électromagnétique et l'échauffement du matériau résultant. L'estimation de la puissance électrique requise se réfère directement à la conception considérant le système de chauffage par induction. En général les résultats ont permis premièrement de modéliser et simuler le processus de traitement par induction de la plaque et ainsi fournir suffisamment d'informations pour comprendre le comportement du profil durci en fonction des paramètres clés du processus, ensuite déterminer la répartition de la température en chaque point traité sur la plaque et à chaque instant du temps de chauffe. Et finalement sélectionner les plages des paramètres de processus clés optimales, noter la densité du courant externe, la vitesse de déplacement de la plaque par rapport à l'inducteur et le gap horizontal qui assurent une distribution de température adéquate et profonde sur la surface de la plaque.

La dernière phase de cette étude avait pour objectif d'étudier les effets des paramètres machine et géométrique. L'objectif était de déterminer les interactions entre les paramètres, en se basant sur des analyses statistiques dans les zones d'intérêt afin de rendre la distribution de la température uniforme sur la pièce, au milieu et à la fin du temps de chauffe. Cette phase du mémoire porte sur le développement d'un modèle prédictif fiable et acceptable qui prédit l'effet des paramètres machines et paramètres géométriques sur la distribution de la température de la plaque étudié précédemment. L'étape de caractérisation thermomécanique fut réalisée en trois parties. La première partie fut dédiée aux travaux de modélisation qui ont été faits précédemment dans la deuxième phase du mémoire, afin de caractériser adéquatement les paramètres machine et les facteurs géométriques qui ont le plus d'influence sur la distribution de la température. En deuxième partie, une campagne de simulation a été

conduite en se basant sur un design orthogonal proposé par la méthode de Taguchi en considérant un facteur géométrique, le gap horizontal entre le coté vide de l'inducteur et la pièce, ainsi que deux facteurs machines, la densité du courant externe, et la vitesse du déplacement de la plaque vis-à-vis l'inducteur. Des analyses statistiques ont été conduites pour développer des modèles de prédiction de profil de température par la méthode de surface de réponse RSM et par ANOVA. La troisième partie fut réalisée pour la validation du modèle de prédiction. Les analyses statistiques ont démontré une bonne concordance entre le modèle de prédiction et les résultats de la simulation, avec une erreur qui ne dépasse pas 50 ºC entre la température prédite et la température mesurée. Malgré les bons résultats trouvés, une validation expérimentale s'impose pour s'assurer du bon fonctionnement des composants et des résultats afin de valoriser le projet.

Un des premiers défis rencontrés durant cette étude était la simulation. Face à la difficulté de lancer le calcul pour plusieurs simulations en même temps avec un grand maillage, même en utilisant la machine virtuelle, on n'a pas réussi à avoir des résultats vu que le projet était grand même pour le computer cluster. Une étude de convergence a été faite afin réduire le temps de calcul sans pour autant perdre en terme de précision. Cette étude de convergence, qui a porté sur le maillage et le pas de temps de calcul, a permis la mise en place d'un modèle numérique robuste et précis.

Finalement, les travaux effectués dans ce projet de recherche ont conduit à une meilleure compréhension du procédé de traitement thermique par induction appliqué sur une plaque an acier 4340. Pour des travaux futurs il est nécessaire de consolider notre étude par des études d'optimisation ciblant d'autre paramètres de ce procédé, ainsi que la validation expérimentale à l'aide d'un compagnon d'essai. D'autres travaux futurs pourraient se réaliser en adoptant cet historique thermique pour calculer les profils de dureté, de contraintes résiduelles ou de tailles des grains, ainsi que des techniques consistantes de modélisation par réseaux de neurones artificiels pour la prédiction des comportements mécaniques des pièces traitées par induction. On a aussi l'impression 3D qui a été proposée comme une application industrielle basée sur l'industrie 4.0. Une solution répondante à la question de savoir s'il serait

possible, à un moment donné, d'imprimer des bobines de cuivre pour réduire le coût élevé de la production des inducteurs et rendre les inducteurs accessibles à tout type de géométrie.

RÉFERENCE BIBLIOGRAPHIQUE

[1] V. Rudnev, D. Loveless, R. Cook, and M. Black, "Induction hardening of Gears: a Review," *Heat Treatment of Metals,* vol. 30, no. 4, pp. 97-103, 2003.

[2] V. Rudnev, G. Fett, A. Griebel, and J. Tartaglia, "Principles of induction hardening and inspection," *ASM Handbook,* vol. 4, pp. 58-86, 2014.

[3] L. Jakubovičová, G. Andrej, K. Peter, and S. Milan, "Optimization of the induction heating process in order to achieve uniform surface temperature," *Procedia Engineering,* vol. 136, pp. 125-131, 2016.

[4] I. Balabozov, H. Brauer, and I. Yatchev, "Modelling of magnetic concentrators in induction heating systems," in *2017 15th International Conference on Electrical Machines, Drives and Power Systems (ELMA)*, 2017: IEEE, pp. 453-456.

[5] V. Rudnev, "Evolution of Induction Heating and Heat Treating as a Subject of Mathematical Modeling, Optimization and Design," in *2019 XXI International Conference Complex Systems: Control and Modeling Problems (CSCMP)*, 2019: IEEE, pp. 43-47.

[6] G. E. Totten, *Steel heat treatment: metallurgy and technologies*. CRC press, 2006.

[7] H. Chandler, *Heat treater's guide: practices and procedures for irons and steels*. ASM international, 1994.

[8] H. Ghasemi-Nanesa, M. Jahazi, M. Heidari, and T. Levasseur, "The influence of deformation-induced microvoids on mechanical failure of AISI A8-Mod martensitic tool steel," in *AIP Conference Proceedings*, 2017, vol. 1896, no. 1: AIP Publishing LLC, p. 020021.

[9] Neonickel. "Acier Allié 4340." https://www.neonickel.com/fr/alloys/alliages-dacier/4340-alloy-steel/ (accessed.

[10] R. E. Haimbaugh, *Practical induction heat treating*. ASM international, 2015.

[11] D. Hömberg *et al.*, "Simulation of multi-frequency-induction-hardening including phase transitions and mechanical effects," *Finite Elements in Analysis and Design,* vol. 121, pp. 86-100, 2016.

[12] P. Woodard, S. Chandrasekar, and H. Yang, "Analysis of temperature and microstructure in the quenching of steel cylinders," *Metallurgical and materials transactions B,* vol. 30, no. 4, pp. 815-822, 1999.

[13] M. Kadanik, L. Burgschat, M. Reich, S. Petersen, and O. Keßler, "Experimental Determination of Heat Transfer using a Polymer Solution Shower during Induction Hardening," *HTM Journal of Heat Treatment and Materials,* vol. 76, no. 4, pp. 249-260, 2021.

[14] Z. Li, B. L. Ferguson, V. Nemkov, R. Goldstein, J. Jackowski, and G. Fett, "Effect of quenching rate on distortion and residual stresses during induction hardening of a full-float truck axle shaft," *Journal of materials engineering and performance,* vol. 23, no. 12, pp. 4170-4180, 2014.
[15] H. Kristoffersen and P. Vomacka, "Influence of process parameters for induction hardening on residual stresses," *Materials & Design,* vol. 22, no. 8, pp. 637-644, 2001.
[16] V. Nemkov, R. Goldstein, J. Jackowski, L. Ferguson, and Z. Li, "Stress and distortion evolution during induction case hardening of tube," *Journal of materials engineering and performance,* vol. 22, no. 7, pp. 1826-1832, 2013.
[17] J. Komotori, M. Shimizu, Y. Misaka, and K. Kawasaki, "Fatigue strength and fracture mechanism of steel modified by super-rapid induction heating and quenching," *International journal of fatigue,* vol. 23, pp. 225-230, 2001.
[18] P. Legutko, "Wpływ parametrów materiałowych stali stopowych na proces hartowania indukcyjnego kół zębatych," *Przegląd Elektrotechniczny,* vol. 97, 2021.
[19] F. Mühl, J. Damon, S. Dietrich, and V. Schulze, "Simulation of induction hardening: Simulative sensitivity analysis with respect to material parameters and the surface layer state," *Computational Materials Science,* vol. 184, p. 109916, 2020.
[20] B. Larregain, N. Vanderesse, F. Bridier, P. Bocher, and P. Arkinson, "Method for accurate surface temperature measurements during fast induction heating," *Journal of materials engineering and performance,* vol. 22, no. 7, pp. 1907-1913, 2013.
[21] N. Barka, "Study of the machine parameters effects on the case depths of 4340 spur gear heated by induction—2D model," *The International Journal of Advanced Manufacturing Technology,* vol. 93, no. 1-4, pp. 1173-1181, 2017.
[22] D. W. Dudley, "Handbook of practical gear design," *Mc Graw-Hill Book Company, 1984,* p. 656, 1984.
[23] M. Faraday, *Experimental researches in chemistry and physics*. CRC Press, 1990.
[24] L. Foucault, *Recueil des travaux scientifiques de Léon Foucault*. Gauthier-villars, 1878.
[25] V. I. Rudnev, "Single-coil dual-frequency induction hardening of gears," *Heat treating progress,* vol. 9, pp. 9-11, 2009.
[26] H.-J. Peter, "Inductive surface hardening with the simultaneous dual frequency induction heat treating," *Harterei-Technische Mitteilungen,* vol. 59, no. 2, pp. 119-124, 2004.
[27] J. Yuan, J. Kang, Y. Rong, and R. Sisson, "FEM modeling of induction hardening processes in steel," *Journal of materials engineering and performance,* vol. 12, no. 5, pp. 589-596, 2003.
[28] V. Nemkov, V. Demidovich, V. Rudnev, and O. Fishman, "Electromagnetic end and edge effects in induction heating," in *Proceedings of UIE Congress, Montreal*, 1991.
[29] V. Rudnev, "Mathematical simulation and optimal control of induction heating of large-dimensional cylinders and slabs," Ph. D. thesis, St. Petersburg El. Eng. Univ., Russia, 1986.
[30] V. Nemkov and V. Demidovich, "Theory and calculation of induction heating devices," *Energoatomizdat, Leningrad,* vol. 280, 1988.

[31] N. Barka, A. Chebak, A. El Ouafi, M. Jahazi, and A. Menou, "A new approach in optimizing the induction heating process using flux concentrators: application to 4340 steel spur gear," *Journal of materials engineering and performance,* vol. 23, no. 9, pp. 3092-3099, 2014.

[32] V. Rudnev, R. Cook, D. Loveless, and M. Black, "Induction heat treatment," *Steel Heat Treatement Handbook, New York, Basel, Hong Kong,* 1997.

[33] J. Grum, "Overview of residual stresses after induction surface hardening," *International Journal of Materials and Product Technology,* vol. 29, no. 1-4, pp. 9-42, 2007.

[34] N. Barka, P. Bocher, and J. Brousseau, "Sensitivity study of hardness profile of 4340 specimen heated by induction process using axisymmetric modeling," *The International Journal of Advanced Manufacturing Technology,* vol. 69, no. 9, pp. 2747-2756, 2013.

[35] D. L. Loveless and V. I. Rudnev, "Multi-frequency heat treatment of a workpiece by induction heating," ed: Google Patents, 2007.

[36] e. induction. "AUTOMOTIVE." https://www.efd-induction.com/en/industries/automotive (accessed.

[37] V. Rudnev, D. Loveless, and R. L. Cook, *Handbook of induction heating*. CRC press, 2017.

[38] S. Semiatin, *Elements of induction heating: design, control, and applications*. ASM International, 1988.

[39] R. Baker, "Classical heat flow problems applied to induction billet heating," *Transactions of the American Institute of Electrical Engineers, Part II: Applications and Industry,* vol. 77, no. 2, pp. 106-112, 1958.

[40] C. V. Dodd, "Solutions to electromagnetic induction problems," Oak Ridge National Lab.(ORNL), Oak Ridge, TN (United States), 1967.

[41] J. Donea, S. Giuliani, and A. Philippe, "Finite elements in the solution of electromagnetic induction problems," *International Journal for Numerical Methods in Engineering,* vol. 8, no. 2, pp. 359-367, 1974.

[42] J. Davies and P. Simpson, *Induction heating handbook*. McGraw-Hill Companies, 1979.

[43] P. Masse, B. Morel, and T. Breville, "A finite element prediction correction scheme for magneto-thermal coupled problem during Curie transition," *IEEE Transactions on magnetics,* vol. 21, no. 5, pp. 1871-1873, 1985.

[44] M. Melander, "Computer predictions of progressive induction hardening of cylindrical components," *Materials science and technology,* vol. 1, no. 10, pp. 877-882, 1985.

[45] G. Meunier, D. Shen, and J.-L. Coulomb, "Modelisation of 2D and axisymmetric magnetodynamic domain by the finite elements method," *IEEE Transactions on magnetics,* vol. 24, no. 1, pp. 166-169, 1988.

[46] K. Wang, S. Chandrasekar, and H. T. Yang, "Finite-element simulation of induction heat treatment," *Journal of Materials Engineering and Performance,* vol. 1, no. 1, pp. 97-112, 1992.

[47] O. Longeot and C. DELALEAU, "Simulation numérique des procédés de traitement par induction," *Traitement thermique (Paris),* no. 280, 1995.
[48] K. Sadeghipour, J. Dopkin, and K. Li, "A computer aided finite element/experimental analysis of induction heating process of steel," *Computers in industry,* vol. 28, no. 3, pp. 195-205, 1996.
[49] C. Chaboudez, S. Clain, R. Glardon, D. Mari, J. Rappaz, and M. Swierkosz, "Numerical modeling in induction heating for axisymmetric geometries," *IEEE transactions on magnetics,* vol. 33, no. 1, pp. 739-745, 1997.
[50] M. Enokizono, T. Todaka, and S. Nishimura, "Finite element analysis of high-frequency induction heating problems considering inhomogeneous flow of exciting currents," *IEEE transactions on magnetics,* vol. 35, no. 3, pp. 1646-1649, 1999.
[51] Y. Favennec, V. Labbé, and F. Bay, "Induction heating processes optimization a general optimal control approach," *Journal of computational physics,* vol. 187, no. 1, pp. 68-94, 2003.
[52] F. Bay, Y. Favennec, and V. Labbe, "A numerical modeling example in multi-physics coupling: analysis and optimization of induction heating processes; Un exemple de modelisation numerique en couplages multiphysiques: analyse et optimisation du chauffage par induction," 2003.
[53] V. Fireteanu, T. Tudorache, A. Geri, and G. Veca, "Transverse flux induction heating: comparison between numerical models and experimental validation," *COMPEL-The international journal for computation and mathematics in electrical and electronic engineering,* 2003.
[54] V. Nemkov and R. Goldstein, "Computer simulation for fundamental study and practical solutions to induction heating problems," *COMPEL-The international journal for computation and mathematics in electrical and electronic engineering,* 2003.
[55] H. Kawaguchi, M. Enokizono, and T. Todaka, "Thermal and magnetic field analysis of induction heating problems," *journal of materials processing technology,* vol. 161, no. 1-2, pp. 193-198, 2005.
[56] I. Magnabosco, P. Ferro, A. Tiziani, and F. Bonollo, "Induction heat treatment of a ISO C45 steel bar: Experimental and numerical analysis," *Computational materials science,* vol. 35, no. 2, pp. 98-106, 2006.
[57] M. Kchaou, M. Yaakoubi, and F. Dammak, "Effect of the superficial hardening on distortion and stress state: application on bearing race," *Int. Rev. Mechan. Eng,* vol. 3, no. 4, 2009.
[58] B. Yang, A. Hattiangadi, W. Li, G. Zhou, and T. McGreevy, "Simulation of steel microstructure evolution during induction heating," *Materials Science and Engineering: A,* vol. 527, no. 12, pp. 2978-2984, 2010.
[59] A. Kohli and H. Singh, "Optimization of processing parameters in induction hardening using response surface methodology," *Sadhana,* vol. 36, no. 2, pp. 141-152, 2011.
[60] W. Jomaa, V. Songmene, and P. Bocher, "An investigation of machining-induced residual stresses and microstructure of induction-hardened AISI 4340 steel," *Materials and Manufacturing Processes,* vol. 31, no. 7, pp. 838-844, 2016.

[61] C. Jiang, H. Chen, Q. Wang, and Y. Li, "Effect of brazing temperature and holding time on joint properties of induction brazed WC-Co/carbon steel using Ag-based alloy," *Journal of Materials Processing Technology,* vol. 229, pp. 562-569, 2016.
[62] P. Guerrier, K. K. Nielsen, S. Menotti, and J. H. Hattel, "An axisymmetrical non-linear finite element model for induction heating in injection molding tools," *Finite Elements in Analysis and Design,* vol. 110, pp. 1-10, 2016.
[63] P. Guerrier, G. Tosello, K. K. Nielsen, and J. H. Hattel, "Three-dimensional numerical modeling of an induction heated injection molding tool with flow visualization," *The International Journal of Advanced Manufacturing Technology,* vol. 85, no. 1, pp. 643-660, 2016.
[64] H. Hammi, A. El Ouafi, N. Barka, and A. Chebak, "Scanning based induction heating for AISI 4340 steel spline shafts-3D simulation and experimental validation," *Advances in Materials Physics and Chemistry,* vol. 7, no. 06, p. 263, 2017.
[65] D. Tong, J. Gu, and G. E. Totten, "Numerical investigation of asynchronous dual-frequency induction hardening of spur gear," *International Journal of Mechanical Sciences,* vol. 142, pp. 1-9, 2018.
[66] M. Kranjc, A. Županič, T. Jarm, and D. Miklavčič, "Optimization of induction heating using numerical modeling and genetic algorithm," in *2009 35th Annual Conference of IEEE Industrial Electronics*, 2009: IEEE, pp. 2104-2108.
[67] Y. Han, H. Wen, and E. Yu, "Study on electromagnetic heating process of heavy-duty sprockets with circular coils and profile coils," *Applied Thermal Engineering,* vol. 100, pp. 861-868, 2016.
[68] A. Senhaji, "Simulation numérique de la chauffe par induction électromagnétique d'un disque en AISI 4340," École de technologie supérieure, 2017.
[69] J. Grum, "Measuring and analysis of residual stresses after induction hardening and grinding," in *Materials science forum*, 2000, vol. 347: Trans Tech Publ, pp. 453-458.
[70] J. Grum, "A review of the influence of grinding conditions on resulting residual stresses after induction surface hardening and grinding," *Journal of Materials Processing Technology,* vol. 114, no. 3, pp. 212-226, 2001.
[71] J. Barglik, A. Smalcerz, R. Przylucki, and I. Doležel, "3D modeling of induction hardening of gear wheels," *Journal of Computational and Applied Mathematics,* vol. 270, pp. 231-240, 2014.
[72] H. Wen and Y. Han, "Study on mobile induction heating process of internal gear rings for wind power generation," *Applied Thermal Engineering,* vol. 112, pp. 507-515, 2017.
[73] A. Candeo, C. Ducassy, P. Bocher, and F. Dughiero, "Multiphysics modeling of induction hardening of ring gears for the aerospace industry," *IEEE Transactions on Magnetics,* vol. 47, no. 5, pp. 918-921, 2011.
[74] M.-S. Huang and Y.-L. Huang, "Effect of multi-layered induction coils on efficiency and uniformity of surface heating," *International Journal of Heat and Mass Transfer,* vol. 53, no. 11-12, pp. 2414-2423, 2010.
[75] P. Kochure and K. Nandurkar, "Application of taguchi methodology in selection of process parameters for induction hardening of EN8 D Steel," *Power (kw),* vol. 10, no. 12, p. 14, 2012.

[76] S. J. Midea and P. Lynch, "Tooth-by-tooth induction hardening of gears (and how to avoid some common problems)," *Proc. Thermal Process. Gear Solutions,* pp. 46-51, 2014.
[77] V. Savaria, F. Bridier, and P. Bocher, "Predicting the effects of material properties gradient and residual stresses on the bending fatigue strength of induction hardened aeronautical gears," *International Journal of Fatigue,* vol. 85, pp. 70-84, 2016.
[78] P. Withers, "Residual stress and its role in failure," *Reports on progress in physics,* vol. 70, no. 12, p. 2211, 2007.
[79] D. Rodman, C. Krause, F. Nürnberger, F.-W. Bach, L. Gerdes, and B. Breidenstein, "Investigation of the surface residual stresses in spray cooled induction hardened gearwheels," *International journal of materials research,* vol. 103, no. 1, pp. 73-79, 2012.
[80] M. N. James, D. G. Hattingh, D. Asquith, M. Newby, and P. Doubell, "Applications of residual stress in combatting fatigue and fracture," *Procedia Structural Integrity,* vol. 2, pp. 11-25, 2016.
[81] H. B. Besserer *et al.*, "Induction Heat Treatment of Sheet-Bulk Metal-Formed Parts Assisted by Water–Air Spray Cooling," *steel research international,* vol. 87, no. 9, pp. 1220-1227, 2016.
[82] D. Coupard, T. Palin-luc, P. Bristiel, V. Ji, and C. Dumas, "Residual stresses in surface induction hardening of steels: Comparison between experiment and simulation," *Materials Science and Engineering: A,* vol. 487, no. 1-2, pp. 328-339, 2008.
[83] D. Deng, "FEM prediction of welding residual stress and distortion in carbon steel considering phase transformation effects," *Materials & Design,* vol. 30, no. 2, pp. 359-366, 2009.
[84] D. Ivanov, L. Markegård, J. I. Asperheim, and H. Kristoffersen, "Simulation of stress and strain for induction-hardening applications," *Journal of materials engineering and performance,* vol. 22, no. 11, pp. 3258-3268, 2013.
[85] M. Meo and R. Vignjevic, "Finite element analysis of residual stress induced by shot peening process," *Advances in Engineering Software,* vol. 34, no. 9, pp. 569-575, 2003.
[86] M. Khalifa, N. Barka, J. Brousseau, and P. Bocher, "Sensitivity study of hardness profile of 4340 steel disc hardened by induction according to machine parameters and geometrical factors," *The International Journal of Advanced Manufacturing Technology,* vol. 101, no. 1-4, pp. 209-221, 2019.
[87] S. Rhein, T. Utz, and K. Graichen, "Optimal control of induction heating processes using FEM software," in *2015 European Control Conference (ECC)*, 2015: IEEE, pp. 515-520.
[88] N. Vanderesse, B. Larregain, F. Bridier, and P. Bocher, "Experimental assessment of high heating rates in induction heating with temperature-sensitive lacquers," *Journal of Materials Engineering and Performance,* vol. 27, no. 8, pp. 3831-3843, 2018.
[89] M. Khalifa, N. Barka, J. Brousseau, and P. Bocher, "Reduction of edge effect using response surface methodology and artificial neural network modeling of a spur gear

treated by induction with flux concentrators," *The International Journal of Advanced Manufacturing Technology,* vol. 104, no. 1-4, pp. 103-117, 2019.
[90] J. Yi, M. Gharghouri, P. Bocher, and M. Medraj, "Distortion and residual stress measurements of induction hardened AISI 4340 discs," *Materials Chemistry and Physics,* vol. 142, no. 1, pp. 248-258, 2013.
[91] H. F. Sabeeh, I. M. Abdulbaqi, and S. M. Mahdi, "Effect of flux concentrator on the surface hardening process of a steel gear," in *2018 1st International Scientific Conference of Engineering Sciences-3rd Scientific Conference of Engineering Science (ISCES)*, 2018: IEEE, pp. 80-85.
[92] M. Khalifa, N. Barka, J. Brousseau, and P. Bocher, "Optimization of the edge effect of 4340 steel specimen heated by induction process with flux concentrators using finite element axis-symmetric simulation and experimental validation," *The International Journal of Advanced Manufacturing Technology,* vol. 104, no. 9-12, pp. 4549-4557, 2019.
[93] T. Zhu, P. Feng, X. Li, F. Li, and Y. Rong, "The study of the effect of magnetic flux concentrator to the induction heating system using coupled electromagnetic-thermal simulation model," in *2013 International Conference on Mechanical and Automation Engineering*, 2013: IEEE, pp. 123-127.
[94] F. Li, X. Li, X. Qin, and Y. K. Rong, "Study on the plane induction heating process strengthened by magnetic flux concentrator based on response surface methodology," *Journal of Mechanical Science and Technology,* vol. 32, no. 5, pp. 2347-2356, 2018.
[95] V. Rudnev, "An objective assessment of magnetic flux concentrators," *Heat treating progress,* pp. 19-23, 2004.
[96] R. G. O'brien, "A general ANOVA method for robust tests of additive models for variances," *Journal of the American Statistical Association,* vol. 74, no. 368, pp. 877-880, 1979.
[97] A. Alin, "Minitab," *Wiley Interdisciplinary Reviews: Computational Statistics,* vol. 2, no. 6, pp. 723-727, 2010.
[98] T. Dahiru, "P-value, a true test of statistical significance? A cautionary note," *Annals of Ibadan postgraduate medicine,* vol. 6, no. 1, pp. 21-26, 2008.
[99] J. J. Faraway, *Practical regression and ANOVA using R*. University of Bath Bath, 2002.
[100] N. Draper and H. Smith, "Aplied regression analisys. reprint," ed: New York: J. Wiley, 2014.
[101] B. Coto, V. G. Navas, O. Gonzalo, A. Aranzabe, and C. Sanz, "Influences of turning parameters in surface residual stresses in AISI 4340 steel," *The International Journal of Advanced Manufacturing Technology,* vol. 53, no. 9-12, pp. 911-919, 2011.
[102] J. Miles, "R-squared, adjusted R-squared," *Encyclopedia of statistics in behavioral science,* 2005.
[103] J. Antony, *Design of experiments for engineers and scientists*. Elsevier, 2014.
[104] M. K. Misra, B. Bhattacharya, O. Singh, and A. Chatterjee, "Multi response optimization of induction hardening process-a new approach," *IFAC Proceedings Volumes,* vol. 47, no. 1, pp. 862-869, 2014.